Mammalian Adenylyl Cyclases: a Novel Class of Membrane Receptors

Dissertation

der Mathematisch-Naturwissenschaftlichen Fakultät

der Eberhard Karls Universität Tübingen

zur Erlangung des Grades eines

Doktors der Naturwissenschaften

(Dr. rer. nat.)

vorgelegt von

Marius Landau

aus Frankenberg (Eder)

Tübingen

2024

Gedruckt mit Genehmigung der Mathematisch-Naturwissenschaftlichen Fakultät der Eberhard Karls Universität Tübingen.

Tag der mündlichen Qualifikation:	09.12.2024
Dekan:	Prof. Dr. Thilo Stehle
1. Berichterstatter/-in:	Prof. Dr. Joachim Schultz
2. Berichterstatter/-in:	Prof. Dr. Doron Rapaport

Acknowledgements

First and foremost, I would like to express my sincere gratitude to my supervisor, Prof. Dr. Joachim E. Schultz, for providing me with the opportunity to work on this fascinating and challenging project. I deeply appreciate the time he invested in guiding me and helping me navigate the world of scientific research. Additionally, I am thankful for his invaluable life advice and his encouraging words during times of scientific setbacks.

I extend my gratitude to Prof. Dr. Doron Rapaport for evaluating my dissertation.

A special thank you goes to Prof. Dr. Harald Groß for his significant contributions to my project, particularly for his support in the laboratory and his assistance with the analysis of the data we acquired.

I am also deeply grateful to Prof. Dr. Andrei N. Lupas for his constant advice, insightful discussions, and for giving me the opportunity to participate in inspiring group meetings, which provided me with further guidance.

I would like to thank my former colleagues, Dr. Sherif Elsabbagh and Dr. Anubha Seth, for their collaboration, which was always seamless and enjoyable. I also appreciate the practical lab techniques they taught me, which were invaluable for my day-to-day work.

My heartfelt thanks go to Ms. Anita Schultz and Ms. Ursula Kurz for their consistent help both in and out of the lab, and for their positive influence on the overall working environment.

I would like to express my appreciation to the members of the Ruth, Lukowski, and Gross groups, especially those working on the 7th and 9th floors, for their excellent cooperation and for fostering a productive working atmosphere.

A special note of gratitude goes to Mr. Andreas Evers, my first chemistry teacher in high school, who ignited my passion for science and Dr. Jost Weber who mentored me throughout my pharmacy studies.

I am deeply indebted to my parents for their unwavering support throughout the years, for always believing in my potential, and for standing by me through every challenge I faced. I am also particularly grateful to my sister, Anna, for her immense support in every aspect of my life.

Finally, I want to thank my girlfriend, Marie, for her emotional support and her consistently positive attitude, which brings a smile to my face even on the most challenging days.

Table of contents

Abbreviations

AC	Adenylyl cyclase
mAC	membrane bound adenylyl cyclase
GPCR	G-protein coupled receptor
TM	Transmembrane (domain)

List of publications

Publications:

Seth, A., **Landau, M.,** Shevchenko, A., Traikov, S., Schultz, A., Elsabbagh, S., & Schultz, J.E. (2022). Distinct glycerophospholipids potentiate Gsα-activated adenylyl cyclase activity. *Cellular Signalling, 97,*110396. https://doi.org/10.1016/j.cellsig.2022.110396

Elsabbagh, S., **Landau, M**., Gross, H., Schultz, A., & Schultz, J.E. (2023). Heme b inhibits class III adenylyl cyclases. *Cellular signalling*, 103, 110568. https://doi.org/10.1016/j.cellsig.2022.110568

Landau, M., Elsabbagh, S., Gross, H., Fuchs, A., Schultz, A., Schultz, J.E. (2024). The membrane domains of mammalian adenylyl cyclases are lipid receptors. *Elife 2024 Vol. 13* https://doi.org/10.7554/eLife.101483.3

Zusammenfassung

Humane Adenylylcyclasen (ACs) spielen eine entscheidende Rolle in der Signalübertragung zwischen dem extrazellulären und intrazellulären Raum. Molekulare Botenstoffe werden von G-Protein-gekoppelten Rezeptoren (GPCRs) auf der Zelloberfläche erkannt, wo sie binden und G-Proteine aktivieren, die das Signal aus dem extrazellulären Raum in das Zytoplasma weiterleiten. Dieses Signal wird an ACs übertragen, die daraufhin den sekundären Botenstoff cyclisches Adenosinmonophosphat (cAMP) erzeugen. cAMP übermittelt das Signal an zytosolische Proteine und löst so eine zelluläre Reaktion aus.

ACs sind pseudo-heterodimere Proteine, die aus einer Transmembran- (TM) Domäne und einer katalytischen (zytosolischen) Domäne bestehen. Die Umwandlung von ATP in cAMP erfolgt, wenn die beiden katalytischen Untereinheiten zusammenkommen und das aktive Zentrum bilden. Der TM-Bereich, der aus zwei hexahelikalen Untereinheiten (TM1 und TM2) besteht, macht etwa 40 % der Proteinstruktur aus. Obwohl eine Funktion darin besteht, als Membrananker zu dienen, deuten neuere Erkenntnisse darauf hin, dass er eine komplexere Funktion haben könnte. Die evolutionäre Konservierung signalübertragender Elemente, die die TM- und katalytischen Domänen verbinden, die erfolgreiche Übertragung anderer Rezeptordomänen auf AC und Substanzen im Serum, die selektiv AC Isoformen hemmen, weisen alle auf eine potenzielle Rezeptorfunktion hin.

Ziel meines Projekts war es, zu untersuchen, ob die TM-Domänen eine Rezeptorfunktion innehaben, indem ein physiologischer Ligand identifiziert wird. Wir stellten fest, dass Glycerophospholipide die Gsα-stimulierte AC-Aktivität auf eine nicht isoform-spezifische Weise in allen neun membranständigen AC-Isoformen verstärken. Unsere Daten deuten darauf hin, dass Glycerophospholipide direkt auf die katalytische Domäne wirken könnten, anstatt auf den TM-Bereich. Ähnlich wurde festgestellt, dass Häm B mehrere Klasse III ACs, einschließlich aller neun menschlichen Isoformen, unspezifisch hemmt. Obwohl diese Moleküle nicht die gesuchten Liganden waren, offenbarten sie neue Ebenen der AC-Regulation.

Freie, ungesättigte Fettsäuren wie Ölsäure und Arachidonsäure beeinflussen die Gsα-stimulierte AC-Aktivität isoform-spezifisch. So stimuliert Ölsäure die Isoformen 2, 3, 7 und 9, während Arachidonsäure die Isoformen 1 und 4 hemmt. Durch den Austausch der TM-Domänen der Isoformen 3 und 5 konnten wir zeigen, dass Rezeptorfunktionen austauschbar sind: Die Hemmung von Isoform 5 durch das Endocannabinoid Anandamid, das auch die Isoformen 1, 4 und 6 hemmt, wurde erfolgreich auf Isoform 3 übertragen. Zudem ging die stimulierende Wirkung der Ölsäure verloren beim Austausch der TM-Domänen.

Zusammenfassend haben wir einen neuen Mechanismus der AC-Regulation über ihre TM-Domäne identifiziert. Die Regulation durch Fettsäuren und ihrer Derivate beweist die regulatorische Rolle der TM-Domänen. Die Ergebnisse positionieren menschliche ACs an einem Knotenpunkt zwischen schneller Neurotransmitter-Signalübertragung (phasische Signaltransduktion) und langsamer, direkter, lipidvermittelter Signalübertragung (tonische Signaltransduktion).

Summary

Human adenylyl cyclases (ACs) play a critical role in signal transduction from extracellular to intracellular compartments. Extracellular signals are recognized by G-protein-coupled receptors (GPCRs) on the cell surface, where they bind and release intracellular G-proteins. The Gsα subunit of the trimeric G-protein binds and activates ACs, which generate cAMP, initiating cellular responses.

ACs are pseudo-heterodimeric proteins composed of transmembrane and cytosolic components. The conversion of ATP to cAMP occurs when the two catalytic subdomains associate and form an active site. The TM region comprises two hexahelical subdomains (TM1 and TM2) and accounts for approximately 40% of the protein. Although the role of the TMs is thought to be membrane anchoring, recent studies suggest additional, possibly more complex functions. Evolutionary conservation of signal-transducing elements connecting TM1 and TM2 and respective catalytic domains, the successful graft of other receptor domains on to ACs, and the rather selective inhibition by serum compounds of ACs with a TM domain are indicative of potential receptor functions.

The aim of my project was to examine whether the TM domains might function as membrane receptors by identifying physiological ligands. Initially, we discovered that glycerophospholipids enhance Gsα-stimulated AC activity in a non-isoform-specific manner. The data suggest that glycerophospholipids may act directly on the catalytic dimer. Similarly, heme B was found to inhibit multiple class III ACs, including all nine human isoforms. Although these molecules are not the ligands we intended to identify, they revealed new layers of AC regulation.

Using acid extracts of bovine lung lipids, we identified unsaturated fatty acids, such as oleic and arachidonic acid, to affect Gsα-stimulated AC activity in a rather isoform-specific manner. Oleic acid enhanced isoforms 2, 3, 7, and 9, whereas arachidonic acid attenuated isoforms 1 and 4. By swapping the TM domains of isoforms 3 and 5, we demonstrated that receptor functions are transferable: the inhibition of isoform 5

by the endocannabinoid anandamide (which inhibits isoforms 1, 4, 5, and 6) was successfully grafted onto isoform 3. Additionally, the enhancing effect of oleic acid vanished.

In conclusion, we identified a novel mechanism of AC regulation, involving its own membrane domains as receptors for fatty acids. This positions mammalian ACs at a crucial junction between rapid neurotransmitter signaling (phasic signaling) and slower, direct lipid-mediated signal transduction (tonic signaling).

1.Introduction

1.1 Signal transduction

Communication is key. This frequently cited phrase in human interactions holds true for all forms of life, whether we are discussing humans, animals, other eukaryotes, or even prokaryotes. Since all cells are enclosed by membranes, the transmission of signals (communication) across these membranes is a fundamental necessity. This process requires membrane-embedded proteins, such as receptors/sensors, to detect signals from the cell's external environment. These signals are conveyed through the binding of ligands (first messengers).

1.2 cAMP-dependent pathway

Since 1958, when Sutherland and Rall first described the presence of cAMP, our understanding of signal transduction expanded significantly [1]. The cAMP-dependent signaling pathway can be summarized in three major steps: First, the binding of a first messenger (such as hormones, neurotransmitters, chemokines) to GPCRs. They constitute the largest class of membrane-embedded proteins involved in signal transduction, with approximately 2% of all human genes coding for these receptors [2]. The sheer number of genes, and consequently proteins, hints at the vast array of ligands that interact with GPCRs. This diversity of ligands leads to a wide range of physiological effects, including roles in neurotransmission, blood pressure regulation, glucose and lipid metabolism, immune responses, and more [2]. Given their widespread influence, it is no surprise that GPCRs play a pivotal role in both health and disease, with about 35% of FDA-approved drugs targeting these receptors [3].

In the next step, the signal (the binding of the ligand) is relayed to the associated G-proteins, which are directly coupled to the GPCRs. G-proteins consist of an α subunit and a βγ dimer subunit. When a ligand binds to the GPCR, the GDP molecule attached to the α subunit is replaced by GTP, resulting in the dissociation of the GTP-bound α subunit from the βγ dimer. G-protein α subunits can be classified into four

subfamilies: $G\alpha_s$, $G\alpha_i$, $G\alpha_q$, and $G\alpha_{12}$ [2]. In the final step, the α subunit binds to a specific site on ACs C2. In the case of Gαs, this binding activates ACs, while $G\alpha_i$, binding to C1, inhibits their activity. ACs then convert ATP into cAMP. This creates a uniform second messenger that transmits a wide variety of signals within the cell.

One of the key effects of cAMP is its activation of protein kinase A (PKA). Once activated, PKA phosphorylates and regulates the activity of several target proteins [4]. Besides PKA, cAMP also interacts with cyclic nucleotide-gated ion channels [5] and exchange proteins activated by cAMP (EPAC) [6].

1.3 Adenylyl cyclases

As previously mentioned, ACs catalyze the conversion of ATP to cAMP. It would be logical to assume that all ACs share a common ancestor, but this is not the case. ACs are classified into six distinct and unrelated groups, labeled as classes I through VI. To date, most research has focused on proteins from class III, primarily because the other classes are predominantly found in a limited range of prokaryotic species [7]. Class III stands out as the most diverse, both functionally and structurally, the largest in number, and the most pharmacologically significant, as it is the only group present in animals [8].

Class III is further subdivided into four subclasses, labeled IIIa to IIId, based on similarities in the sequences of their catalytic domains [8]. An overview of the evolutionary relationships between the subclasses is shown in Figure 1. This thesis mainly deals with subclass IIIa ACs.

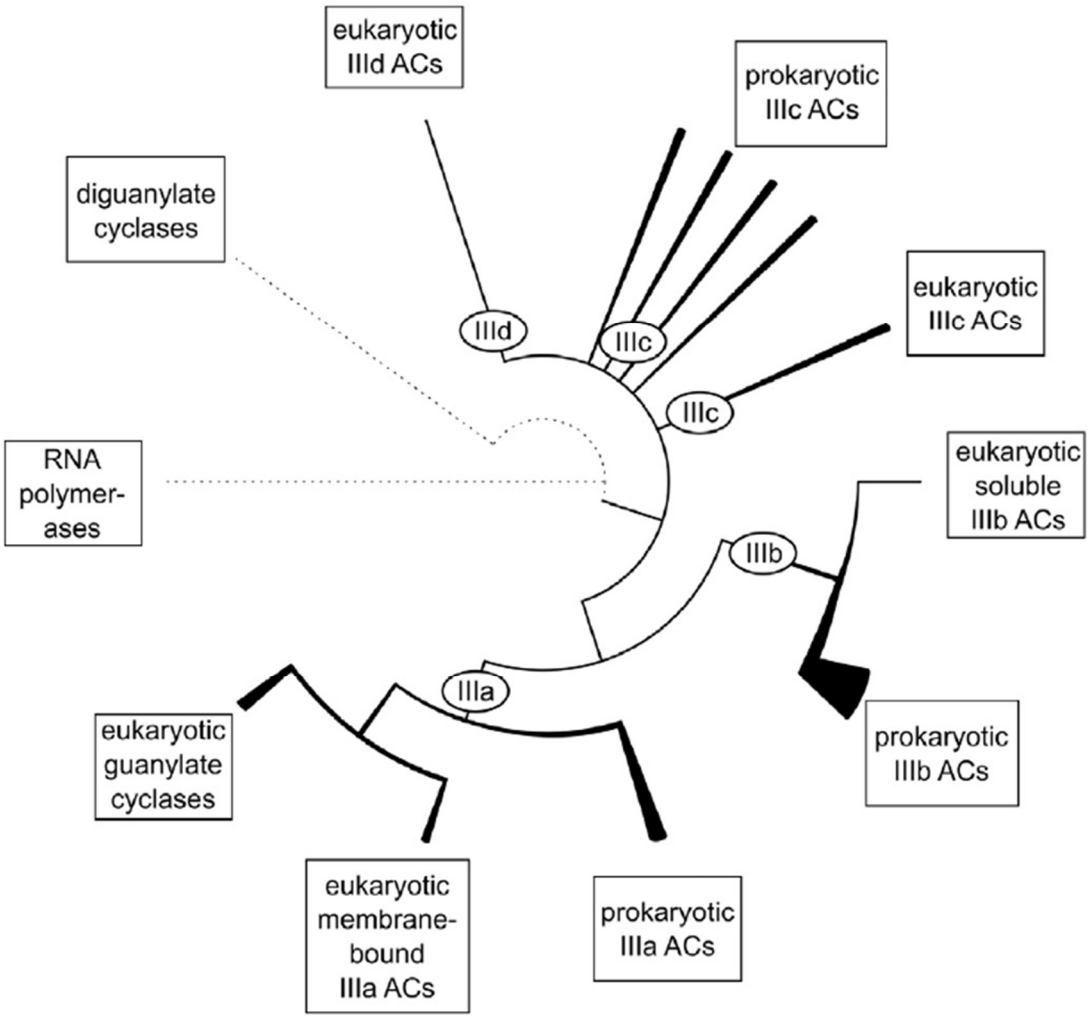

Figure 1. Evolutionary relationship between the catalytic domains of class III ACs.
Dotted lines: remote homology to other protein families. Solid lines: relations between major subgroups. Line thickness indicates diversity of domain architecture within a branch. (from [8])

All class III ACs share a common requirement for dimerization in order to become active. In bacteria, this occurs through homodimerization, where two identical domains come together. In eukaryotes, however, ACs form what is known as a pseudoheterodimer, in which two complementary domains are linked within the same protein [8]. The catalytic mechanism at the core of these enzymes has been well-characterized and confirmed through computational, biochemical, and structural studies [9-11]. Three pairs of residues are essential for the successful conversion of ATP: two aspartate residues that coordinate a divalent metal ion cofactor (Mn^{2+} or Mg^{2+}), which facilitates a nucleophilic inline attack by the ribose's 3'-OH group on the α-phosphoryl group of ATP. An arginine and asparagine residue help stabilize the resulting transition state. Lastly, a lysine and aspartate pair plays a crucial role in distinguishing ATP from GTP as substrates [7].

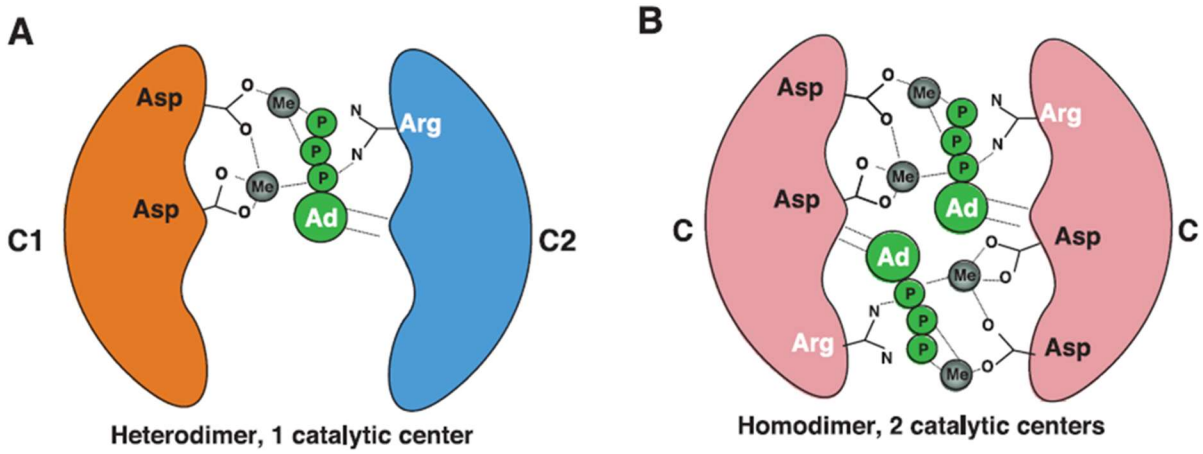

Figure 2. Dimeric structure of class III adenylyl cyclase catalytic domains. Cyclase homology dimers form heterodimers with one catalytic center (A) or homodimers with two catalytic centers (B). Ad: adenosine; P: phosphate group; Me: divalent cation. The transition state stabilizing arginine and the two metal-cofactor coordinating aspartate residues are provided by the opposite catalytic domain. (Figure adapted from [7])

1.4 Mammalian adenylyl cyclases:

ACs catalyze the conversion of ATP into cAMP through a cyclization reaction. The human genome encodes nine membrane-bound AC isoforms and one soluble AC. While the overall structure of membrane-bound ACs (mACs) is similar across isoforms, they vary in sequence and length [12]. These pseudoheterodimeric proteins are composed of a TM domain, which consists of two hexahelical transmembrane subdomains. These are connected to two cytosolic subdomains, C1 and C2, which are further divided into four subdomains (C1a, C1b, C2a, C2b) (figure 3). The catalytic site is formed by the two catalytic subdomains, each providing key residues necessary for ATP binding and stabilizing the transition state during the cyclization process.

The transition state is further stabilized by two divalent cations, either magnesium or manganese, with magnesium being the likely physiological cofactor, while manganese acts as a more potent cofactor [13].

The various mAC isoforms are grouped into four classes based on similarities in their membrane domains [8]. Group I is formed by the isoforms 1, 3, and 8, group II by 2, 4, and 7, group III by 5 and 6, and group IV consists of only isoform 9.

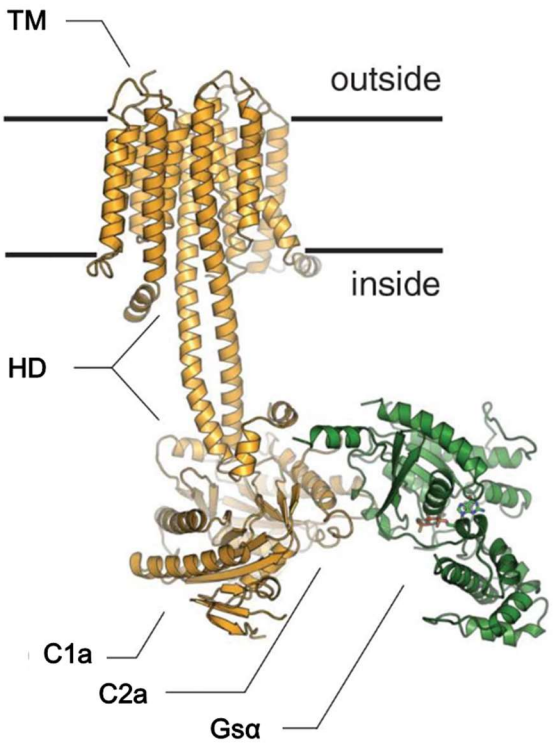

Figure 3. Cryo-EM structure of bovine AC isoform 9 as a model for mammalian AC structures (resolution approximately 3.6 Å).
Depicted structural AC elements: TM: transmembrane domain; HD: helical domain (including the cyclase transducing elements described in [14]); C1a/C2a :subdomains of the two catalytic domains C1/C2. (modified after [15]).

1.5 Transmembrane domains as potential receptors

In 1989, when Krupinski et al. published the first amino acid sequence of an adenylyl cyclase (AC), questions arose regarding the role of the relatively large transmembrane (TM) domain, suggesting it might serve more than just a membrane-anchoring function. In their publication, Krupinski et al. hypothesized that the TM domain might function as an ion channel or transporter [16]. Other proposals included a potential role as a voltage sensor [17] or a factor involved in dimerization [18], though none of these ideas have been confirmed to date.

However, when Tang & Gilman demonstrated the creation of a forskolin- and Gsα-sensitive soluble AC by directly linking the cytosolic domains of AC1 and AC2, effectively omitting the entire TM domain, it led to the prevailing view that the TM domain did not influence enzyme activity and was solely responsible for membrane anchoring [19].

On the other hand, bioinformatic studies have revealed significant variability in the TM domains across all nine human AC isoforms, pointing toward a possible receptor function and different regulatory mechanisms or ligands for each isoform. Remarkably, these TM domains exhibit isoform-specific evolutionary conservation spanning over 0.5 billion years [8, 20]. If the TM domains merely served as membrane anchors, why would such a high degree of conservation persist for so long?

In 2016, Beltz et al. described a chimera comprising the quorum-sensing receptor from *Vibrio harveyi* (CqsS) and the mycobacterial class IIIa AC Rv1625c, which represents one half of the structure of human ACs, featuring a 6-TM domain linked to a cytosolic, catalytic domain. For activity, this chimera requires dimerization, forming a homodimer comparable to the pseudoheterodimeric structure of human ACs [21, 22]. The lipophilic compound (*S*)-3-hydroxy-tridecan-4-one, also known as Cholerae AutoInducer-1, acts as a ligand for CqsS. Cholerae AutoInducer-1 concentration-

dependently increased cAMP production, suggesting that inputs from the TM domain can affect the catalytic domain [22].

To facilitate signal transduction between the TM and catalytic domains, a transducer element is essential. In 2017, Ziegler et al. identified a cyclase transducer element (CTE) in various class IIIa/b ACs, further supporting the potential receptor function of the TM domains[14].

Following the functional characterization of the CqsS-Rv1625c chimera, Seth et al. engineered a chimera of CqsS and mammalian AC2, replacing the two hexahelical TM domains of AC2 with the TM domain of CqsS. Although this chimera was not directly regulated by Cholerae AutoInducer-1, Gsα stimulation was inhibited. Additionally, they found that unidentified compounds in human serum inhibited Gsα activation in various AC isoforms and reduced AC activity in rat brain cortical membranes [23]. Based on these results, they proposed a three-state model of AC regulation via its TM domains (figure 4).

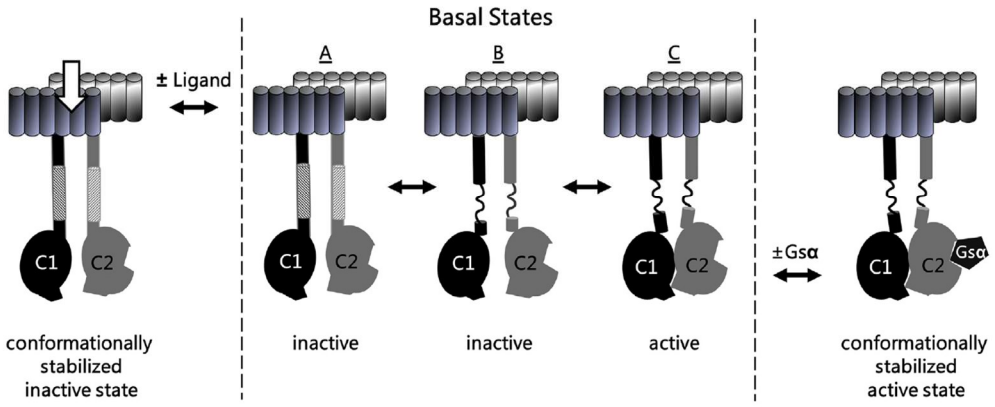

Figure 4. Hypothetical three-state model of AC regulation.
The model shows three basal states of the enzyme present in a thermodynamic equilibrium. A and B represent inactive states while C represents an active state. A and B differ in conformation stability of the catalytic C1/C2 domains. Gsα binding on the cytosolic side leads to a conformationally stabilized active state (right). The potential ligand binding on the other hand leads to a conformationally stabilized inactive state (left) (figure from [23]).

The forthcoming elucidation of AC structures yields more insights on where potential ligand binding sites can be found in TM domains. Cryo-EM structures of human AC isoforms 5, 8, 9 and the mycobacterial AC Rv1625c revealed extracellular cavities at the TM dimers interface, that resemble potential binding sites for potential ligands like small molecules, ions, peptides or lipids [15, 24-26].

2. Objective

The evolutionary conservation, the presence of signal-transducing elements, the ability to transfer receptor properties of quorum-sensing receptors onto ACs, the compounds in serum that affect holoenzyme ACs but not the CqsS-AC chimera, and the identification of potential ligand-binding sites through structural analysis, all suggest an orphan receptor function for the TM domain of ACs. My task was to identify (physiological) ligands that bind directly to the TM domain and regulate the enzyme's activity. The research question was clearly defined, allowing me to stay focused on this main objective without being sidetracked by other, albeit interesting, data. From the outset, it was understood that this project was not solely about analyzing different starting materials and identifying their components, but rather a bioassay-guided identification of potential ligands.

Naturally, some follow-up questions arose alongside the main one:

a) What would be a suitable starting material to use?
b) If ligands are found, are they exclusively inhibitory?
c) Do the ligands bind in an isoform-specific manner?
d) Do they directly regulate ACs, or is the regulation coupled to GPCR/Gsα?
e) Do potential ligands regulate cAMP formation *in vivo*?
f) Do they regulate cAMP formation in mammalian tissues?

3. Results and discussion

3.1. Publication I:

Seth, A., **Landau, M**., Shevchenko, A., Traikov, S., Schultz, A., Elsabbagh, S., Schultz, J. E. (2022). Distinct glycerophospholipids potentiate Gsα-activated adenylyl cyclase activity. *Cellular signalling*, 97,110396. https://doi.org/10.1016/j.cellsig.2022.110396

Position in list of authors: 2 (contributed equally with first author Seth A.)

Personal contributions:

Designed, carried out and analyzed experiments for the data represented in figures 1, 4, 5, 6 and in part for figure 3 in the main manuscript.

Designed, carried out and analyzed experiments for supplementary tables 2, 3 and figure 4. Also contributed data for supplementary figure 3.

Maintained cell culture and harvested membranes for testing.

Revised and edited the manuscript together with all authors.

Estimated contribution: 50%.

Cellular Signalling 97 (2022) 110396

Contents lists available at ScienceDirect

Cellular Signalling

journal homepage: www.elsevier.com/locate/cellsig

Distinct glycerophospholipids potentiate Gsα-activated adenylyl cyclase activity

Anubha Seth [a,1,2], Marius Landau [b,1], Andrej Shevchenko [c], Sofia Traikov [c], Anita Schultz [b], Sherif Elsabbagh [b], Joachim E. Schultz [b,*]

[a] Max-Planck-Institut für Biologie, Tübingen, Germany
[b] Pharmazeutisches Institut der Universität Tübingen, Tübingen, Germany
[c] Max-Planck-Institut für molekulare Zellbiologie und Genetik, Dresden, Germany

ARTICLE INFO

Keywords:
Adenylyl cyclase
Membrane anchor
Receptor
Glycerophospholipids
Phosphatidic acid
Cyclic AMP

ABSTRACT

Nine mammalian adenylyl cyclases (AC) are pseudoheterodimers with two hexahelical membrane domains, which are isoform-specifically conserved. Previously we proposed that these membrane domains are orphan receptors (https://doi.org/10.7554/eLife.13098; https://doi.org/10.1016/j.cellsig.2020.109538). Lipids extracted from fetal bovine serum at pH 1 inhibited several mAC activities. Guided by a lipidomic analysis we tested glycerophospholipids as potential ligands. Contrary to expectations we surprisingly discovered that 1-stearoyl-2-docosahexaenoyl-phosphatidic acid (SDPA) potentiated Gsα-activated activity of human AC isoform 3 seven-fold. The specificity of fatty acyl esters at glycerol positions 1 and 2 was rather stringent. 1-Stearoyl-2-docosahexaenoyl-phosphatidylserine and 1-stearoyl-2-docosahexaenoyl-phosphatidylethanolamine significantly potentiated several Gsα-activated mAC isoforms to different extents. SDPA appears not interact with forskolin activation of AC isoform 3. SDPA enhanced Gsα-activated AC activities in membranes from mouse brain cortex. The action of SDPA was reversible. Unexpectedly, SDPA did not affect cAMP generation in HEK293 cells stimulated by isoproterenol, PGE_2 and adenosine, virtually excluding a role as an extracellular ligand and, instead, suggesting an intracellular role. In summary, we discovered a new dimension of intracellular AC regulation by chemically defined glycerophospholipids.

1. Introduction

cAMP is a universal regulator of numerous cellular processes [7,32,36,38]. Its biosynthesis is via adenylyl cyclases. This report deals with the nine mammalian, membrane-bound pseudoheterodimeric ACs (mACs; reviewed in [2,7,24,32]. Currently, a direct regulation of mACs does not exist. The accepted regulation is indirect and includes *(i)* the extracellular activation of G-protein-coupled receptors, *(ii)* intracellular release of the Gsα subunit from a trimeric G-protein and, *(iii)*, as a last step mAC activation by the free α-subunit [7,30]. Secondarily, calmodulin, Ca^{2+} ions, $G_{\beta\gamma}$ and phosphorylation are cytosolic effectors. In contrast, we recently have assigned a direct regulatory role mediated by the membrane domains of mACs acting as receptors [3,34]. In this proposal, the mAC receptors are comprised of the two hexahelical domains each connected to a cytosolic catalytic domain, C1 and C2, via highly conserved cyclase transducing elements [7,34,46]. These transducing elements, also termed helical domains, are perfectly suited to mediate signal transduction between membrane anchors and the catalytic dimer as shown by the cryo-EM structure of AC9 holoenzyme [27]. The proposal for a receptor function is based on: *(i)* the evolutionary conservation of the membrane anchors in an isoform-specific manner for >0.5 billion years [2], *(ii)* on highly conserved cyclase-transducing-elements [46], and *(iii)* on catalytic domains conserved from cyanobacteria to mammals [2,16,18,34], *(iv)* on a most recent cryo-EM structure of the mycobacterial cyclase Cya at 3.6A resolution in which a potential intramembrane binding pocket for lipophilic compounds was identified (Metha et al. 2022; https://doi.org/10.1101/2021.12.01.470738).

Abbreviations: mAC, membrane-delimited adenylyl cyclase; GPL, glycerophospholipid; SDPA, 1-stearoyl-2-docosahexaenoyl-phosphatidic acid.

* Corresponding author at: Pharmazeutisches Institut der Universität Tübingen, Auf der Morgenstelle 8, 72076 Tübingen, Germany.
E-mail address: joachim.schultz@uni-tuebingen.de (J.E. Schultz).

[1] Both contributed equally.
[2] Present address: Dept. of Pharmacology, Yale University School of Medicine, 333 Cedar Street, New Haven, CT 06520-8066, USA.

https://doi.org/10.1016/j.cellsig.2022.110396
Received 6 June 2022; Received in revised form 27 June 2022; Accepted 28 June 2022
Available online 2 July 2022

Recently we reported ligand-mediated inhibition of a Gsα-activated mAC2 in a chimera in which the AC membrane domains were replaced by the hexahelical quorum-sensing receptor CqsS from *Vibrio* sp. that has a known lipophilic ligand, cholera-auto-inducer-1 [3,22,34]. In an initial approach to identify ligands for the mAC receptors we used fetal bovine serum (FBS) which had been shown to contain inhibitory components [34]. Eliminating peptides or proteins as possible ligands we fractionated lipids by extraction with chloroform/methanol at different pH values [4]. Expecting to isolate inhibitory components we report the most surprising discovery that 1-stearoyl-2-docosahexaenoyl-phosphatidic acid (SDPA) potentiated Gsα-activated mAC3 activity up to 7-fold. The actions of SDPA resemble, to a limited extent, those of the plant diterpene forskolin [7]. The data establish a new layer of direct mAC regulation and emphasize the importance of glycerophospholipids (GPLs) in regulation of intracellular cAMP generation.

2. Materials and methods

2.1. Reagents and materials

The genes of the human AC isoforms 1–9 cloned into the expression plasmid pcDNA3.1+/C-(K)-DYK were purchased from GenScript and contained a C-terminal flag-tag. Creatine kinase was purchased from Sigma, restriction enzymes from New England Biolabs or Roche Molecular. All chemicals were from Avanti Lipids and Sigma-Merck. _ENREF_24The constitutively active GsαQ227L point mutant was expressed and purified as described earlier [8,10,11]. Forskolin was a gift from Hoechst, Frankfurt, Germany. Human serum (catalog # 4522 from human male AB plasma) and fetal bovine serum were from Gibco, Life Technologies, Darmstadt, Germany (catalog #: 10270; lot number: 42Q8269K).

2.2. Plasmid construction and protein expression

ACIC1_ACIIC2 was generated in pQE60 with *NcoI*/*Hin*dIII restrictions sites according to Tang et al. [39]. The construct boundaries were: $MRGSH_6$-HA-hAC1-$C1_{M268-R482}$-AAAGGMPPAAAGGM -hAC2-$C2_{R822-S1091}$. HEK293 cells were maintained in Dulbecco's modified Eagle's medium (DMEM) containing 10% fetal bovine serum at 37 °C with 5% CO2. Transfection of HEK293 cells with single mAC plasmids was with PolyJet (SignaGen, Frederick, MD, USA). Permanent cell lines were generated by selection for 7 days with G418 (600 μg/mL) and maintained with 300 μg/mL G418 [1,6,37].Clonal selection was omitted. For membrane preparation cells were tyrpsinized and collected by centrifugation (3000 ×*g*, 5 min). Cells were lysed and homogenized in 20 mM HEPES, pH 7.5, 1 mM EDTA, 2 mM $MgCl_2$, 1 mM DTT, and one tablet of cOmplete, EDTA-free (for 50 mL), 250 mM sucrose by 20 strokes in a potter homogenizer. Debris was removed by centrifugation for 5 min at 1000 x*g*, membranes were then collected by centrifugation at 100,000 x*g* for 60 min at 0 °C, resuspended and stored at −80 °C in 20 mM MOPS, pH 7.5, 0.5 mM EDTA, 2 mM $MgCl_2$. Expression was checked by Western blotting.

Membrane preparation from mouse brain cortex was according to [33,34]. For each preparation three cerebral cortices were dissected and homogenized in 4.5 mL cold 48 mM Tris-HCl, pH 7.4, 12 mM $MgCl_2$, and 0.1 mM EGTA with a Polytron hand disperser (Kinematica AG, Switzerland). The homogenate was centrifuged for 15 min at 12,000 *g* at 4 °C and the pellet was washed once with 5 mL 1 mM potassium bicarbonate. The final suspension in 2 mL 1 mM $KHCO_3$ was stored in aliquots at −80 °C.

2.3. Adenylyl cyclase assay

AC activities were determined in a volume of 10 μl using 1 mM ATP, 2 mM $MgCl_2$, 3 mM creatine phosphate, 60 μg/mL creatine kinase, 50 mM MOPS, pH 7.5. Ca^{2+}, usually present at low μM concentrations, was not complexed by EGTA. The cAMP assay kit from Cisbio (Codolet, France) was used according to the supplier's instructions. For each assay a cAMP standard curve was established [34]. Lipids were dissolved in 100% ethanol or DMSO at high concentrations and acutely diluted in 20 mM MOPS pH 7.5 at concentrations, which limited organic solvent in the assay at maximally 1%. Up to 2% neither ethanol nor DMSO had any effect on AC activity.

Table 1
Lipid extraction of FBS with chloroform/methanol.

% Gsα activated Adenylyl Cyclase Activity			
	pH 14	pH 6	pH 1
hAC1	99 ± 5	91 ± 5	25 ± 1
hAC2	176 ± 8	158 ± 4	149 ± 9
hAC3	183 ± 40	175 ± 41	31 ± 11
hAC5	98 ± 7	123 ± 12	50 ± 7
hAC6	91 ± 4	89 ± 2	57 ± 4
hAC7	140 ± 6	131 ± 4	79 ± 6
hAC8	192 ± 11	193 ± 7	115 ± 4
hAC9	201 ± 22	251 ± 12	140 ± 12

2 mL FBS were extracted with chloroform/methanol (1:2) according to [4]. The organic phase was evaporated, and the residue was dissolved in 35 μl DMSO. Adenylyl cyclases were activated by 600 nM Gsα and 33 nl of the DMSO extracts were added. Basal AC activities were in the order of the table: 0.11, 0.43, 0.02, 0.4, 0.16, 0.02, 0.33, and 0.04 nmol $cAMP{\cdot}mg^{-1}{\cdot}min^{-1}$, respectively. 600 nM Gsα-activated activities were 0.49, 1.31, 0.36, 2.23, 0.71, 0.25, 3.16 and 1.67 nmol $cAMP{\cdot}mg^{-1}{\cdot}min^{-1}$. $n = 4–12$.

2.4. Lipidomic analysis

Lipids were extracted from MonoQ purified aqueous fractions by methyl-*tert*-butyl ether/methanol as described [21] after adjusting their pH to 1.0 and 6.0, respectively. The collected extracts were dried under vacuum, and re-dissolved in 500 μl of water/acetonitrile 1:1 (*v*/v). Lipids were analyzed by LC-MS/MS on a Xevo G2-S QTof (Waters) mass spectrometer interfaced to Agilent 1200 liquid chromatograph. Lipids were separated on a Cortecs C18 2.7 μm beads; 2.1 mm ID x 100 mm (Waters) using a mobile phase gradient: solvent A: 50% aqueous acetonitrile; solvent B: 25% of acetonitrile in isopropanol; both A and B contained 0.1% formic acid (v/v) and 10 mM ammonium formate. The linear gradient was delivered with flow rate of 300 μl /min in 0 min to 12 min from 20% to 100% B; from 12 min to 17 min maintained at 100% B, and from 17 min to 25 min at 20% B. Mass spectra were acquired within the range of m/z 50 to m/z 1200 at the mass resolution of 20,000 (FWHM). The chromatogram was searched against web-accessible XCMS compound database at https://xcmsonline.scripps.edu/landing_page.php?pgcontent=mainPage. Lipids were quantified using Skyline 21.1.0.278 software using synthetic lipid standards [42] spiked into the analyzed fractions prior lipid extraction.

2.5. Data analysis and statistical analysis

All incubations were in duplicates or triplicates. For easier presentation, data were normalized to respective controls and S.E.M values are indicated. Data analysis was with GraphPad prism 8.1.2 using a two-tailed *t*-test.

3. Results

3.1. Lipids as possible mAC effectors

In exploratory experiments, we extracted lipids from FBS with chloroform/methanol at pH 1, pH 6, and pH 14 [4]. After evaporation of solvent the solid residues were dissolved in DMSO and tested against human mAC isoforms 1, 2, 3, 5, 6, 7, 8, and 9 in membrane preparations from HEK293 cells transfected with the respective ACs (Table 1). The

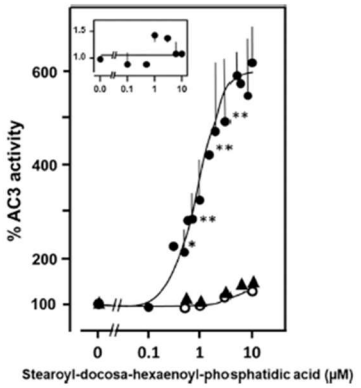

Fig. 1. 1-Stearoyl-2-docosahexaenoyl-phosphatidic acid concentration-dependently potentiates mAC3 activated by 600 nM Gsα (filled circles). 100% Gsα-activated mAC3 activity corresponded to 707 ± 187 pmoles cAMP•mg^{-1}•min^{-1}. Basal mAC3 activity is not significantly affected by SDPA (open circles; 100% basal activity corresponds to 34 pmoles cAMP•mg^{-1}•min^{-1}). Triangles: Effect of SDPA on the C1-C2 soluble AC construct activated by 600 nM Gsα (Basal activity was 12 pmol cAMP•mg^{-1}•min^{-1}. 600 nM Gsα activated activity was 150 pmol cAMP•mg^{-1}•min^{-1} corresponding to 100%). Insert: Activity of the mycobacterial AC Rv1625c is unaffected by SDPA (activity was 23 nmoles cAMP•mg^{-1}•min^{-1}). Data were normalized to respective 100% activities. Significances in a two-tailed *t*-test: *: $p < 0.05$; **: $p < 0.01$ compared to 100% activity. For clarity, not all significances are marked. $N = 4$–6; error bars denote S.E.M.'s.

pH 1 extract inhibited Gsα-activated AC 1, 2, 5, 6, and 7 to different extents. The pH 6 and pH 14 extracts appeared to enhance Gsα-activated AC isoforms 2, 3, 8, and 9 (Table 1).

We then carried out a lipidomic analysis with the pH 1 and the pH 6 fractions [21,42]. Based on previous data we expected ligands which inhibit Gsα-activated mAC activities [34]. Therefore, we concentrated on lipids present in the pH 1 fraction. Apart from several. Based on previous data we expected potential ligands which inhibit Gsα-activated mAC activities and concentrated on lipids present in the pH 1 fraction [34]. Apart from several minor constituents from different lipid classes the major constituents in the acidic fraction were phosphatidic acids, phosphatidylcholine, phosphatidylethanolamine and phosphatidylserines (see Appendix Fig. 1 and 2). Next, we examined the effect of commercially available bulk lipids on Gsα-activated mACs. Egg phosphatidic acids significantly stimulated, whereas other bulk lipids such as egg and liver phosphatidylcholine, brain gangliosides, sulfatides and cerebrosides had no significant effects.

The lipidomic analysis showed that highly unsaturated fatty acids such as arachidonic acid and docosahexaenoic acid are prominent acyl substituents in phosphatidic acids (Appendix Fig. 2). These acyl residues are only minor components in the tested egg or liver phosphatidic acids. Therefore, we assayed commercially available synthetic GPLs containing polyunsaturated fatty acids as acyl substituents. The general structure of glycerophospholipids is shown below (see Appendix Table 1 for a complete list of lipids examined in this study).

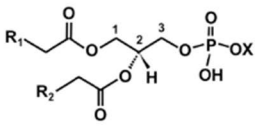

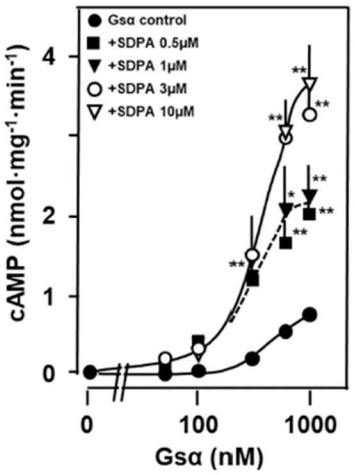

Fig. 2. SDPA increases the affinity of mAC3 for Gsα. The EC_{50} concentration for Gsα in the absence of SDPA was 518 nM and in the presence it was 336 ± 29 nM ($p < 0.02$; $n = 5$–6). Basal AC3 activity was 27 ± 21 pmoles cAMP•mg^{-1}•min^{-1}; 1000 nM Gsα increased mAC3 activity to 791 ± 128 pmoles cAMP•mg^{-1}•min^{-1}). Significances: *: $p < 0.05$; **: $p < 0.01$ compared to corresponding activities without SDPA. n = 5–6; error bars denote S.E.M. Often error bars did not exceed the symbol size.

Basic structure of glycerophospholipids: $R_1$and R_2 are fatty acyl residues esterified at glycerol positions 1 and 2; X can be a proton H^+ as in phosphatidic acid, choline (phosphatidylcholine), serine (phosphatidylserine), glycerol (phosphatidylglycerol), or ethanolamine (phosphatidylethanolamine).

The assays used membranes containing human mAC isoforms expressed in HEK293 cells. The mACs were activated by 600 nM of a constitutively active Gsα (Q227L, here termed Gsα) because we expected to characterize an inhibitory input [11,34]. Most surprisingly, we discovered that 1-stearoyl-2-docosahexaenoyl-phosphatidic acid (SDPA) potentiated mAC3 up to 7-fold above the 16-fold activation already exerted by 600 nM Gsα alone (Fig. 1). The EC_{50} of SDPA was 0.9 μM. In the absence of Gsα 10 μM SDPA had no significant effect (Fig. 1). As far as the synergism between Gsα-activated mAC3 is concerned, the effect of SDPA was reminiscent of the known cooperativity between forskolin and Gsα activated mACs [7].

Does the action of SDPA require a membrane-anchored AC holoenzyme or is the activity of a Gsα-activated C1/C2 catalytic dimer potentiated as well? We produced a soluble active AC construct connecting the catalytic C1 domain of mAC1 and the C2 domain of mAC2 by a flexible linker [39] [39]. The construct was expressed in *E. coli* and purified via its His_6-tag. It was activated 12-fold by Gsα (from 12 to 150 pmol cAMP•mg^{-1}•min^{-1}). SDPA up to 10 μM did not affect basal activity and failed to significantly enhance Gsα-activated activity of the chimera. We tentatively conclude that the SDPA action requires membrane anchoring of mACs.

We investigated whether SDPA affects the activity of a Gsα-insensitive membrane-bound bacterial AC. We used the mycobacterial AC Rv1625c, a monomeric progenitor of mammalian mACs, which has a hexahelical membrane domain and is active as a dimer [12] [12]. The activity of the Rv1625c holoenzyme was unaffected by SDPA (Fig. 1 insert). The particular intrinsic properties of the mammalian membrane domains in conjunction with Gsα-activation may be required to confer SDPA sensitivity.

Next, we examined which kinetic parameters are affected by SDPA.

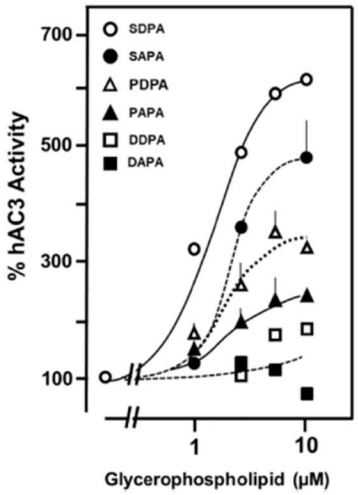

Fig. 3. Specificity of fatty acyl esters in phosphatidic acids for potentiation of Gsα-activated mAC3. 600 nM Gsα-activated activity (100%) was 446 pmol cAMP•mg^{-1}•min^{-1} (basal mAC3 activity was 15.2 pmol cAMP•mg^{-1}•min^{-1}). Abbreviations: SAPA, 1-stearoyl-2-arachidonoyl-phosphatidic acid; PDPA, 1-palmitoyl-2-docosahexaenoyl-phosphatidic acid; PAPA, 1-palmitoyl-2-arachidonoyl-phosphatidic acid; DDPA, di-docosahexaenoyl-phosphatidic acid; DAPA, di-arachidonoyl-phosphatidic acid. The EC_{50} concentrations were 4.8, 1.3, and 1.4 μM, for SAPA, PDPA, and DDPA, respectively (differences not significant; $n = 3$). Error bars denote S.E.M. For comparison, a curve presenting SDPA is included.

For mAC3, the enzymatic reaction rates ± SDPA were linear with respect to protein concentration and time up to 30 min. The Km for substrate ATP (0.1 mM) was unaffected. The most striking effect of SDPA was the increase in Vmax (from 4 to 8 nmol cAMP•mg^{-1}•min^{-1}). Concentration-response curves for Gsα in the presence of different SDPA concentrations showed that the affinity of mAC3 for Gsα was significantly increased (Fig. 2). Most likely, Gsα and SDPA act at distinct sites of the protein and potentiation by SDPA is due to concerted structural interactions, reminiscent of the cooperativity between Gsα and forskolin [7].

3.2. Specificity of 1- and 2-acyl substituents in phosphatidic acid

Phosphatidic acid is the simplest GPL consisting of a glycerol backbone to which two fatty acids and phosphoric acid are esterified. At physiological pH it carries about 1.5 negative charges. Generally, at positions 1 and 2 of glycerol a variety of fatty acyl residues haves been identified. We examined the biochemical specificity of the fatty acyl substituents in phosphatidic acid (Fig. 3).

10 μM 1-Stearoyl-2-arachidonoyl-phosphatidic acid (SAPA) potentiated Gsα-activated mAC3 about 5-fold (EC_{50} = 4.8 μM; Fig. 3). Exchanging the stearic acid at position 1 by a palmitic acid, i.e. 1-palmitoyl-2-docosahexaenoyl-phosphatidic acid (PDPA) reduced activity by about 50% compared to SDPA (EC_{50} = 1.3 μM). Strikingly, the corresponding 1-palmitoyl-2-arachidonoyl-phosphatidic acid (PAPA) lost about 70% of activity compared to SDPA (Fig. 3), highlighting the structural contribution of the 1-fatty acyl substituent to biochemical activity. The importance of the substituent at position 1 was further emphasized when assaying 1, 2-di-docosahexaenoyl-phosphatidic acid (DDPA). The efficiency was reduced by 80% compared to SDPA (Fig. 3). The EC_{50} for DDPA was 1.4 μM. Even more drastic was the absence of an effect using 1, 2-di-arachidonoyl-phosphatidic acid (DAPA; Fig. 3). Expectedly then, 1-stearoyl-2-linoleoyl-phosphatidic acid was inactive (not shown). The data show a remarkable positional specificity for the 1- and 2-acyl substituents of the glycerol backbone and indicate a specific and concerted interaction between the fatty acyl esters. The specificity of fatty acyl-substitution also strongly indicated that SDPA is not acting in its property as a general membrane GPL because other phosphatidic acids should be equally suitable as membrane lipids. Further, the peculiar biochemical properties of SDPA in its relation with AC isoforms suggest that the negative charges of phosphatidic acid are not sufficient to determine specificity, but that the lipid substitutions on position 1- as well as 2- probably are equally important.

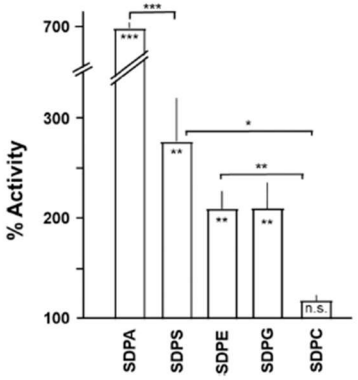

Fig. 4. Head group specificity of glycerophospholipids enhancing Gsα-activated mAC3 activity. Basal mAC3 activity was 0.03. Gsα-stimulated activity was 0.56 nmol cAMP•mg^{-1}•min^{-1} (corresponding to 100%). Concentration of lipids was 10 μM. Error bars denote S.E.M. Significances: *: $p < 0.05$; **: $p < 0.01$; ***: $p < 0.001$; $n = 3$–9.

3.3. Head group specificity of glycerophospholipids

The next question is whether 1-stearoyl-2-docosahexaenoyl-GPLs with different head groups might affect Gsα-activated mAC3. First, we replaced the phosphate head group in SDPA by phosphoserine generating SDPS. This greatly reduced potentiation of Gsα-activated mAC3 activity (2.8-fold potentiation; Fig. 4). A concentration-response curve of SDPS with mAC3 showed that the EC_{50} concentration was similar to that of SDPA (1.2 vs 0.9 μM; $n = 6$–9; n.s.), but its efficacy is significantly lower suggesting that identical binding sites are involved.

We further used 1-stearoyl-2-docosahexaenoyl-ethanolamine (SDPE), 1-stearoyl-2-docosahexaenoyl-phosphatidylglycerol (SDPG) and 1-stearoyl-2-docosahexaenoyl-phosphatidylcholine (SDPC; Fig. 4). In this order, efficacy to enhance the Gsα-activated mAC3 declined, with SDPC having no significant effect (Fig. 4). The surprising specificity of the 1- and 2-fatty acyl-substituents of the glycerol backbone was emphasized once again when we used 1-stearoyl-2-arachidonoyl-phosphatidyl-ethanolamine (SAPE) and 1-stearoyl-2-arachidonoyl-phosphatidylcholine. In both instances biochemical activity was lost (not shown). Consequently, we did not further probe GPLs with differing fatty acyl combinations at the glycerol 1- and 2-positions because, as demonstrated, changes in acyl substitutions resulted in considerable reduction or loss of biological activity (see Fig. 3).

3.4. Effect of glycerophospholipids on Gsα-activated adenylyl cyclase isoforms

So far, we examined only the mAC3 isoform that showed a

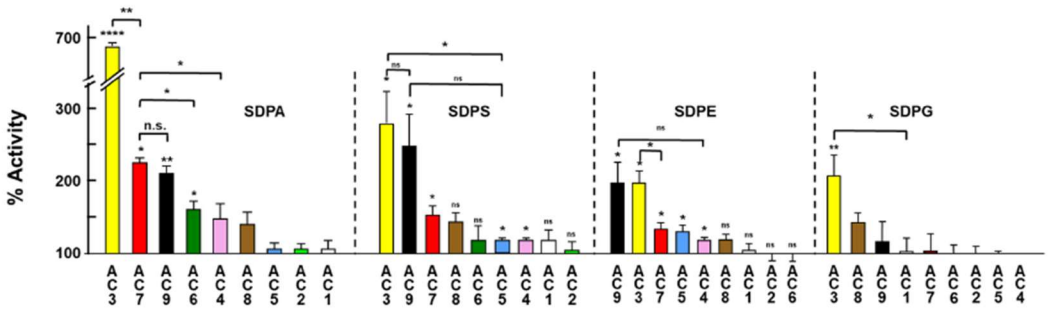

Fig. 5. Effect of 10 μM of glycerophospholipids on various mAC isoforms activated by 600 nM Gsα. Basal activities and Gsα-activated activities are listed in Appendix Table 2). Error bars denote S.E.M. Significances: *: $p < 0.05$; **: $p < 0.01$; ***: $p < 0.001$; ****: $p < 0.0001$ compared to Gsα-activated activity (set at 100%). n = 3–9.

particularly high synergism between Gsα and SDPA. Does SDPA equally potentiate the Gsα-activated activities of the other mAC isoforms? More generally, do GPLs display an mAC isoform specificity in the regulation of intracellular cAMP biosynthesis? We expressed the nine human mAC isoforms in HEK293 and, first, tested how SDPA affected the Gsα-activated activities (Fig. 5).

Under identical experimental conditions 10 μM SDPA significantly potentiated mAC7 (2.4-fold), mAC9 (2.1-fold) and mAC6 activities (1.5-fold). Concentration-response curves were carried for mACs 1, 2, 6, 7 and 9 (Appendix Fig. 3). The EC_{50} concentrations of SDPA for mAC6, 7 and 9 were 0.7 μM, i.e. not significantly different from suggesting equal binding affinities. The other Gsα-activated mAC isoforms were not significantly affected (Fig. 5 and Appendix Fig. 3). In summary, the data demonstrated that the mAC isoform specificity of SDPA was not absolutely stringent. The data then pose the question whether other GPLs may exert similar effects on mAC activities or display a different panel of isoform specificity. This was investigated using four more stearoyl-2-docosahexaenoyl-GPLs (Fig. 5). 10 μM SDPS potentiated mAC3 and mAC9. Smaller, yet significant effects were measured with mACs 7, 8, 5, and 6 (Fig. 5). 10 μM SDPE significantly potentiated Gsα-activated mAC isoforms 9, 3, 7, 5, and 4 (in this order). 10 μM SDPG significantly enhanced only mAC3 activity (Fig. 5). Compared to the seven-fold effect of SDPA on mAC3 these effects were small, yet, in mammalian biology such enhancements in mAC activity may well have profound physiological consequences. Up to 20 μM SDPC which is a major constituent of the outer leaflet of membranes had no effect on any mAC isoform (not shown). Taken together, the data then demonstrate the capacity of chemically defined GPLs to enhance or potentiate the activation of Gsα-activated mACs. We can virtually exclude coincidental and unspecific effects of the amphiphilic phospholipids because mAC isoforms were affected differentially. The results strongly suggest that a defined conformational space must exist at mACs that allows specific interactions with GPLs. Presently, the molecular details of the binding mode remain unknown.

3.5. Relationship between SDPA and forskolin

SDPA failed to activate basal mAC3 activity and only potentiates Gsα-activated mAC3 activity (Fig. 1). The plant diterpene forskolin stimulates basal as well as Gsα-activated mAC activities [7,41,44], i.e. the effects of SDPA and forskolin are only partly similar. Forskolin stimulates mACs expressed in Sf9 cells to rather different extents and with discrepant potencies, e.g. the EC_{50} concentrations for AC1 (0.7 μM) and AC2 (8.7 μM) differ >12-fold [25]. We established forskolin concentration-response curves for all mAC isoforms expressed in HEK293 cells under identical experimental conditions using Mg^{2+} as divalent cation, a comprehensive study which is lacking so far

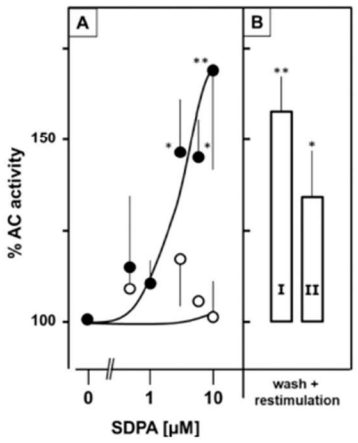

Fig. 6. 1-Stearoyl-2-docosahexaenoyl-phosphatidic acid (SDPA) concentration-dependently potentiates Gsα activated adenylyl cyclase activity in brain cortical membranes from mouse. (A) 600 nM Gsα was used to activate mACs in cortical membranes (solid circles: 100% Gsα-activated activity is 7.9 ± 1.9 nmol $cAMP \bullet mg^{-1} \bullet min^{-1}$); open circles: basal activity (in absence of Gsα) is 0.3 ± 0.2 nmol $cAMP \bullet mg^{-1} \bullet min^{-1}$. $n = 6$. (B) Reversibility of SDPA action. Cortical brain membranes were incubated for 15 min without (I) and with (II) 10 μM SDPA. Membranes were then collected by centrifugation, and re-assayed +600 nM Gsα and 10 μM SDPA. Error bars denote S.E.M., *: $p < 0.05$; **: $p < 0.01$ (n = 6).

(Appendix Fig. 4).

Stimulations at 1 mM forskolin were between 3-fold for mAC1 and remarkable 42-fold for mAC3. The EC_{50} concentrations ranged from 2 μM (mAC1) to 512 μM forskolin (mAC7; Appendix Fig. 4). We also observed forskolin activation of mAC9 although the current consensus regarding this isoform is that it is forskolin insensitive. The latter conclusion is based on experiments with mAC9 expressed in insect Sf9 cells using Mn^{2+} as a cation [7]. Another report described a 2.3-fold forskolin activation of mAC9 when expressed in CMT cells [26], in line with our data (6-fold activation; appendix Fig. 4). We examined potential interactions between forskolin and SDPA using mAC3 activated by 600 nM Gsα. Up to 10 μM, SDPA did not significantly affect forskolin stimulation. We reason that the absence of interactions or cooperativity between forskolin and SDPA suggests that both agents affect mAC regions which exclude mutual cooperative interactions.

Nevertheless, considering the structural dissimilarity of forskolin and SDPA and the obvious lack of a molecular fit an identical binding site for both lipophilic agents is rather unlikely. On the other hand, both agents do interact with distantly binding Gsα in a cooperative manner.

3.6. SDPA enhances Gsα-stimulated cAMP formation in mouse brain cortical membranes

Above we tested GPLs with individual mAC isoforms. Next, we asked whether SDPA would potentiate mAC activity in membranes isolated from mouse brain. In mouse brain cortex all mAC isoforms except for mAC4 are expressed [20,31]. We expected to measure at least some potentiation of the Gsα-activated AC activity by SDPA. The basal AC activity in cortical membranes of 0.3 nmoles $cAMP{\cdot}mg^{-1}{\cdot}min^{-1}$ was unaffected by 10 μM SDPA (Fig. 6A). 600 nM Gsα stimulated AC activity 20-fold (7.9 nmoles $cAMP{\cdot}mg^{-1}{\cdot}min^{-1}$) and this was further enhanced 1.7-fold by 10 μM SDPA (13.4 nmoles $cAMP{\cdot}mg^{-1}{\cdot}min^{-1}$). An SDPA concentration-response curve yielded an EC_{50} of 1.2 μM, i.e. similar to those established in HEK293-expressed mAC isoforms (Fig. 6A; compare to Fig. 1 and Appendix Fig. 3). This demonstrated that the SDPA effect on mAC activities was not due to peculiar membrane properties of the HEK293 cells and supported the suggestion that the effects of GPLs may be of physiologically important.

Next, we asked whether SDPA acts directly via a membrane-receptor domain of hAC3 or is a cytosolic effector. We used HEK293 cells transfected with hAC3. 2.5 μM isoproterenol increased cAMP levels from 0.06 to 0.24 pmol/10^4 cells within 45 min (6-fold). 10 μM SDPA did not affect isoproterenol stimulation. Addition of SDPA did not enhance intracellular cAMP generation (see Appendix Table 3). These unequivocal data virtually excluded that SDPA acted via extracellular binding sites (receptors) or via an efficient and rapid uptake system. In fact, although SDPA is a GPL, it is unlikely that it can pass into intact cells. First, the negatively charged headgroup of SDPA is dissociated at the pH of incubations. Second, SDPA might slide into the outer leaflet of the membrane, but it would require a flippase for incorporation into the inner leaflet and potential release into the cytosol. Considering the negative surface charge of the inner leaflet due to the predominance of phosphatidylserine we consider this as unlikely. Third, we did not observe significant incorporation of SDPA into brain cortical membranes (see below). Thus, the data tentatively suggest a cytosolic site for the action of GPLs.

3.7. Is SDPA a ligand?

GPLs are common building blocks of cell membranes. Major constituents of the inner leaflet are phosphatidylserines and phosphatidylethanolamines, whereas the outer leaflet contains predominantly phosphatidylcholine and sphingomyelin. In many tissues docosahexaenoic acid is a major substituent in membrane GPLs [14]. Phosphatidic acids are indispensable, yet minor membrane components [17]. The SDPA potentiation of Gsα-activated mAC3 could be due to a lack of SDPA. Added SDPA might be incorporated into the membrane close to mACs resulting in a reordering of mAC domains. Alternatively, SDPA may transiently bind to the cyclase. Under these latter circumstances the SDPA effect should be reversible. We attempted to dissect these possibilities. We incubated brain cortical membranes for 15 min at 37 °C with 10 μM SDPA. The membranes were then collected at 100,000 g and washed once. The membranes were susceptible to Gsα stimulation and potentiation by SDPA like naïve membranes (Fig. 6B). Furthermore, the supernatant of a 50 μM SDPA preincubation potentiated the Gsα activation in naïve membranes, i.e., SDPA was not significantly incorporated into the membrane preparation. This supports the notion that SDPA, and most likely other GPLs, serve as intracellular effectors for mACs.

4. Discussion

Our results were contrary to the hypothesis at the outset because we expected to find an mAC inhibitory input. Most surprisingly we identified SDPA and other GPLs as positive effectors of mAC activities. Obviously, we have discovered a new system of intracellular mAC regulation. At this state our findings open more questions than can be answered with this initial report.

We used non-clonal HEK293 cells permanently transfected with mACs. HEK293 cells express considerable endogenous AC3 and 6 activities [37]. These endogenous mAC activities appear to be negligible in this context. First, upon transfection of mAC isoforms we observed very different basal AC activities virtually excluding that 'contaminating' endogenous AC activities affected our results (see Appendix Table 2 for a list of basal activities in transfected HEK293 cells). Second, we tested HEK293 cells in which mACs 3 and 6 were knocked out [37]. Upon mAC3 transfection SDPA similarly potentiated Gsα-activated mAC3 activity. Because these engineered cells proliferated rather slowly they were not used routinely.

Diacylglycerols' and PA are lipid second messengers that regulate physiological and pathological processes, e.g. phosphatidic acids were reported to effect ion channel regulation and SDPA to act on the serotonin transporter in the brain [19,29,35]. So far, the specificity of fatty acyl residues and head groups in these lipids was not explored. Here, we observed a striking exclusivity of fatty-acyl esters at positions 1- and 2- of the glycerol backbone supporting a specific effector-mAC interaction. Usually, fatty acyl substitutions are regulated because they impart specific biophysical and biochemical properties [14]. We demonstrated that the combined fatty acyl ligands 1-stearoyl-2-docosahexaenoyl are more or less exclusive for the actions of SDPA. Even seemingly minor changes caused substantial changes in activity and efficacy, e.g., a change from stearoyl to palmitoyl at glycerol position 1 (Fig. 3). This argues for a specific steric interaction between the flexible stearoyl- and docosahexaenoyl carbon-chains. Acyl chain substitutions might then impair specific protein-ligand interactions, e.g. by a shrinkage of the binding surface. Apparently, such interactions are substantially diminished when only one of the two acyl residues is altered. Notably, didocosahexaenoyl- and di-arachidonoyl-phosphatidic acids (DDPA and DAPA) had mostly lost the capability to promote AC3 activity (Fig. 3). A particularly interesting point is the preference for 2-docosahexaenoyl acylation in the GPLs. Docosahexaenoic acid is an essential omega-3 fatty acid that cannot be synthesized at adequate quantities in infants or seniors [28]. Therefore it is widely sold as a nutraceutical and should be included into a balanced diet. Docosahexaenoic acid is particularly abundant in membrane lipids in the retina (about 60% of all lipids contain docosahexaenoic acid), testes, brain, heart and skeletal muscle [14]. A sodium-dependent symporter for uptake of this fatty acid, packaged as a lysophosphatidic acid, has been characterized and its structure was elucidated by cryo-EM [5,23,43]. Docosahexaenoic acid is needed for normal brain development and cognitive functions, a role in depression, aging and Alzheimer's disease is discussed [9,13,14,23,45]. So far, mACs have not yet been noticed in metabolic disturbances caused by a lack of docosahexaenoic acid. The data presented here provides evidence that docosahexaenoic acid is involved in stimulating the cAMP generating system.

Examination of head group specificity displayed different patterns of mAC susceptibility and activity (Fig. 5). Notably, mAC isoforms 1 and 2 were not significantly affected by any of the GPLs assayed. This may be due to a general insensitivity for GPLs or that we did not identify the suitable bioactive GPLs. We did not examine the specificity of acyl substitution at the glycerol backbone in SDPS, SDPE, SDPG and SDPC because of the specificity of the stearic/docosahexaenoic acid couple in SDPA. We tested 1-stearoyl-2-arachidonoyl-phosphatidyl choline and the corresponding phosphatidyl-ethanolamine. Biological activity was absent with mACs 3, 5, 7, and 9, bolstering the assertion that fatty acyl specificity is stringent in these GPLs as well. Presently we cannot

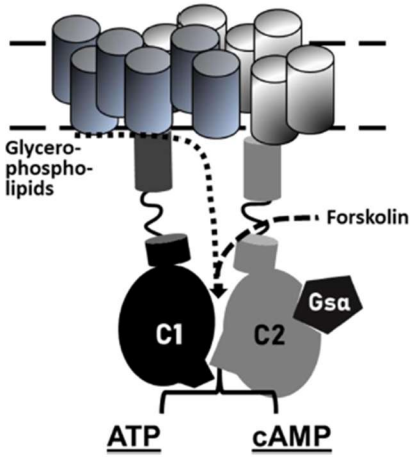

Fig. 7. Tentative scheme of a 2X6TM-adenylyl cyclase with regulatory input from Gsα, binding to the C2 catalytic domain, forskolin, binding to a degenerated second substrate-binding site [12,40], and glycerophospholipids, here proposed to enter and bind at the membrane anchor-receptor and extending towards the catalytic dimer.

completely exclude that GPLs acylated by different couples of acid substituents at the 1- and 2-positions might possess equal or better effector properties. In view of the large variety of GPLs this cannot be tested with a reasonable effort. Currently, we consider such a possibility as remote. We do not know how GPLs mechanistically potentiate AC activity in a synergistic interaction together with Gsα. The tentative scheme in Fig. 7 is intended to illustrate an approximation of potential interaction sites in relation to Gsα and forskolin. The precise nature of such interactions requires structural details (in progress).

Another question which is not answered in this study concerns the intracellular origin of GPLs, how their biosynthesis and release is regulated and tied into the cAMP regulatory system. Despite being water insoluble, an efficient traffic of phospholipids in cells exists, e.g. between locations of uptake and biosynthesis, to and from low-density-, high-density- and very low density lipoproteins, and the diversity of membrane-enclosed organelles such as mitochondria, nucleus, endoplasmic reticulum, endosomes, lysosomes, and the plasma membrane itself. Thus, lipid trafficking is a continuous cellular process connected to diverse signaling systems [14,35]. Part of the biosynthetic pathways for phosphatidic acid is the hydrolysis of GPLs with choline, ethanolamine or serine as headgroups by phospholipase D which generates phosphatidic acids [15]. Chemically, GPLs are excellently suited to serve as mAC effectors because termination of SDPA signaling is easily accomplished by phospholipase C. The relationship between SDPA and forskolin is debatable. The agents do not cooperatively interact at mAC proteins. Certainly, the structural changes caused by either agent promote the interactions between AC and Gsα. Yet this is no proof that such changes are identical or even similar.

A critical observation was the potentiation by SDPA of Gsα-activated mAC activity in mouse brain cortical membranes. mAC3 has been reported to be abundantly expressed in brain [20,31]. The efficacy of SDPA was comparable to that determined in mAC3-HEK293 membranes. This demonstrated that the effect of GPLs observed in HEK293 expressed AC isoforms is of physiological significance. Our approach has then discovered intracellular processes, which in conjunction with the established canonical GPCR/Gsα-regulation of mACs add a new dimension of mAC regulation. Currently, we cannot exclude the possibility that other GPLs exist which have an inhibitory input. Actually, thermodynamic considerations would argue in favor of such a possibility. Whether this is realized as a biological mechanism remains an open possibility. Presently, many important questions remain unanswered, such as how are intracellular GPL levels regulated, which of the intracellular GPLs have access to the membrane delimited ACs, are GPL concentrations persistently or acutely adjusted in a cell, e.g., by stress, diet, diurnal, or seasonal effects or by peculiar disease states? In other word, are we dealing with a long-term regulation of the Gsα-sensitivity of the cAMP generating system or with coordinated short term signaling events? Answering these medically relevant questions remains a formidable challenge in the future.

Credit author statement

Anubha Seth, Marius Landau, Anita Schultz, Sheif Elsabagh: Investigation. Andrej Shevchenko and Sofia Traikov: Methodology; Joachim E. Schultz: Conceptualization, Formal analysis, Funding acquisition, supervision, Writing - original draft.

Declaration of Competing Interest

None.

Acknowledgements

We thank U. Kurz for a continuous supply of Gsα (Q227L), Dr. V. Watts, for suppling us with HEK293ΔmAC3ΔmAC6 cells, and Prof. Dr. A. Lupas for continuous encouragement. We gratefully acknowledge constructive suggestions from Dr. J. Linder. Supported by the Deutsche Forschungsgemeinschaft and institutional funds from the Max-Planck-Society.

Appendix A. Supplementary data

Supplementary data to this article can be found online at https://doi.org/10.1016/j.cellsig.2022.110396.

References

[1] T.A. Baldwin, Y. Li, C.S. Brand, V.J. Watts, C.W. Dessauer, Insights into the regulatory properties of human adenylyl cyclase type 9, Mol. Pharmacol. 95 (2019) 349–360.
[2] J. Bassler, J.E. Schultz, A.N. Lupas, Adenylate cyclases: receivers, transducers, and generators of signals, Cell. Signal. 46 (2018) 135–144.
[3] S. Beltz, J. Bassler, J.E. Schultz, Regulation by the quorum sensor from Vibrio indicates a receptor function for the membrane anchors of adenylate cyclases, Elife (2016) 5.
[4] E.G. Bligh, W.J. Dyer, A rapid method of total lipid extraction and purification, Can. J. Biochem. Physiol. 37 (1959) 911–917.
[5] R.J. Cater, G.L. Chua, S.K. Erramilli, J.E. Keener, B.C. Choy, P. Tokarz, C.F. Chin, D. Q.Y. Quek, B. Kloss, J.G. Pepe, et al., Structural basis of omega-3 fatty acid transport across the blood-brain barrier, Nature 595 (2021) 315–319.
[6] M.G. Cumbay, V.J. Watts, Novel regulatory properties of human type 9 adenylate cyclase, J. Pharmacol. Exp. Ther. 310 (2004) 108–115.
[7] C.W. Dessauer, V.J. Watts, R.S. Ostrom, M. Conti, S. Dove, R. Seifert, International union of basic and clinical pharmacology. CI. Structures and small molecule modulators of mammalian adenylyl Cyclases, Pharmacol. Rev. 69 (2017) 93–139.
[8] S. Diel, K. Klass, B. Wittig, C. Kleuss, Gbetagamma activation site in adenylyl cyclase type II. Adenylyl cyclase type III is inhibited by Gbetagamma, J. Biol. Chem. 281 (2006) 288–294.
[9] J. Duan, Y. Song, X. Zhang, C. Wang, Effect of omega-3 polyunsaturated fatty acids-derived bioactive lipids on metabolic disorders, Front. Physiol. 12 (2021), 646491.
[10] M.P. Graziano, M. Freissmuth, A.G. Gilman, Expression of Gs alpha in Escherichia coli. Purification and properties of two forms of the protein, J. Biol. Chem. 264 (1989) 409–418.
[11] M.P. Graziano, M. Freissmuth, A.G. Gilman, Purification of recombinant Gs alpha, Methods Enzymol. 195 (1991) 192–202.
[12] Y.L. Guo, T. Seebacher, U. Kurz, J.U. Linder, J.E. Schultz, Adenylyl cyclase Rv1625c of Mycobacterium tuberculosis: a progenitor of mammalian adenylyl cyclases, EMBO J. 20 (2001) 3667–3675.
[13] D. Heras-Sandoval, J. Pedraza-Chaverri, J.M. Perez-Rojas, Role of docosahexaenoic acid in the modulation of glial cells in Alzheimer's disease, J. Neuroinflammation 13 (2016) 61.

[14] D. Hishikawa, W.J. Valentine, Y. Iizuka-Hishikawa, H. Shindou, T. Shimizu, Metabolism and functions of docosahexaenoic acid-containing membrane glycerophospholipids, FEBS Lett. 591 (2017) 2730–2744.
[15] J.H. Jang, C.S. Lee, D. Hwang, S.H. Ryu, Understanding of the roles of phospholipase D and phosphatidic acid through their binding partners, Prog. Lipid Res. 51 (2012) 71–81.
[16] T. Kanacher, A. Schultz, J.U. Linder, J.E. Schultz, A GAF-domain-regulated adenylyl cyclase from Anabaena is a self-activating cAMP switch, EMBO J. 21 (2002) 3672–3680.
[17] E.E. Kooijman, K.N. Burger, Biophysics and function of phosphatidic acid: a molecular perspective, Biochim. Biophys. Acta 1791 (2009) 881–888.
[18] J.U. Linder, J.E. Schultz, The class III adenylyl cyclases: multi-purpose signalling modules, Cell. Signal. 15 (2003) 1081–1089.
[19] Q. Lu, C. Murakami, Y. Murakami, F. Hochino, M. Asami, T. Uzuki, H. Sakai, F. Sakane, 1-Stearoyl-2-docosahexaenoyl-phosphatidic acid interacts with and activates Praja-1, the E3 ubiquitin ligase acting on the serotonin transporter in the brain, FEBS Lett. 594 (2020) 1787–1796.
[20] M.G. Ludwig, K. Seuwen, Characterization of the human adenylyl cyclase gene family: cDNA, gene structure, and tissue distribution of the nine isoforms, J. Recept. Signal Transduct. Res. 22 (2002) 79–110.
[21] V. Matyash, G. Liebisch, T.V. Kurzchalia, A. Shevchenko, D. Schwudke, Lipid extraction by methyl-tert-butyl ether for high-throughput lipidomics, J. Lipid Res. 49 (2008) 1137–1146.
[22] W.L. Ng, Y. Wei, L.J. Perez, J. Cong, T. Long, M. Koch, M.F. Semmelhack, N. S. Wingreen, B.L. Bassler, Probing bacterial transmembrane histidine kinase receptor-ligand interactions with natural and synthetic molecules, Proc. Natl. Acad. Sci. U. S. A. 107 (2010) 5575–5580.
[23] L.N. Nguyen, D. Ma, G. Shui, P. Wong, A. Cazenave-Gassiot, X. Zhang, M.R. Wenk, E.L. Goh, D.L. Silver, Mfsd2a is a transporter for the essential omega-3 fatty acid docosahexaenoic acid, Nature 509 (2014) 503–506.
[24] K.F. Ostrom, J.E. LaVigne, T.F. Brust, R. Seifert, C.W. Dessauer, V.J. Watts, R. S. Ostrom, Physiological roles of mammalian transmembrane adenylyl cyclase isoforms, Physiol. Rev. 102 (2022) 815–857.
[25] C. Pinto, D. Papa, M. Hubner, T.C. Mou, G.H. Lushington, R. Seifert, Activation and inhibition of adenylyl cyclase isoforms by forskolin analogs, J. Pharmacol. Exp. Ther. 325 (2008) 27–36.
[26] R.T. Premont, I. Matsuoka, M.G. Mattei, Y. Pouille, N. Defer, J. Hanoune, Identification and characterization of a widely expressed form of adenylyl cyclase, J. Biol. Chem. 271 (1996) 13900–13907.
[27] C. Qi, S. Sorrentino, O. Medalia, V.M. Korkhov, The structure of a membrane adenylyl cyclase bound to an activated stimulatory G protein, Science 364 (2019) 389–394.
[28] X. Qiu, Biosynthesis of docosahexaenoic acid (DHA, 22:6-4, 7,10,13,16,19): two distinct pathways, Prostaglandins Leukot. Essent. Fat. Acids 68 (2003) 181–186.
[29] C.V. Robinson, T. Rohacs, S.B. Hansen, Tools for understanding nanoscale lipid regulation of ion channels, Trends Biochem. Sci. 44 (2019) 795–806.
[30] R. Sadana, C.W. Dessauer, Physiological roles for G protein-regulated adenylyl cyclase isoforms: insights from knockout and overexpression studies, Neurosignals 17 (2009) 5–22.
[31] C. Sanabra, G. Mengod, Neuroanatomical distribution and neurochemical characterization of cells expressing adenylyl cyclase isoforms in mouse and rat brain, J. Chem. Neuroanat. 41 (2011) 43–54.
[32] J.E. Schultz, J. Natarajan, Regulated unfolding: a basic principle of intraprotein signaling in modular proteins, Trends Biochem. Sci. 38 (2013) 538–545.
[33] J.E. Schultz, B.H. Schmidt, Treatment of rats with thyrotropin (TSH) reduces the adrenoceptor sensitivity of adenylate cyclase from cerebral cortex, Neurochem. Int. 10 (1987) 173–178.
[34] A. Seth, M. Finkbeiner, J. Grischin, Schultz JE (2020) Gsalpha stimulation of mammalian adenylate cyclases regulated by their hexahelical membrane anchors, Cell. Signal. 68 (2020), 109538.
[35] J.J. Shin, C.J. Loewen, Putting the pH into phosphatidic acid signaling, BMC Biol. 9 (2011) 85.
[36] S.C. Sinha, S.R. Sprang, Structures, mechanism, regulation and evolution of class III nucleotidyl cyclases, Rev. Physiol. Biochem. Pharmacol. 157 (2006) 105–140.
[37] M. Soto-Velasquez, M.P. Hayes, A. Alpsoy, E.C. Dykhuizen, V.J. Watts, A novel CRISPR/Cas9-based cellular model to explore adenylyl cyclase and cAMP signaling, Mol. Pharmacol. 94 (2018) 963–972.
[38] R.K. Sunahara, R. Taussig, Isoforms of mammalian adenylyl cyclase: multiplicities of signaling, Mol. Interv. 2 (2002) 168–184.
[39] W.J. Tang, A.G. Gilman, Construction of a soluble adenylyl cyclase activated by Gs alpha and forskolin, Science 268 (1995) 1769–1772.
[40] J.J. Tesmer, S.R. Sprang, The structure, catalytic mechanism and regulation of adenylyl cyclase, Curr. Opin. Struct. Biol. 8 (1998) 713–719.
[41] J.J. Tesmer, R.K. Sunahara, A.G. Gilman, S.R. Sprang, Crystal structure of the catalytic domains of adenylyl cyclase in a complex with Gsalpha.GTPgammaS, Science 278 (1997) 1907–1916.
[42] O. Vvedenskaya, T.D. Rose, O. Knittelfelder, A. Palladini, J.A.H. Wodke, K. Schuhmann, J.M. Ackerman, Y. Wang, C. Has, M. Brooch, et al., Nonalcoholic fatty liver disease stratification by liver lipidomics, J. Lipid Res. 62 (2021), 100104.
[43] C.A.P. Wood, J. Zhang, D. Aydin, Y. Xu, B.J. Andreone, U.H. Langen, R.O. Dror, C. Gu, L. Feng, Structure and mechanism of blood-brain-barrier lipid transporter MFSD2A, Nature 596 (2021) 444–448.
[44] G. Zhang, Y. Liu, A.E. Ruoho, J.H. Hurley, Structure of the adenylyl cyclase catalytic core, Nature 386 (1997) 247–253.
[45] Z. Zhu, Z. Tan, Y. Li, H. Luo, X. Hu, M. Tang, J. Hescheler, Y. Mu, L. Zhang, Docosahexaenoic acid alters Gsalpha localization in lipid raft and potentiates adenylate cyclase, Nutrition 31 (2015) 1025–1030.
[46] M. Ziegler, J. Bassler, S. Beltz, A. Schultz, A.N. Lupas, J.E. Schultz, A novel signal transducer element intrinsic to class IIIa and IIIb adenylate cyclases, FEBS J. 284 (2017) 1204–1217.

Supplemental Material

Appendix Figure 1

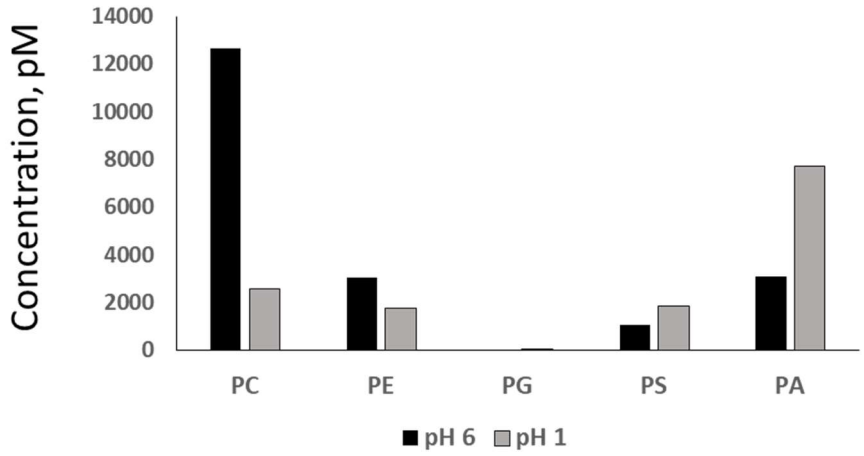

Lipid class composition of MTBE / methanol extracts. MonoQ-purified fractions were extracted at pH 1.0 and pH 6.0. Expectantly, the extract recovered under acidic conditions was enriched with PA. Y-axis: total abundance of lipid classes, pmol/L (n=2).

Appendix Figure 2

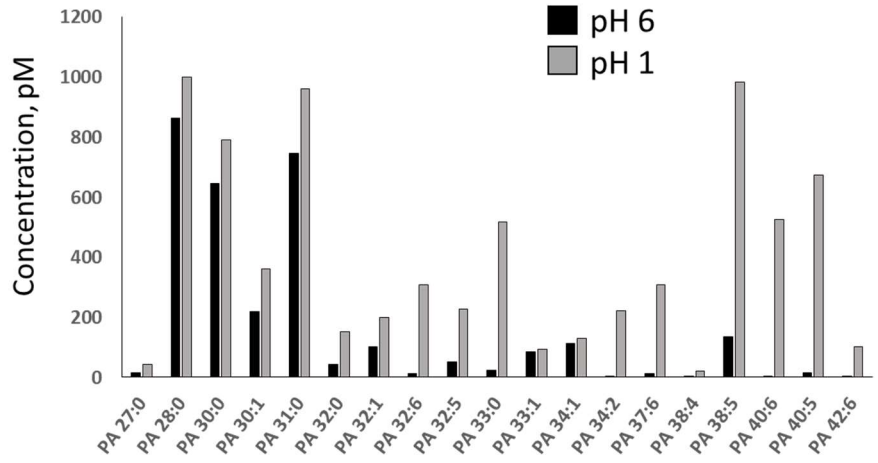

Molecular composition of PA species extracted by MTBE / methanol from the fractions with pH 6.0 and pH 1.0. Acidic extraction increased the recovery of PA by more than 2-fold and also enriched the extract with the molecular species comprising long polyunsaturated fatty acid moieties. Y-axes: molar abundance of lipid species, in pmol/L (n=2).

Appendix Table 1:

List of lipids tested:

from Avanti lipids:

- 131303P Cerebrosides
- 131305P Sulfatides
- 800818C-1-stearoyl-2-arachidonoyl-sn-glycerol
- 800819 --stearoyl-2-docosahexaenoyl-sn-glycerol
- 830855C 1,2-dipalmitoyl-sn-glycero-3-phosphate
- 840051P L-α-phosphatidylcholine (Egg, Chicken)
- 840055C L-α-phosphatidylcholine (Liver, Bovine)
- 840065C 1-stearoyl-2-docosahexaenoyl-sn-glycero-3-phospho-L-serine
- 840101C L-α-phosphatidic acid (Egg, Chicken) (sodium salt)
- 840859C 1-palmitoyl-2-arachidonoyl-sn-glycero-3-phosphate (sodium salt)
- 840860C 1-palmitoyl-2-docosahexaenoyl-sn-glycero-3-phosphate (sodium salt)
- 840862C 1-stearoyl-2-linoleoyl-sn-glycero-3-phosphate (sodium salt)
- 840863C 1-stearoyl-2-arachidonoyl-sn-glycero-3-phosphate (sodium salt)
- 840864C 1-stearoyl-2-docosahexaenoyl-sn-glycero-3-phosphate (sodium salt)
- 840875C 1,2-dioleoyl-sn-glycero-3-phosphate (sodium salt)
- 840885C 1,2-dilinoleoyl-sn-glycero-3-phosphate (sodium salt)
- 840886C 1,2-diarachidonoyl-sn-glycero-3-phosphate (sodium salt)
- 840887C 1,2-didocosahexaenoyl-sn-glycero-3-phosphate (sodium salt)
- 850469C 1-stearoyl-2-arachidonoyl-sn-glycero-3-phosphocholine
- 850472C 1-stearoyl-2-docosahexaenoyl-sn-glycero-3-phosphocholine
- 850804C 1-stearoyl-2-arachidonoyl-sn-glycero-3-phosphoethanolamine
- 850806C 1-stearoyl-2-docosahexaenoyl-sn-glycero-3-phosphoethanolamine
- 850852C 1,2-dioleoyl-sn-glycero-3-phosphoethanolamine-N,N-dimethyl
- 857130P 1-oleoyl-2-hydroxy-sn-glycero-3-phosphate (sodium salt)
- 857328P 1-oleoyl-sn-glycero-2,3-cyclic-phosphate (ammonium salt)
- 860053P total ganglioside extract (Brain, Porcine-Ammonium Salt)
- 860492 Sphingosine-1-phosphate; D-erythro-sphingosine-1-phosphate

- LIPOID (Heidelberg) donated the following lipids:

- 30. 556200 Lipoid PC 14:0/14:0; 1,2-Dimyristoyl-sn-glycero-3-phosphatidylcholine (DMPC)
- 31. 556300 Lipoid PC 16:0/16:0;1,2-Dipalmitoyl-sn-glycero-3-phosphatidylcholine (DPPC)
- 32. 556500 Lipoid PC 18:0/18:0; 1,2-Distearoyl-sn-glycero-3-phosphocholine (DSPC)
- 33. 556600 Lipoid PC 18:1/18:1; 1,2-Dioleoyl-sn-glycero-3-phosphocholine (DOPC)
- 34. 556400 Lipoid PC 16:0/18:1; 1-Palmitoyl-2-oleoyl-sn-glycero-3-phosphocholine (POPC)
- 35. 557100 Lipoid PC 22:1/22:1; 1,2-Dierucoyl-sn-glycero-3-phosphocholine (DEPC)
- 36. 566300 Lipoid PA 16:0/16:0; 1,2-Dipalmitoyl-sn-glycero-3-phosphate, mono-sodium salt (DPPA-Na)
- 37. 567600 Lipoid PS 18:1/18:1; 1,2-Dioleoyl-sn-glycero-3-phosphoserine, sodium salt (DOPS-Na)
- 38. 560200 Lipoid PG 14:0/14:0; 1,2-Dimyristoyl-sn-glycero-3-phospho-rac-glycerol-Na (DMPG)
- 39. 560300 Lipoid PG 16:0/16:0; 1,2-Dipalmitoyl-sn-glycero-3-phospho-rac-glycerol-Na (DPPG)
- 40. 560400 Lipoid PG 18:0/18:0; 1,2-Distearoyl-sn-glycero-3-phospho-rac-glycerol-Na (DSPG)
- 41. 565600 Lipoid PE 14:0/14:0; 1,2-Dimyristoyl-sn-glycero-3-phosphoethanolamine (DMPE)
- 42. 565300 Lipoid PE 16:0/16:0; 1,2-Dipalmitoyl-sn-glycero-3-phosphoethanolamine (DPPE)
- 43. 565400 Lipoid PE 18:0/18:0; 1,2-Distearoyl-sn-glycero-3-phosphoethanolamine (DSPE)
- 44. 565600 Lipoid PE 18:1/18:1; 1,2-Dioleoyl-sn-glycero-3-phosphoethanolamine (DOPE)

Appendix Table 2

mAC activities in HEK293 cell membranes transfected with human mAC isoforms

nmol cAMP•mg^{-1}•min^{-1}

	basal activity	**+ 0.6 µM Gsα**	
HEK293	0.02	0.19	(10-fold)
HEK293 AC1	0.16	0.71	(4-fold)
HEK293 AC2	0.34	5.17	(15-fold)
HEK293 AC3	0.03	0.55	(16-fold)
HEK293 AC4	0.02	0.2	(9-fold)
HEK293 AC5	0.07	2.46	(37-fold)
HEK293 AC6	0.08	1.41	(18-fold)
HEK293 AC7	0.03	0.19	(7-fold)
HEK293 AC8	0.15	1.08	(7-fold)
HEK293 AC9	0.03	1.87	(71-fold)
HEK293ΔAC3,6	0.006	0.06	(10-fold)

(n= 5-12)

Appendix Figure 3

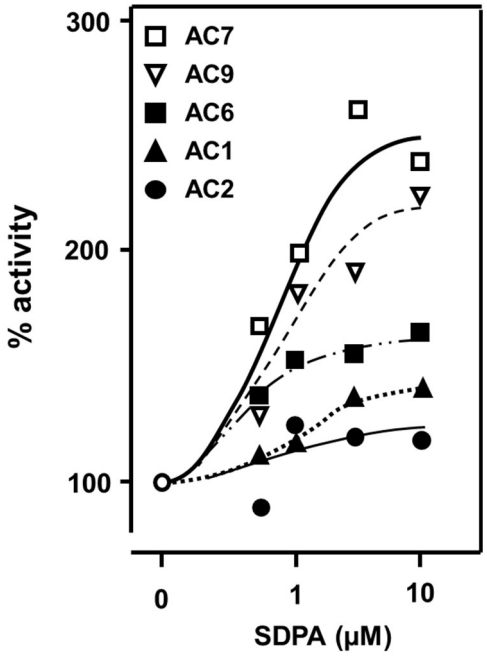

Concentration-response curves for SDPA potentiation of mAC isoforms 7, 9, 6, 1, and 2. Basal and Gsα-activated activities are listed in Appendix table 2. n=2-5.

Appendix Figure 4:

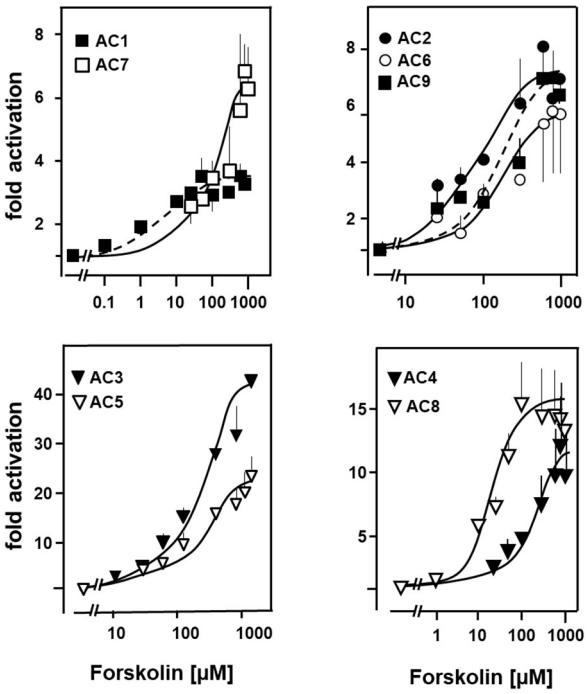

AC	EC_{50} [µM]
AC1	2
AC2	91
AC3	240
AC4	233
AC5	233
AC6	479
AC7	513
AC8	21
AC9	417

Forskolin concentration-response curves for the nine human mAC isoforms expressed in HEK293 cells. Error bars denote S.E.M. The calculated EC_{50} concentrations are listed at right. n = 2-4.

Appendix Table 3

With hAC3 transfected HEK293 cells in a 396 well plate were incubated and stimulated at 37°C for 45 min by adenosine, isoproterenol and prostaglandin E_2 ± 10 µM SDPA.

n = 3 to 4, mean ± S.E.M. Incubations were stopped by addition of detection and lysis buffer of the cAMP assay kit (10 µl/well; Cisbio).

	pMoles cAMP/ 10^4 cells
basal	**0.06 ± 0.02**
SDPA, 10 µM	**0.02 ± 0.01**
2.5 µM isoproterenol	**0.24 ± 0.03**
2.5 µM isoproterenol + 10 µM SDPA	**0.25 ± 0.03**
1 µM prostaglandin E_2	**0.10 ± 0.01**
1 µM prostaglandin E_2 + 10 µM SDPA	**0.11 ± 0.02**
10 µM adenosine	**0.17 ± 0.07**
10 µM adenosine + 10 µM SDPA	**0.07 ± 0.01**

[Please note that isolated HEK293 membrane preparations did not respond to adenosine, isoproterenol or PGE_2]

Additional, unpublished data

Since Seth et al. published the three-state-model of AC regulation, we wanted to directly address the question of correlation between potential ligands and the regulation via GPCRs by adding Gsα to the assays [23]. To determine a suitable concentration of Gsα I carried out concentration-response experiments for all 9 human isoforms (Figure 5). Since we were expecting ligands with predominantly inhibitory influence, I decided to use 600 nM Gsα since this is not a maximal concentration, so there is room for potential activity-enhancing ligands, but also a concentration bigger than the EC_{50} for each isoform (except mAC9) which should be stimulating sufficiently to clearly identify inhibitory effects of potential ligands (EC_{50} values are shown in table 1). After seeing enhancing effects of potential ligands on Gsα-stimulated ACs, I decided to reduce the Gsα concentration to 300 nM.

Isoform	(approximate) **EC_{50} (nM) for Gsα**
mAC1	273
mAC2	475
mAC3	518
mAC4	553
mAC5	390
mAC6	363
mAC7	466
mAC8	175
mAC9	~ 700

Table 1. Approximate Gsα EC_{50} for mAC isoforms.

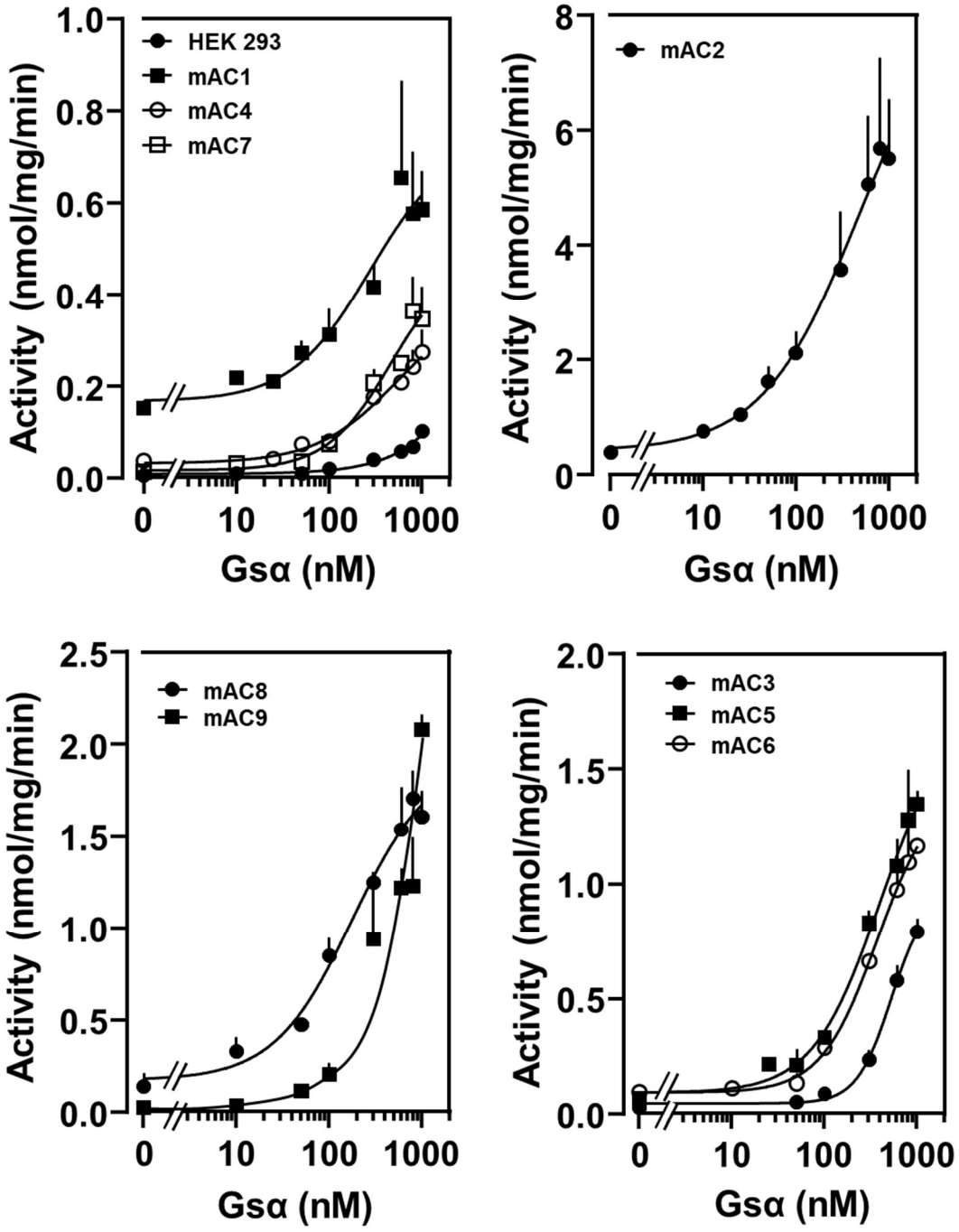

Figure 5. Concentration-response curves of Gsα for all nine mAC isoforms.

Docosahexaenoic acid (C22:6), which is the fatty acid at position 2 of SDPA, is a poly-unsaturated ω3 fatty acid. It is found in nearly all human tissues, but most prominently in neural tissues [27]. The number one docosahexaenoic acid source for humans is marine food but it can also be synthesized from α-linolenic and linoleic acid by multiple elongation and desaturation steps [28]. Next, we examined whether the fatty acid itself would enhance mAC3 activity or if the glycerol backbone, the phosphate group and the second fatty acid is necessary. Figure 6 shows docosahexaenoic acid is not enhancing Gsα-stimulated AC3 activity in comparison to SDPA in terms of potency and efficiency.

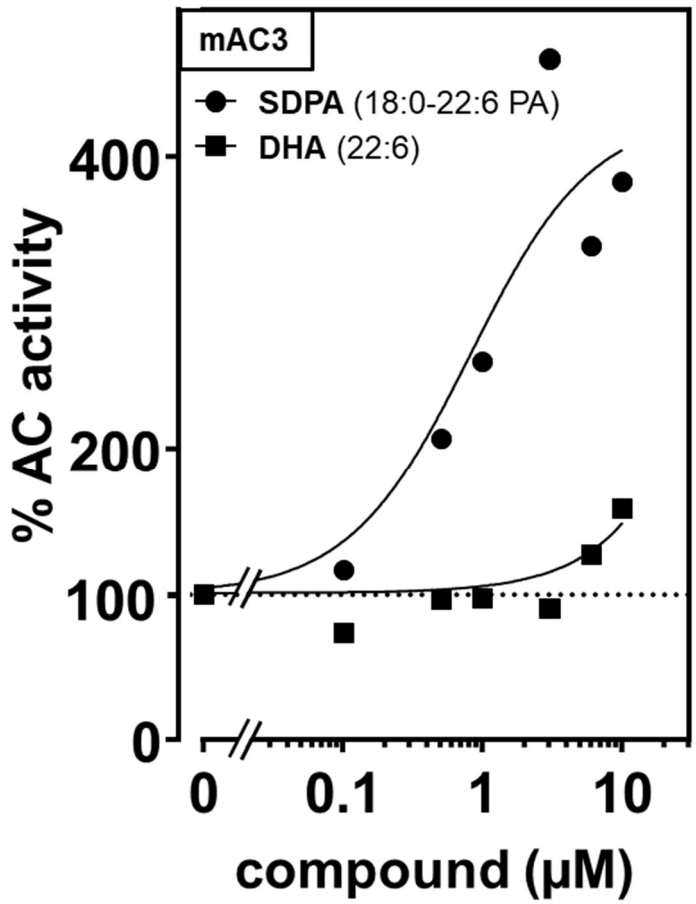

Figure 6. Effect of SDPA and docosahexaenoic acid (DHA) on 600 nM Gsα-stimulated mAC3
Basal and Gsα activities of mAC3 were 0.03 and 0.26 nmol cAMP•mg^{-1}•min^{-1}, respectively. n= 1. EC_{50} value of SDPA was 0.8 μM.

The diterpene forskolin is a potent stimulator of AC activity [12]. In publication I it is only mentioned that SDPA is not further enhancing forskolin-stimulated AC activity, but I also wanted to investigate whether the synergistic effect of forskolin plus Gsα can be enhanced by SDPA. The results showed, strikingly, that 25μM forskolin and 600nM Gsα alone are indeed stimulating mAC3 activity. The addition of both together increased the activity of mAC3 from a basal level of 0.011 to 6.49 nmol cAMP•mg^{-1}•min^{-1}. This enormous stimulation could not be further enhanced by the presence of up to 10 μM SDPA (figure 8), which might be explained by a potential similar way of enhancing Gsα action or by reaching the maximum of mAC3 activity that cannot be enhanced any further. The fact that I was able to measure mAC3 activities higher than 6.49 nmol cAMP•mg^{-1}•min^{-1} is indicating that SDPA and forskolin might share a similar mechanism of enhancing Gsα stimulation, although the chemical and structural differences of forskolin and SDPA are virtually excluding a shared binding site (figure 7).

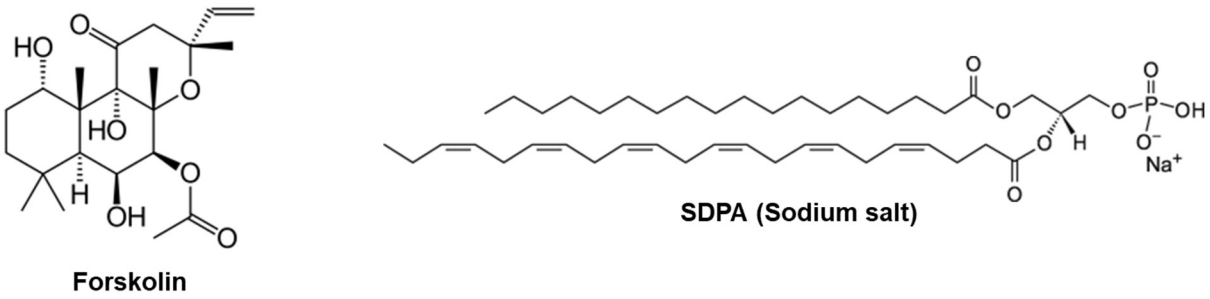

Figure 7. Structures of forskolin and SDPA.

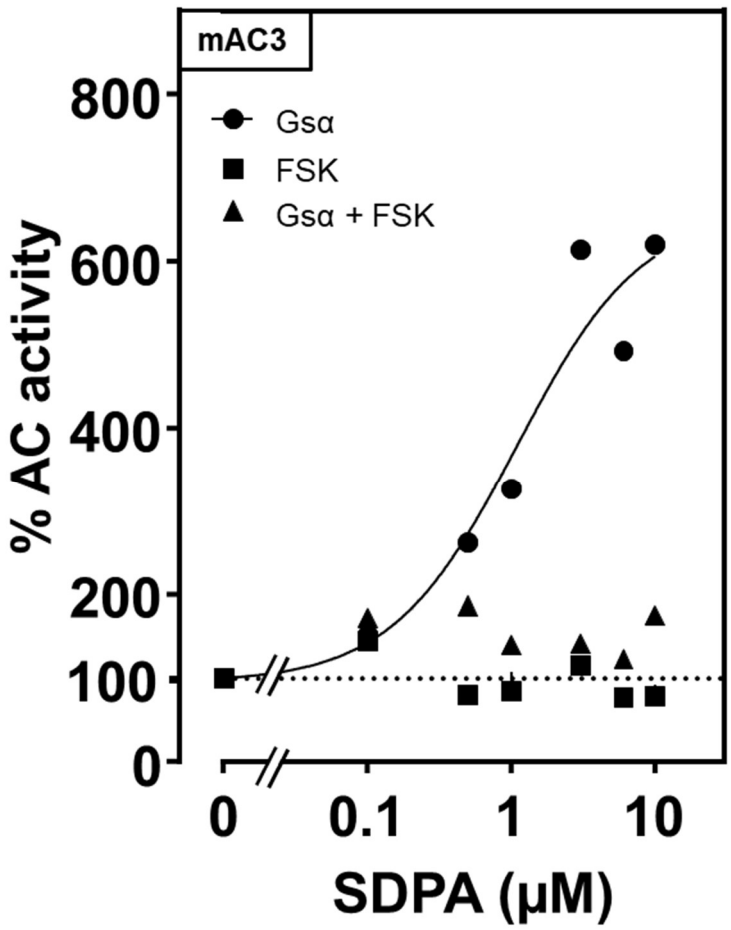

Figure 8. Effect of SDPA on 600 nM Gsα-, 25 μM Forskolin- (FSK-) and 600 nM Gsα + 25μM FSK- stimulated mAC3.
Basal and Gsα, FSK, and Gsα + FSK activities of mAC3 were 0.01 and 0.32, 0.18, and 6.49 nmol cAMP•mg^{-1}•min^{-1}, respectively. N=2. 100% corresponds to Gsα-, FSK- and Gsα + FSK- activity, respectively. Error bars are not shown for clarity.

3.2 Publication II:

Elsabbagh, S., **Landau, M**., Gross, H., Schultz, A., & Schultz, J.E. (2023). Heme b inhibits class III adenylyl cyclases. *Cellular signalling*, 103, 110568. https://doi.org/10.1016/j.cellsig.2022.110568

Position in list of authors: 2

Personal contributions:

Designed, carried out and analyzed experiments for the data represented in figure 8B in the main manuscript.

Maintained cell culture and harvested membranes for testing.

Revised and edited the manuscript together with all authors.

Estimated contribution: 10%.

Cellular Signalling 103 (2023) 110568

Contents lists available at ScienceDirect

Cellular Signalling

journal homepage: www.elsevier.com/locate/cellsig

Heme b inhibits class III adenylyl cyclases

Sherif Elsabbagh, Marius Landau, Harald Gross, Anita Schultz, Joachim E. Schultz *

Pharmazeutisches Institut der Universität Tübingen, Tübingen, Germany

ARTICLE INFO

Keywords:
Adenylyl cyclase
Membrane anchor
Heme b
Hemin
Hematin
Protoporphyrin IX
Biliverdin
Chlorophyll

ABSTRACT

Acidic lipid extracts from mouse liver, kidney, heart, brain, and lung inhibited human pseudoheterodimeric adenylyl cyclases (hACs) expressed in HEK293 cells. Using an acidic lipid extract from bovine lung, a combined MS- and bioassay-guided fractionation identified heme b as inhibitor of membrane-bound ACs. IC_{50} concentrations were 8–12 μM for the hAC isoforms. Hemopexin and bacterial hemophore attenuated heme b inhibition of hAC5. Structurally related compounds, such as hematin, protoporphyrin IX, and biliverdin, were significantly less effective. Monomeric bacterial class III ACs (mycobacterial ACs Rv1625c; Rv3645; Rv1264; cyanobacterial AC CyaG) were inhibited by heme b with similar efficiency. Surprisingly, structurally related chlorophyll *a* similarly inhibited hAC5. Heme b inhibited isoproterenol-stimulated cAMP accumulation in HEK293 cells. Using cortical membranes from mouse brain hemin efficiently and reversibly inhibited basal and Gsα-stimulated AC activity. The physiological relevance of heme b inhibition of the cAMP generating system in certain pathologies is discussed.

1. Introduction

The regulation of vertebrate adenylyl cyclases is a field attracting researchers from many diverse areas and across most subspecialties in medicine [1–5]. The reasons are obvious: the enzymatic product is the universal second messenger 3′, 5′-cyclic AMP (cAMP). After nine distinct membrane-bound ACs were sequenced [2,5–7], biochemical studies on regulation were considerably expanded. The initial speculation of a function of the two hexahelical membrane anchors as ion channels or transporters was never confirmed [6]. Subsequently, the regulation of the vertebrate ACs via the GPCR/Gsα axis was nearly 'codified'. Additional regulatory inputs are phosphorylation of amino acid residues at the cytosolic side, Ca^{2+}, calmodulin, and Gβγ [2]. Surprisingly, it was tacitly accepted that the AC membrane anchors which comprise up to 40% of the proteins were just that and otherwise functionally inert.

Since 1990, our laboratory is attempting to find a physiological function beyond anchoring using a variety of approaches [8–13]. In 2016 we demonstrated that an isosteric hexahelical membrane receptor, the quorum-sensing receptor CqsS from *Vibrio*, regulated the canonical mycobacterial class III AC Rv1625c [12]. We further characterized a conserved cyclase-transducing element, CTE, also termed helical domain, which is located between the membrane and catalytic domains [12,14–16]. In 2020, we reported that the quorum-sensing receptor CqsS from *Vibrio* regulated the extent of Gsα activation of the mammalian AC2 [17]. We further demonstrated that fetal bovine serum (FBS) contains components which concentration-dependently attenuated the Gsα activated AC2 [17]. Based on these findings, we proposed a model for AC regulation in which all AC domains were assigned specific functionalities. The AC membrane anchors were proposed to be orphan receptors for yet unknown ligands. Since then, our efforts have been focused on identification of potential AC ligands. Here, we report the surprising finding that heme b, isolated from a bovine lung homogenate, inhibited all human membrane bound ACs at low micromolar concentrations and with high structural specificity in vitro and in HEK293 cells.

2. Materials and methods

2.1. Reagents and materials

ATP, creatine kinase, creatine phosphate, bovine hemin (Cat.# H9039; ≥90% pure), protoporphyrin IX (Cat. # 258385), biliverdin (Cat.# 30,891), hematin (Cat.# H3281) and chlorophyll *a* (Cat. # C6144) were purchased from Merck-Sigma as was hemopexin from human plasma (Cat. # SRP6514). Porcine hemin >98% pure was supplied by Roth chemicals (Cat. # 7629.1). Porcine hemin was used to exclude interference by potential impurities in bovine hemin (see

Abbreviations: AC, adenylyl cyclase..

* Corresponding author at: Pharmazeutisches Institut der Universität Tübingen, Auf der Morgenstelle 8, 72076 Tübingen, Germany.
E-mail address: joachim.schultz@uni-tuebingen.de (J.E. Schultz).

https://doi.org/10.1016/j.cellsig.2022.110568
Received 9 November 2022; Received in revised form 12 December 2022; Accepted 19 December 2022
Available online 21 December 2022
0898-6568/

Appendix Table 1). The constitutively active GsαQ227L mutant was expressed and purified as described earlier [18–20]. Forskolin was a gift from Hoechst, Frankfurt, Germany. Fetal bovine serum (FBS) was from Gibco, Life Technologies, Darmstadt, Germany (Cat. # 10270; lot number: 42Q8269K). Sera for sheep, rabbit, goat, and chicken were from Sigma (Cat. Numbers S2263; R4505; G6767; C5405), and fish serum was from my BioSource, San Diego, CA, USA (Cat. # MBS318429). NADH, D-Lactic dehydrogenase from *Lactobacillus leichmannii*, sodium pyruvate, trypsin from porcine pancreas, N-α-benzoyl-L-arginine ethyl ester (BAEE) were purchased from Merck-Sigma.

2.2. General experimental procedures

HPLC was performed using a Waters system, with a Waters 996 controller and pump and photodiode array detector, a Rheodyne 7725i injector and a 200 series PerkinElmer vacuum degasser. For LC-MS analysis, a 1100 Series HPLC system (Agilent Technologies) was fitted with a G1322A degasser, a G1312A binary pump, a G1329A autosampler and a G1315A diode array detector. The Agilent HPLC components were connected to an ABSCIEX 3200 QTRAP LC/MS/MS mass spectrometer (Sciex, Darmstadt, Germany). The high resolution mass spectrum was recorded on an HR-ESI-TOF-MS Bruker maXis 4G mass spectrometer. All solvents were purchased as HPLC or LC-MS grade.

2.3. Extraction of lung tissue

1.24 kg bovine lung was minced using a meat grinder and 1.2 l 50 mM MOPS pH 7.5 were added into in a waring blender (4 °C) resulting in 2.3 l homogenate. It was centrifuged (30 min at 4 °C, 7200 ×g) resulting in 1.2 l supernatant. The pH of the supernatant was adjusted to 1 using 7% HCl. Equal volumes of CH_2Cl_2: MeOH (2:1) were mixed with the supernatant in a separatory funnel and shaken vigorously. Centrifugation was at 5300 ×*g* for 30 min. The lower organic (CH_2Cl_2) layer was recovered, and the solvent evaporated using a rotary evaporator at 35 °C. 2 g of dried crude extract was obtained.

2.4. Fractionation

The material was dissolved in petrol ether (40–60 °C boiling point) and chromatographed on silica gel 60H (Supelco; vacuum liquid chromatography; VLC). The column was developed stepwise with solvents of increasing polarity, i.e., from 10:90 EtOAc/petrol ether to 100% EtOAc, followed by 100% MeOH. 17 fractions (A to Q) of 300 ml each were collected. Fraction O (eluted with 100% MeOH) was further subjected to RP-HPLC using a linear gradient from 70:30 to 100% MeOH/H_2O (0.1% TFA) over a period of 20 mins (Knauer Eurospher II C18P 250 × 8 mm, 1 ml/min, UV monitoring at 215 and 380 nm). Three subfractions, designated O-1, O-2 and O-3, were obtained.

For LC/MS, fractions were dissolved in methanol and injected into the LC/MS using an acetonitrile/H_2O (0.1%TFA) gradient 10/90 to 50/50 over 24 min. Commercial hemin was dissolved in DMSO (10 mM), diluted in methanol, and analyzed.

2.5. Lactate dehydrogenase assay

LDH, pyruvate and NADH were dissolved in 67.2 mM Tris/HCl pH 7.5 The reaction was monitored for 3 min at 340 nm. Hemin, final concentration (40 μM) was added from a 10 mM DMSO stock.

2.6. Trypsin assay

Trypsin and the substrate N-α-benzoyl-L-arginine ethyl ester were dissolved in 67 mM Tris-HCl, pH 9, buffer. The reaction was monitored at 253 nm for 3 min.

2.7. Plasmid construction and protein expression

HEK293 cells were maintained in Dulbecco's modified Eagle's medium (DMEM) containing 10% FBS at 37 °C with 5% CO_2. Transfection of HEK293 cells with single mAC plasmids was with PolyJet (SignaGen, Frederick, MD, USA). Permanent cell lines were generated by selection for 7 days with G418 (600 μg/ml) and maintained with 300 μg/ml G418 [21–23]. For membrane preparation, cells were tyrpsinized and collected by centrifugation (3000 ×*g*, 5 min). Cells were lysed and homogenized in 20 mM HEPES, pH 7.5, 1 mM EDTA, 2 mM $MgCl_2$, 1 mM DTT, and one tablet of complete, EDTA-free (for 50 ml), 250 mM sucrose by 20 strokes in a potter homogenizer. Debris was removed by centrifugation (5 min at 1000 ×*g*), membranes were then collected by centrifugation at 100000 ×*g* for 60 min at 0 °C, resuspended and stored at −80 °C in 20 mM MOPS, pH 7.5, 0.5 mM EDTA, 2 mM $MgCl_2$. Membrane preparation from mouse brain cortex was according to [17,24]. For each preparation three cerebral cortices were dissected and homogenized in 4.5 ml cold 48 mM Tris-HCl, pH 7.4, 12 mM $MgCl_2$, and 0.1 mM EGTA with a Polytron hand disperser (Kinematica AG, Switzerland). The homogenate was centrifuged for 15 min at 12000 ×*g* at 4 °C and the pellet was washed once with 5 ml 1 mM potassium bicarbonate. The final suspension in 2 ml 1 mM $KHCO_3$ was stored in aliquots at −80 °C.

2.8. Adenylyl cyclase assay

mAC activities were determined in a volume of 10 μl using 1 mM ATP, 2 mM $MgCl_2$ (3 mM $MnCl_2$ with bacterial ACs), 3 mM creatine phosphate, 60 μg/ml creatine kinase, 50 mM MOPS, pH 7.5. The cAMP assay kit from Cisbio (Codolet, France) was used according to the supplier's instructions. For each assay a cAMP standard curve was established.

2.9. HasA preparation

pQE32-pHisHasA-ApR plasmid was transformed into *E. coli* $BL21DE3_{[pRep4]}$. The cells were cultured in LB medium containing 100 μg/ml ampicillin and 25 μg/ml kanamycin to an OD_{600} of 0.62 at 30 °C. After induction (1 mM IPTG) incubation was continued for 4 h at 30 °C. Cells were harvested by centrifugation and resuspended in 20 mM MOPS, pH 7.5 containing complete EDTA free protease inhibitor (buffer A). Cells were disrupted by French press and the lysate was centrifuged (4300 ×*g*; 30 min) followed by ultracentrifugation (100,000 *g*, 60 min). The supernatant was loaded onto a Ni-NTA column equilibrated with buffer A + 20 mM imidazole. After washing with buffer A (+ 5 mM and 15 mM imidazole) HasA was eluted with buffer A + 250 mM imidazole and dialyzed against 20 mM MOPS, pH 7.5, to remove imidazole.

2.10. cAMP accumulation assay

HEK293 cells stably expressing AC3, AC5, AC7, and AC9 were plated at 2500–10000 cells/well into 384 well plates. Cells were then treated with varying concentrations of hemin and incubation was continued for 15–45 min. 10 μM isoproterenol was added to stimulate cAMP production and the incubation was continued for 10–30 min. Cisbio HTRF detection reagents were then added and incubated for 1 h at room temperature.

2.11. Data and statistical analysis of assay results

All incubations were in duplicates or triplicates. For easier presentation data were mostly normalized to respective controls and n and S.E.M values are indicated in all figures. Data analysis was with GraphPad prism 8.1.2 using a two-tailed *t*-test.

Table 1
The effect of different animal sera on Gsα stimulated activity of hAC5 expressed in Sf9 cells. The % activities listed are at 20% serum. Basal hAC5 activity was 0.29 ± 0.09 and 600 nM Gsα stimulated activity (100%) was 5.2 ± 1.15 nmol cAMP•mg^{-1}•min^{-1}. Means ± S.E.M of 3–4 experiments, each with two technical replicates are depicted.

Serum	% hAC5 activity
FBS	11 ± 1
Rabbit	9 ± 1
Sheep	40 ± 14
Goat	13 ± 5
Chicken	16 ± 4
Fish	10 ± 1

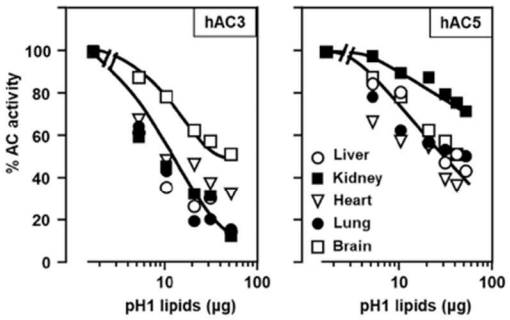

Fig. 1. Effect of acidic lipid extracts from mouse tissues on Gsα-stimulated hAC3 and 5. The dried residues from each tissue were dissolved at 10 mg/ml DMSO, hAC3 and hAC5 were stimulated by 300 nM Gsα. hAC3, 100% activity was 0.6 nmol cAMP•mg^{-1}•min^{-1} (basal activity was 0.01). hAC5, 100% activity was 2.74 nmol cAMP•mg^{-1}•min^{-1} (basal activity was 0.03). Data are from one experiment with two technical replicates.

3. Results

3.1. Identification of heme b

We have reported that components present in FBS attenuated Gsα-activated hAC2 expressed in Sf9 cells [17]. Here, we examined sera from sheep, goat, rabbit, chicken, and fish using Gsα-activated hAC5 expressed in Sf9 cells (Table 1). We observed that these sera attenuated hAC5 with comparable efficacies reported earlier [17]. We concluded that yet unidentified components are present in sera from different species possibly indicating a common evolutionary history with eukaryotic ACs because birds (chicken) and fish (salmon) diverged from mammals several hundred million years ago. The conservation of vertebrate ACs goes back about 0.5 billion years to the coelacanth and elephant shark [7,15]. For chemical identification of potential ligands, the use of serum as a source material is deemed unsuitable, not least because of the projected cost.

Expecting the presence of AC ligands in other tissues, we prepared pH 1 lipid extracts from mouse liver, kidney, heart, lung and brain [25]. Inhibition of Gsα-activated AC3 and AC5 expressed in HEK293 cells were observed with all acidic lipid extracts. AC5 was somewhat less attenuated indicating graded responses (Fig. 1).

Because the extract from lung had a high 'inhibitory' efficiency we continued with bovine lung as a source material. A lung homogenate was acidified to pH 1 and lipids were extracted with dichloromethane/methanol [25]. After solvent removal the solids were dissolved in petrol ether and separated by VLC on silica gel 60H (see scheme). Stepwise elution with petrol ether, ethyl acetate and methanol resulted in 17 fractions (A-Q; 300 ml each) which were brought to dryness. The residues were dissolved at 5 mg/ml DMSO and tested with Gsα-activated hAC5. Fractions with inhibitory potency (F, J-Q) were analyzed by low resolution LC/MS. In the slightly brownish fractions K to Q, a peak at *m/z* 616.3 was prominent. Since fraction O represented contained the compound already in a semi-pure form, we continued working with it. 24 mg of fraction O were dissolved in 0.5 ml methanol and were subjected to RP-HPLC (Fig. 2, left).

Three major peaks were resolved (O-1, O-2, and O-3). The absorption profile at 380 nm indicated the presence of compounds with highly conjugated π-electron systems. The three fractions were taken to dryness, dissolved at 5 mg/ml DMSO, and tested against Gsα-stimulated hAC5 activity (Fig. 2 right).

Fraction O-3 with the best inhibitory efficiency was analyzed by low resolution LC/MS (Appendix Fig. 2). Its mass spectrum displayed a prominent peak at *m/z* 616.3, beside some minor peaks at *m/z* 614, 617 and 618. High resolution ESI-MS analysis of fraction O-3 revealed an $[M-2H^+ + Fe^{3+}]^+$ ion (*m/z* 616.1772) consistent with a molecular formula of $C_{34}H_{32}FeN_4O_4$ (Appendix Fig. 3). A literature and database search identified the compound as heme b (*syn.* Fe^{III}-protoporphyrin IX). This was supported by the analysis of the MS isotope pattern. The ratio of the peak areas for 614:616:617:618 were determined to be 7:100:43.8:12.6 (Appendix Fig. 2) which was in agreement with the predicted Fe isotope distribution of 6.3:100:40.9:9.3 attributable to ^{54}Fe, ^{56}Fe, ^{57}Fe and ^{58}Fe [26]. Furthermore, the fragment at 557.1640 and a minor at 498.1508, observed in the HR-MS spectrum, indicated the sequential loss of two ethanoic acid groups ($C_2H_3O_2$) (Appendix Fig. 3), which is also characteristic for this compound class [27]. We further corroborated the identity of heme b by comparing the retention time and mass-spectra of

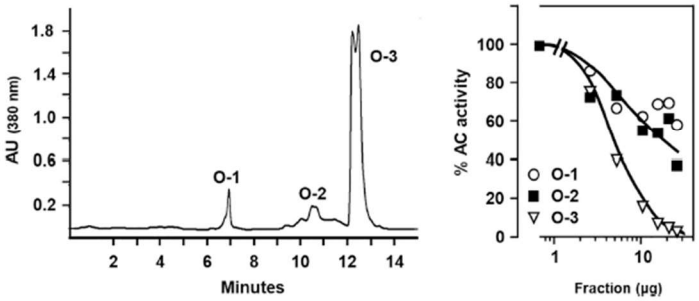

Fig. 2. Left: Fraction O is resolved into three subfractions by RP-HPLC. Right: Effect of subfractions O-1, O-2, and O-3 on 300 nM Gsα stimulated hAC5. 100% activity corresponded to 1.43 nmol cAMP•mg^{-1}•min^{-1} (basal activity was 0.035). The data represent the mean of two experiments with two technical replicates.

Acidic lipid extract from bovine lung

Si-VLC

Fraction	A	B	C	D	E	F	G	H	I	J	K	L	M	N	O	P	Q
Solvent	100% PE	90:10 PE:EA	80:20 PE:EA	60:40 PE:EA	40:60 PE:EA	20:80 PE:EA	100% EA	25:75 MeOH:EA	100% MeOH	100% MeOH	100% MeOH	100% MeOH	100% MeOH	100% MeOH	100% MeOH	100% MeOH	100% MeOH
weight [mg]	3.1	4.5	459.1	404	285.8	70.1	29.5	21.6	344.6	753.3	95.7	85.3	175.5	136.3	54.7	27.4	17.9
AC5 % activity	116.5	125	100.5	80	85	48.5	84	87.5	102.5	44.5	11	1	30	50	44.5	38	25
m/z 616.3	-	-	-	-	-	-	-	-	-	-	+	+	+	+	+	+	+

RP18-HPLC

Fraction	O-1	O-2	O-3
weight [mg]	20	0.94	0.52
m/z 616.3	-	-	+

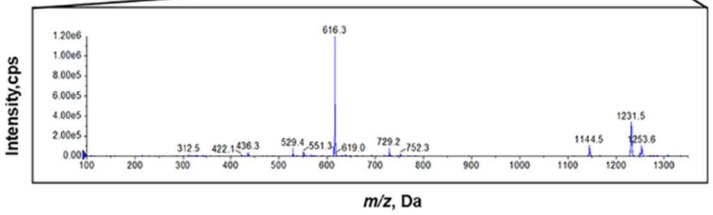

Fractionation Scheme. Si-VLC: Silica-Vacuum Liquid Chromatography, RP-HPLC: Reversed phase-High performance liquid chromatography, EA: Ethyl acetate, PE: Petrol ether, MeOH: Methanol. % remaining AC5 activity; values represent mean of 2 experiments in triplicates. 1 µg of fractions (5 mg/mL in DMSO) were added to the assay. Basal AC5 activity was 0.05 nmol cAMP•mg^{-1}•min^{-1}; 300 nM Gsα-stimulated AC5 activity was 2.1 nmol cAMP•mg^{-1}•min^{-1}.

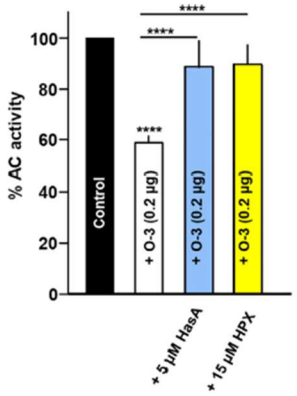

Fig. 3. Hemophore (HasA) and hemopexin (HPX) attenuate inhibition of hAC5 by fraction O-3. Basal activity was 0.04 ± 0.017 nmol cAMP•mg^{-1}•min^{-1}. 300 nM Gsα activity (100%) was 0.63 ± 0.17 nmol cAMP•mg^{-1}•min^{-1}. HPX and Has A did not affect basal or Gsα-stimulated hCA5 activity. ****: $p < 0.0001$. Error bars denote SEM ($n = 4$ with two technical repetitions).

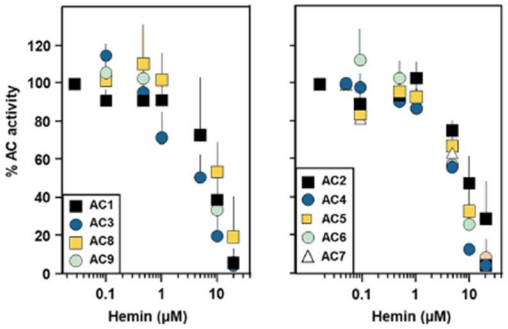

Fig. 4. Concentration-response curves for hemin inhibition of 300 nM Gsα-stimulated hAC isoforms. Basal and 100% Gsα stimulated activities together with the IC_{50} concentrations are listed in appendix Table 1. Error bars denote SEM of 3–4 experiments with two technical replicates.

a commercial heme b standard (hemin) with fraction O-3 (Appendix Fig. 4). Hemin is heme b chloride. Below, we denote the isolated material from lung as heme b and the commercial sample used for most assays as hemin.

To biologically confirm the identity of heme b, we used the hemin-binding proteins human hemopexin and bacterial hemophore HasA. In mammals, hemopexin, produced by the liver serves as heme b scavenger with high affinity (K_D values 320 to 0.1 pM [28,29]). Hemopexin is involved in heme b detoxification [30]. We produced the heme b-binding protein hemophore (Has A) from *Serratia marcescens*. HasA is an extracellular heme-binding protein for iron acquisition, binding heme with a Kd of 5×10^{10} (M^{-1}) [31]. Hemopexin as well as hemophore significantly inhibited the action of fraction O-3 (Fig. 3).

3.2. Action of hemin on mammalian and bacterial class III adenylyl cyclases

Hemin attenuated Gsα-activated AC activity of all nine membranous AC isoforms expressed in HEK293 cells with IC_{50} concentrations of 7.5 to 12 µM (Fig. 4; Appendix Table 1). The IC_{50} was independent from the concentration of Gsα used for hAC stimulation, e.g., at 700 nM Gsα the IC_{50} for hAC5 was 10.4 µM (data not shown). This indicated that Gsα and hemin were not competing for identical binding sites. Similarly, we investigated the effect of hemin on basal activities of hAC1, 2, 5 and 9 (one from each subclass). Basal activities were similarly inhibited in a concentration dependent manner (see Appendix Fig. 5).

To examine the structure-activity relationship for hemin we used hematin, protoporphyrin IX, biliverdin and chlorophyll *a* (the structural formula are depicted in Appendix Fig. 1). Hematin is the ferric protoporphyrin hydroxide [32]. Protoporphyrin IX is the last common precursor in heme and chlorophyll biosynthesis and lacks a central metal ion. Biliverdin, a product of heme catabolism, has an opened porphyrin ring system and lacks the ferric ion [33]. At 10 µM, protoporphyrin IX, hematin and biliverdin had no significant effect on Gsα-stimulated hAC5 activity (Fig. 5). At 40 µM, only up to 30% inhibition was observed for protoporphyrin IX or hematin, much less than with hemin (Fig. 5; Appendix Table 2).

The catalytic domains of eukaryotic ACs share extensive sequence similarity with their bacterial class III progenitors [15]. The possibly regulatory N-termini in bacterial AC isoforms vary considerably [9,15]. The bacterial membrane anchoring domains have two, four and six α-helices and many bacterial ACs have none and are soluble [15]. Bacterial ACs are not regulated by Gsα. We investigated the effect of hemin and structurally related compounds using the mycobacterial AC Rv1625c, a likely precursor of human ACs with a hexahelical membrane anchor [10], the mycobacterial AC Rv3645 which has a hexahelical membrane anchor and a HAMP domain between membrane exit and catalytic domain [11], the membrane-bound cyanobacterial AC CyaG from *Arthrospira maxima* with two membrane spans, an S-helix and a HAMP domain in front of the catalytic domain [34] and the soluble mycobacterial AC Rv1264 which is regulated by pH [35]. Further, we analyzed the soluble construct of Rv1625c, D204-G443 [10]. Without exception, hemin inhibited these bacterial ACs with comparable efficacy to the human AC isoforms (Fig. 5; Appendix Table 2). Significant differences in sensitivity were apparent for hematin, protoporphyrin IX, and biliverdin (Fig. 5, Appendix Table 2). The soluble AC Rv1264 and the soluble construct Rv1625c-D204-G443 construct were inhibited by hematin, protoporphyrin IX and biliverdin (Appendix Fig. 6 and table 2). The data suggest a direct inhibitory attack at the catalytic dimer. The presence of a HAMP domain (Rv3645) or a HAMP domain in line with an S-helix in front of the catalytic domain as in CyaG did not affect inhibition by hemin (Fig. 5, Appendix Fig. 6 and table 2).

Structurally, chlorophyll is closely related to hemin. It shares the tetrapyrrole ring system and several side chains. It carries a central magnesium atom (Mg^{2+}) and a tetra-isoprenoid C20 phytol esterified to a propionic acid sidechain. To determine whether redox reactions, possibly mediated by the central Fe^{3+} of hemin, might be involved in inhibition we examined the effect of chlorophyll *a* on hAC5. Surprisingly, chlorophyll *a* inhibited hAC5 and the membranous mycobacterial Rv1625c AC (Fig. 6). The inhibition was only somewhat less pronounced compared with hemin. Calculated IC_{50} concentrations were 30 and 10 µM for hAC5 and Rv1625c, respectively. The data excluded redox processes as a cause for class III AC inhibition by hemin.

3.3. Hemin inhibits cAMP accumulation in HEK293 cells

The effect of hemin on cAMP accumulation in intact HEK293 cells transfected with hAC3, 5, 7 and 9, i.e., one of each subclass was examined. Hemin at concentrations above 50 µM has been reported to be cytotoxic during extended incubations of astrocytes (12 to 24 h; [36]). We checked hemin toxicity for HEK293 cells under our incubation conditions (50 µM hemin, 45 min). Cells remained viable. Isoproterenol was used for stimulating intracellular cAMP production in HEK293 cells. Hemin inhibited cAMP accumulation with IC_{50} concentrations comparable to HEK293 membrane preparations (Fig. 7). This left the

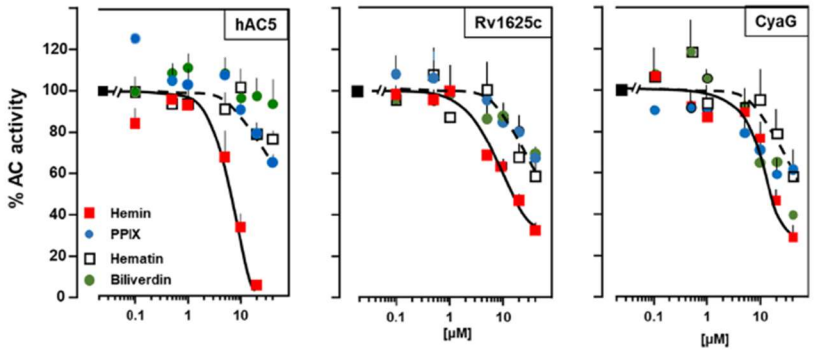

Fig. 5. Structural activity relationship of hemin inhibition of hAC5, mycobacterial AC Rv1625c and cyanobacterial AC CyaG from *Arthrospira maxima*. hAC5 Gsα (300 nM) activity (100%) corresponded to 1.56 ± 0.05 nmol cAMP•mg^{-1}• min^{-1} (basal was 0.02 ± 0.002). Rv1625c activity (100%) was 2.5 ± 0.9 μmol cAMP•mg^{-1}• min^{-1}. CyaG activity (100%) was 0. 6 ± 0.07 μmol cAMP•mg^{-1}• min^{-1}. Error bars denote SEM of 3–5 experiments with two technical repetitions.

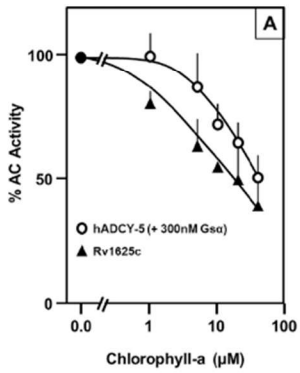

Fig. 6. Chlorophyll *a* inhibits hAC5 expressed in HEK293 membranes and mycobacterial AC Rv1625c. hAC5 Gsα activity (100%) corresponded to 1.4 ± 0.2 nmol cAMP•mg^{-1}• min^{-1} (basal activity was 0.03). Rv1625c activity (100%) was 2.3 ± 0.3 μmol cAMP•mg^{-1}• min^{-1}. Error bars denote SEM of 4–6 experiments with two technical repetitions.

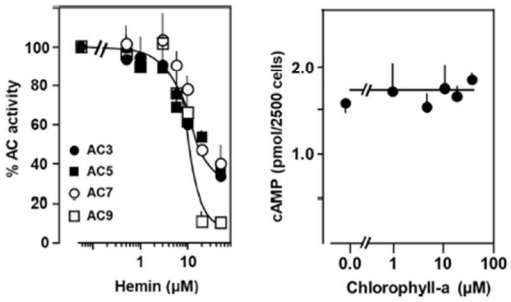

Fig. 7. Hemin inhibits cAMP accumulation in HEK293 cells, chlorophyll *a* does not. HEK293 cells transfected with respective hAC isoforms were stimulated with 10 μM isoproterenol. Basal and isoproterenol stimulated activities are listed in appendix Table 3. IC_{50} of hemin against AC3, 5, 7 and 9 were 8.8, 8.9, 11.8 and 11.6 μM, respectively. Error bars denote SEM of 3–4 experiments each with three technical replicates.

possibility open that hemin acted via an extracellular binding site. However, because the hydrophobic hemin can pass the cell membrane such a conclusion is premature [37,38]. Chlorophyll *a* did not inhibit isoproterenol-stimulated cAMP formation in HEK293 cells (Fig. 7, right). Probably chlorophyll with its C20 phytylester cannot cross into the cytosol. This data supports the notion that the membrane anchors of hACs are not involved in the inhibitory action of hemin, in line with the inhibition of ACs without membrane anchors such as Rv1264 or Rv1625c-D204-G443.

3.4. Hemin inhibits adenylyl cyclases in brain cortical membranes

Next, we prepared membranes from mouse brain cortex in which most mAC isoforms are expressed (except mAC4) [39]. Basal, as well as Gsα stimulated activities of mACs were significantly inhibited by hemin (Fig. 8A and Appendix Fig. 7). Hemin concentration response curves showed an IC_{50} of 9 and 8.5 μM for basal and Gsα stimulated activities, respectively. These concentrations are almost identical to those observed in hAC isoforms expressed in HEK293 cells. The data suggest that (a) ACs in brain cortex are similarly sensitive to hemin inhibition, and, (b) the effect of hemin may have physiological relevance. Hemin inhibition was also observed when Gsα-stimulation was synergistically enhanced by 10 μM forskolin (Appendix Fig. 8). This indicated that forskolin activation and hemin inhibition possibly were acting at separate sites of the protein.

Due to its lipophilicity, hemin may irreversibly enter the hydrophobic phospholipid layer causing membrane disorder and inhibition of membrane bound ACs. Alternatively, hemin may reversibly affect the catalytic activity. We used cortical membranes to test these possibilities. Membranes were incubated for 15 min with 10 μM hemin. After collection and washing, the isolated membranes were again subjected to Gsα-stimulation ± hemin (Fig. 8B). The data indicated that hemin inhibition is reversible, i.e., it is not tightly lodged in the membrane and inhibition probably is not caused by permanently disturbing membrane integrity or covalently binding to the hAC protein.

Hemin is a reactive compound, and at higher concentrations a rather toxic blood component. Therefore, it may also affect the activity of other proteins and enzymes. As a control we used the tetrameric enzyme lactate dehydrogenase and the monomeric protease trypsin The activity of both enzymes was not affected by 40 μM hemin (Appendix Fig. 9).

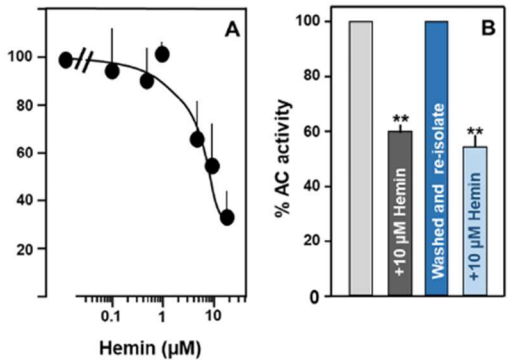

Fig. 8. A) Hemin inhibits Gsα-stimulated cAMP accumulation in mouse brain cortical membranes. 300 nM Gsα stimulated activity (100%) was 6.8 ± 0.64 nmol cAMP•mg^{-1}• min^{-1}. The IC_{50} for hemin was 8.5 μM. Error bars denote SEM. $N = 3$, each with two technical replications. B) Inhibition of Gsα stimulated brain cortical membranes by hemin is reversible. After stimulation by 600 nM Gsα ± 10 μM hemin, membranes were collected by centrifugation at 100,000 *g* and re-assayed. $N = 4$, error bars denote SEM. 100% stimulation was 6.6 ± 0.3 nmol cAMP/mg/min. $p < 0.01$.

4. Discussion

This work started with the intention to identify a ligand or ligands for the tandem of membrane anchors of nine mammalian AC isoforms. We screened bovine lung extracts for inhibitory activity because lung is a rather complex tissue composed of various cell types and is easily available. The identification of non-protein bound heme b, a well-known blood component, as an efficient and general inhibitor of class III ACs, particularly mammalian ACs, was surprising. The chemical identity of heme b was unequivocally proven by LC/MS and by direct comparison with commercial hemin (see Appendix Fig.s 2–4). The biochemical identity and functionality were demonstrated using the human cytoprotective agent hemopexin which is secreted into the blood from the liver, binds heme b with high affinity and delivers it to the liver for degradation. Further, we used the bacterial hemophore HasA from *Serratia marcescens* which similarly binds heme b with very high affinity. HasA is used to fill the bacterial need for iron. Hemopexin and HasA attenuated heme b inhibition of hAC5 by fraction O-3, unequivocally demonstrating the biological activity (Fig. 3).

So far, the connections between cAMP and heme b were induction of heme oxygenase-1 by the membrane-permeable cAMP derivative dibutyryl cAMP in smooth muscle cells [40–42], an inhibitory effect on isoproterenol-stimulated lipolysis in fat cells [43], and stimulation of cAMP production in blood mononuclear cells [44]. Our data indicate that free hemin efficiently inhibited all membrane-delimited mammalian ACs. Therefore, free heme b does not qualify as a specific ligand for any individual isoform. Further, for a specific AC ligand we would not expect a compound such as heme b, which is abundant. Our data do not allow to propose a mechanism of action for heme b. Hemin inhibited basal as well as Gsα-stimulated (± forskolin) hAC activities. This indicated that heme b possibly bound at the AC proteins at sites differing from Gsα or forskolin. We assume that heme b binds directly at the catalytic dimer. This assumption is in line with the inhibition of the soluble AC Rv1264 and the soluble AC construct from Rv1625c (Appendix Fig. 6 and Appendix Table 2). The inhibition of isoproterenol-stimulated cAMP in HEK293 cells presumably involves entry of heme b into the cells as it readily crosses cell membranes ([45] and ref.'s therein). Chlorophyll *a* inhibited in vitro but not in intact cells (Fig. 6 and 7). Chlorophyll *a* with its tetra-isoprenoid C20 phytol ester probably is retained in the membrane and cannot cross into the cytosol. This differs from hemin.

The structural specificity of hemin action as compared to protoporphyrin IX, an immediate biosynthetic precursor, to biliverdin, the first metabolic degradation product by heme-oxygenase-1, and to hematin was remarkable. Several reasons might explain this observation. The large loss of efficiency of the more lipophilic protoporphyrin IX strongly indicates that subtle structural differences caused by the centrally coordinated metal ion may contribute to specific binding and inhibition. Biliverdin is an open chain of four pyrrolic rings and its geometry differs profoundly from hemin or protoporphyrin, thus more easily explaining the loss of inhibitory activity. The scant inhibitory efficiency of hematin was a further surprise because it differs from hemin only by replacement of the coordinated chloride at the Fe^{3+} ion by a hydroxy group. The covalent radii of the chloride anion (102 pm) and a hydroxy group (110 pm) are similar. A major difference is that the hydroxy group is a hydrogen bond acceptor and donor whereas the chloride in heme b cannot form hydrogen bridges; it may form weak van der Waals contacts. The formation of hydrogen bridges may attenuate hematin binding and be responsible for loss of inhibitory efficiency. Heme can bind in either of two flipped orientations defined by the asymmetry of the vinyl and propionyl substituents of the porphyrin skeleton [46]. It is possible that hemin binds in an inhibitory orientation which is disfavored in hematin. Such disparate properties obviously could contribute to differences in biochemical properties.

An unexpected result was that chlorophyll *a* inhibited hAC5 as well as the mycobacterial Rv1625 AC (Fig. 6). In chlorophyll the tetrapyrrole ring system has Mg^{2+} at the center. These data virtually exclude that the inhibitory action of hemin is caused by redox reactions. Chlorophyll *a* had no effect on cAMP formation in intact HEK293 cells (Fig. 7).

Another aspect merits discussion, the β-subunit of the soluble guanylyl cyclase contains a ferrous b-type haem prosthetic group (heme b) facilitating NO binding and regulation [47,48]. The heme binds via its carboxylic groups to tyrosine (Y135) and arginine (R139). Histidine (H105) is a reversible axial ligand at the Fe^{2+} in heme b [48]. This heme-binding triad is N-terminal to the catalytic site. An alignment with mammalian ACs shows that such a binding triad is absent in ACs. The coincidence that heme b inhibits soluble guanylyl cyclases and inhibits class III ACs provokes the question concerning the evolution of these proteins and their disparate properties.

Taken together, the data add a novel aspect of heme b activity within the existing broad spectrum of physiological and toxic actions which applies to all cells and tissues. Heme is a known pro-oxidant and has pro-inflammatory and cytotoxic effects [49]. Heme b is further reported to be a signalling molecule regulating transcription factors and MAP kinases [45]. An important question is whether the concentrations of extracellular heme b under pathophysiological conditions are sufficient to attenuate AC activities [50]. Normally, concentrations of extracellular heme b are low (about 1 μM) and tightly controlled by binding to hemopexin, and, less specifically, to serum albumin. In addition, heme-oxygenase's effectively keep cytosolic heme b concentrations low under normal conditions [49,51]. However, in several haemolytic pathologies, such as sickle cell disease, extravascular haemolysis, malaria attacks, sepsis and septic shock, atherosclerosis, and after transfusion of packed red blood cells, heme b concentrations are reported to increase considerably [49,52]. Serum levels from 20 up to 350 μM have been observed [50,53]. Considering the low concentrations of heme b required for inhibition of hAC activities it may well contribute to pathologic symptoms which are common to these disease states. Therefore, this report may and should call medical attention to a central second messenger system in pathophysiological conditions of elevated heme b concentrations.

Funding

Funder	Grant reference number	Author
Deutsche Forschungsgemeinschaft	Sch275/45	Marius Landau Sherif Elsabbagh

The funders had no role in study design, data collection and interpretation, or the decision to submit the work for publication.

Credit author statement

SE, ML, AS, acquisition of data, analysis, and interpretation of data; SE, ML, culture of HEK293 cell lines transfected with human adenylyl cyclases, SE, HG interpretation of HPLC and MS data, JES, conception and design, analysis and interpretation of data, design of figures, writing manuscript.

Declaration of Competing Interest

None.

Data availability

Data will be made available on request.

Acknowledgements

We are indebted to Prof. Dr. P. Delepelaire, Univ. of Paris, for providing the HasA plasmid. We thank U. Kurz for a continuous supply of Gsα (Q227L), and Prof. Dr. A. Lupas for encouragement and support. Supported by the Deutsche Forschungsgemeinschaft and institutional funds from the Max-Planck-Society.

Appendix A. Appendix

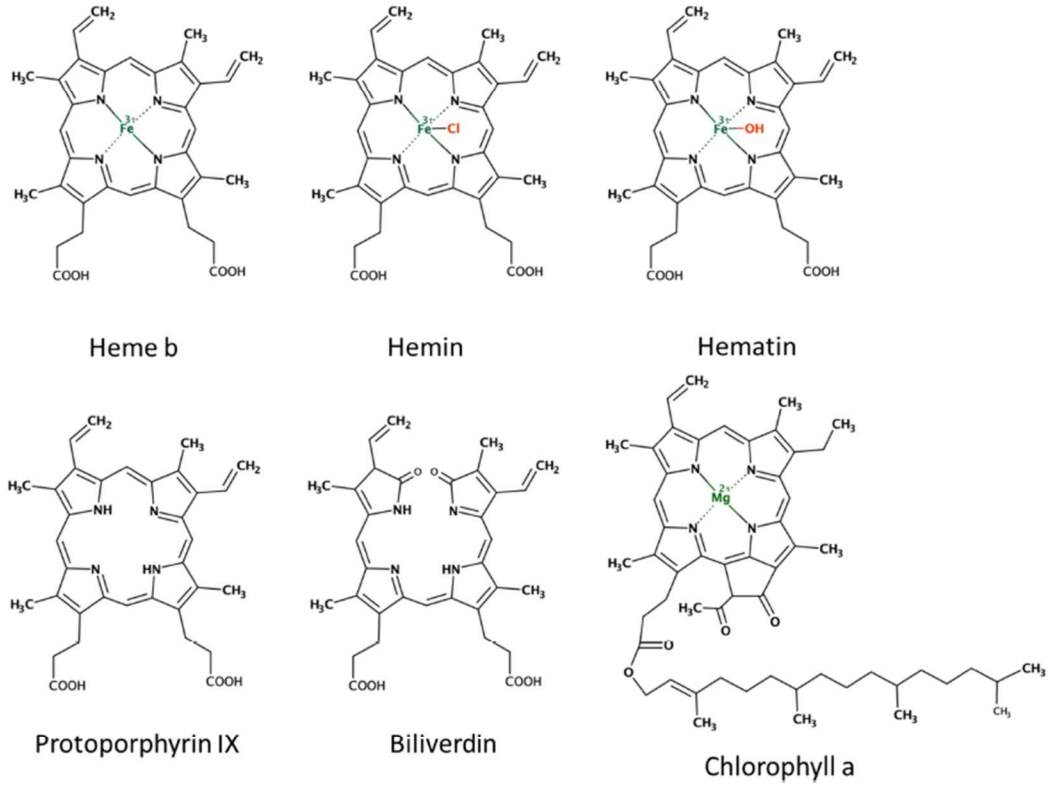

Appendix Fig. 1. Structures of Heme b and close congeners used in this study.

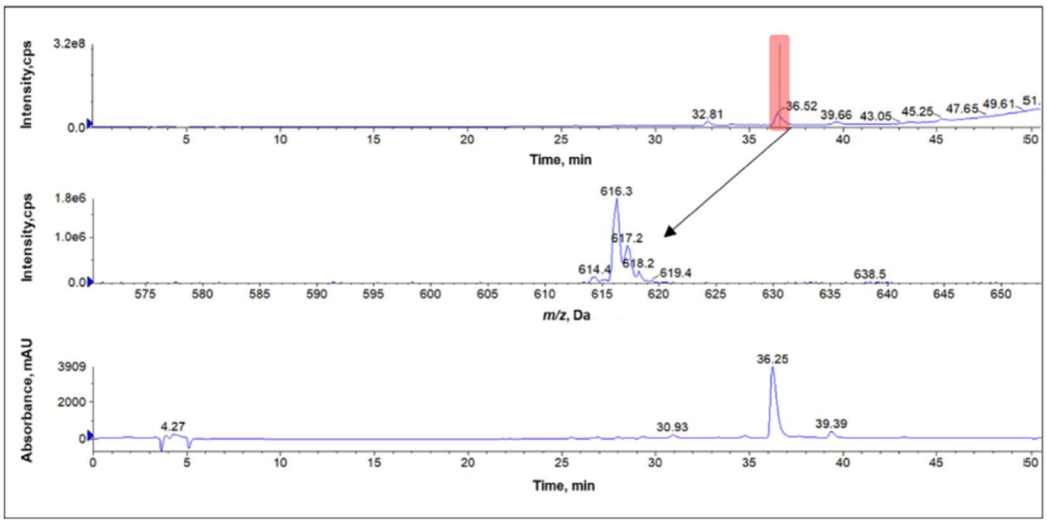

Appendix Fig. 2. Low-resolution-LC-MS of fraction O-3.
Top panel: LC-MS Total ion chromatogram (TIC) of fraction O-3.
Middle panel: MS spectrum of the peak at 36.52 min (shaded in red). It shows the dominant ion of *m/z* 616.3 $[Fe(III)PTP]^+$ and further ions at *m/z* 614, 617 and 618, corresponding to the predicted isotopic composition of Fe^{3+} (^{54}Fe, ^{57}Fe and ^{58}Fe).
Bottom panel: Extracted wavelength chromatogram (XWC) from 380 to 400 nm is shown.
Abbreviations: cps: counts per second, mAU: milli absorbance units

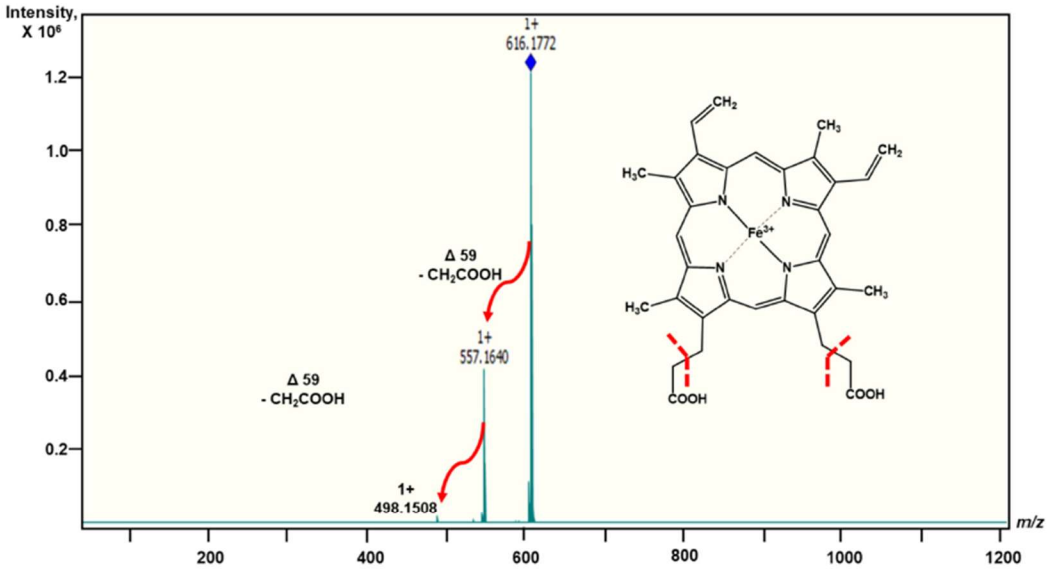

Appendix Fig. 3. HR-ESI-MS/MS spectrum of fraction O-3 and fragmentation pattern
m/z 616.1772 $[^{54}Fe(III)PTP]^+$ calculated for $C_{34}H_{32}{}^{54}FeN_4O_4$ *m/z* 616.1773, Δ (mass error) = −0.2 ppm. The x-axis is stretched such that the Fe-isotope pattern is not clearly visible (compare to appendix Fig. 2).

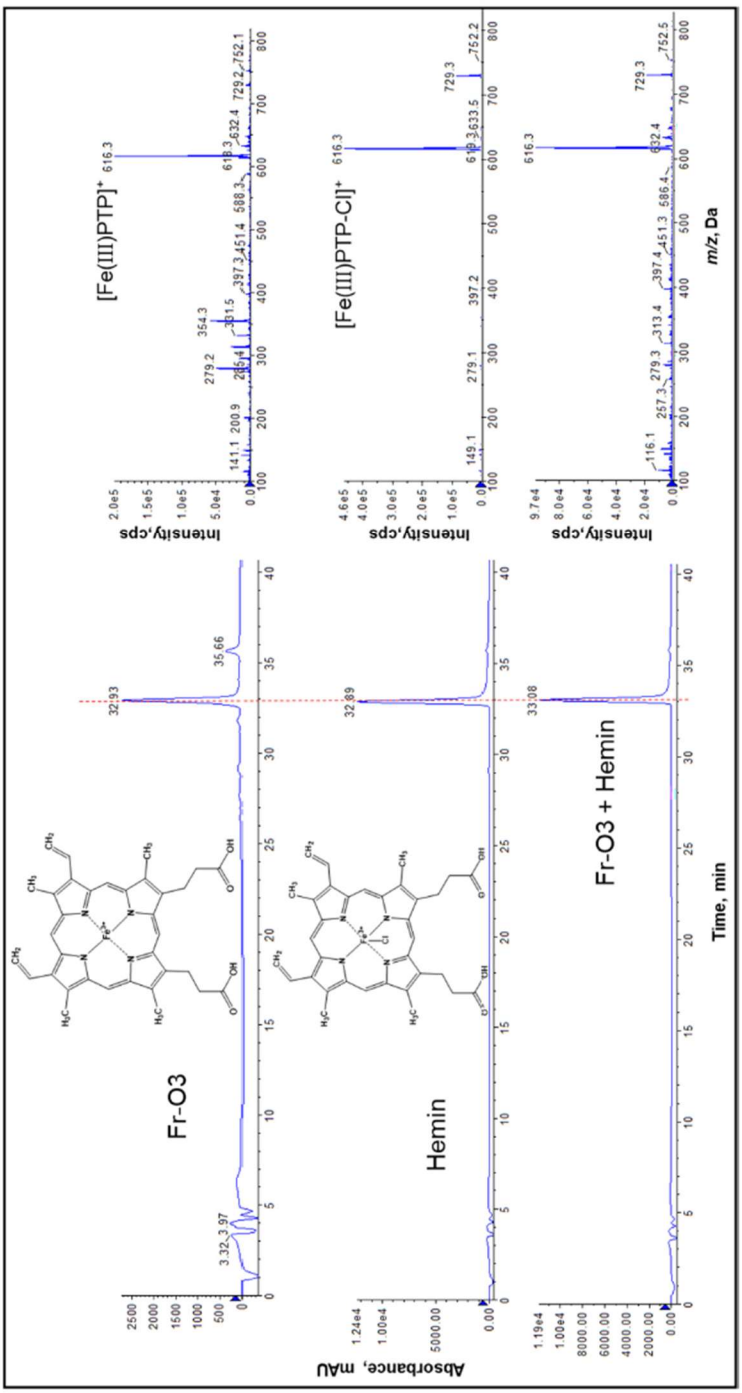

Appendix Fig. 4. Comparison of standard hemin and fraction O-3 harbouring heme b
Top panel:
Left: Extracted wavelength chromatogram (XWC) at 380 nm of an LC-MS run of fraction O-3 harbouring heme b.
Right: LR-MS spectrum, extracted at 32.93 min, showing the ion peak $[M\text{-}2H^{+}+Fe^{3+}]^{+}$ at *m/z* 616.3.
Middle panel:
Left: XWC at 380 nm of an LC-MS run of the reference compound hemin (ferric chloride heme).
Right: LR-MS spectrum, extracted at 32.89 min, showing a pseudo-molecular ion peak $[M\text{-}2H^{+}\text{-}Cl + Fe^{3+}]^{+}$ at *m/z* 616.3. In agreement with literature reports, the true chlorinated molecular ion of hemin $[M\text{-}2H^{+}+Cl + Fe^{3+}]^{+}$ was not detectable at *m/z* 651.3 under ESI-MS conditions.
Bottom panel:
Left: XWC at 380 nm of an LC-MS run of fraction O-3 and co-injected hemin standard. In agreement with literature reports [27], both compounds coelute forming a broader peak at a slightly higher retention time.
Right: LR-MS spectrum, extracted at 33.08 min, showing congruently the pseudo-molecular ion peak $[M\text{-}2H^{+}\text{-}Cl + Fe^{3+}]^{+}$ of hemin and the molecular ion $[M\text{-}2H^{+}+Fe^{3+}]^{+}$ of heme-b, both at *m/z* 616.3.
Abbreviations: cps: counts per second, mAU: milli absorbance units

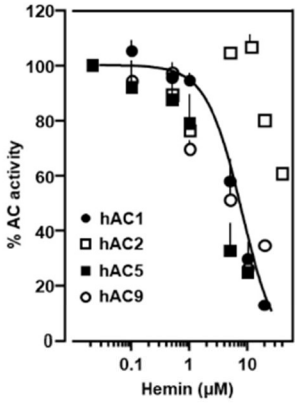

Appendix Fig. 5. Hemin inhibition of hAC basal activities
Basal activities of hAC1, 2, 5 and 9 were 0.016 ± 0.05, 0.03 ± 0.004, 0.013 ± 0.002 and 0.01 ± 0.003 nmol cAMP•mg^{-1}•min^{-1}, respectively. Hemin IC_{50} values against AC1, 2, 5 and 9 were 6.3, ≈ 40, 2 and 3 μM respectively. Error bars denote SEM of 3–4 experiments with two technical replicates.

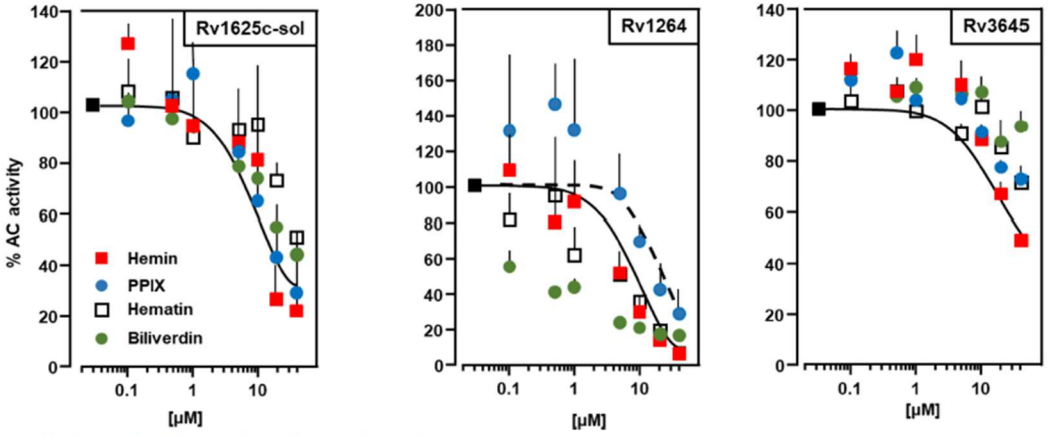

Appendix Fig. 6. Effect of hemin and its analogues on bacterial ACs.
Rv1625c soluble monomer (sol) basal activity (100%) was 52.7 ± 10.9 μmol cAMP•mg^{-1}•min^{-1}. Rv1264 basal activity (100%) was 10.18 ± 2.6 μmol cAMP•mg^{-1}•min^{-1}. Rv3645 basal activity (100%) was 0.93 ± 0.09 μmol cAMP•mg^{-1}•min^{-1}. Error bars denote SEM of 3–5 experiments.

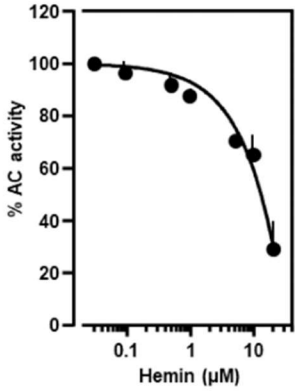

Appendix Fig. 7. Hemin inhibits basal activity of adenylyl cyclase in brain cortical membrane prepared from mouse
Basal activity (100%) was 0.238 ± 0.02 nmol cAMP•mg^{-1}•min^{-1}. Error bars denote SEM. $N = 3$. The calculated IC_{50} of hemin was 9 μM.

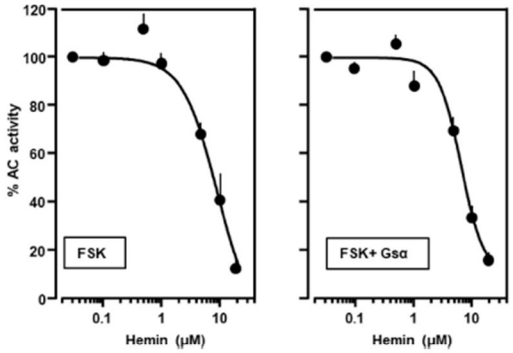

Appendix Fig. 8. Hemin inhibition of hAC5 activity stimulated by forskolin and forskolin + Gsα.
Left: Inhibition of 250 μM forskolin stimulated hAC5. 100% activity was 1.3 ± 0.5 nmol cAMP•mg^{-1}•min^{-1}. Basal activity was 0.008 ± 0.001 nmol cAMP•mg^{-1}•min^{-1}. Hemin IC_{50} concentration was 8.8 μM. Right: Inhibition of hAC5 activity stimulated by 10 μM forskolin and 300 nM Gsα. 100% stimulation was 3.44 ± 0.4 nmol cAMP•mg^{-1}•min^{-1}. The IC_{50} concentration of hemin was 6.9 μM. Error bars denote SEM of 3 experiments.

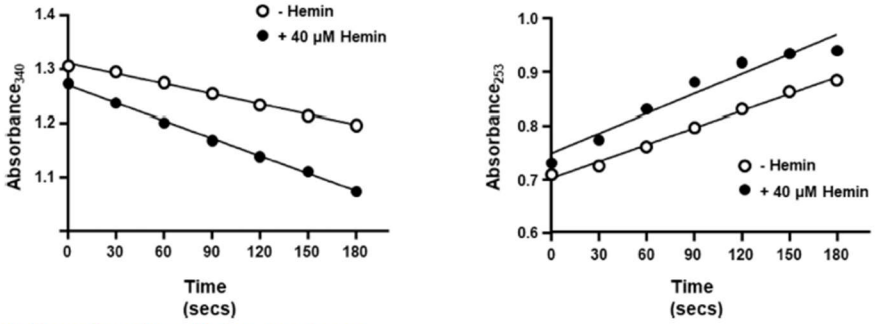

Appendix Fig. 9. Hemin effect on lactate dehydrogenase and trypsin.
Left: 40 μM hemin did not inhibit lactate dehydrogenase activity. Absorbance at 340 nm was recorded for 3 mins.
Right: Trypsin activity was not affected by hemin. Absorbance at 253 nm was monitored for 3 min.

Appendix Table 1
Basal and Gsα stimulated activities of hACs cultured in HEK293 cells.

hAC isoform	Basal Activity nmol cAMP•mg^{-1}•min^{-1}	300 nM Gsα stimulated Activity nmol cAMP•mg^{-1}•min^{-1}	IC_{50} of hemin (μM)
AC1	0.07 ± 0.02	0.3 ± 0.06	10
AC2	0.19 ± 0.08	2.82 ± 0.79	7.4
AC3	0.02 ± 0.01	0.2 ± 0.03	8.5
AC4	0.01 ± 0.01	0.11 ± 0.05	5.5
AC5	0.05 ± 0.01	1.76 ± 0.37	8.4
AC5 (Porcine hemin)	0.01 ± 0.004	1.21 ± 0.05	8.6
AC6	0.01 ± 0.01	0.11 ± 0.01	7.5
AC7	0.01 ± 0.002	0.14 ± 0.05	7.9
AC8	0.21 ± 0.03	2.27 ± 0.78	13.7
AC9	0.04 ± 0.01	1.38 ± 0.09	12

Activities are mean ± SEM. $N = 3$–4 with 2–3 technical repetitions each.
Porcine hemin was ≥98% pure.

Appendix Table 2
IC_{50} values (μM) of hemin and its analogues against ACs.

	Hemin	Protoporphyrin IX	Hematin	Biliverdin
hAC5	8.5	≈ 100	> 100	≈ 1000
Rv1625c	11	≈ 100	≈ 100	> 100
Rv3645	14	≈ 100	> 100	> 100
Rv1625c soluble monomer	12	10(1)	≈ 30	≈ 40
Rv1264	6	≈ 20(2)	≈ 10	≈ 1
CyaG	15	> 100	≈ 80	≈ 20

Significances:
(1) Rv1625c soluble monomer; PPIX IC_{50} differs significantly from hematin and biliverdin, $p < 0.05$.
(2) Rv1264; PPIX IC_{50} differs significantly from hemin, $p < 0.05$, and hematin and biliverdin, $p < 0.01$.

Appendix Table 3
Basal and isoproterenol stimulated activities of hACs transfected in HEK293 cells.

hAC isoform	Basal activity cAMP pmol/20 μL	Isoproterenol stimulated activity cAMP pmol/20 μL
AC3	0.05 ± 0.03	1.92 ± 0.69
AC5	0.89 ± 0.25	1.95 ± 0.54
AC7	0.32 ± 0.01	0.43 ± 0.07
AC9	0.21 ± 0.04	0.72 ± 0.01

Activities are mean ± SEM. N = 3–4 with two technical repetitions each.

References

[1] K.F. Ostrom, et al., Physiological roles of mammalian transmembrane adenylyl cyclase isoforms, Physiol. Rev. 102 (2022) 815–857.
[2] C.W. Desseauer, et al., International Union of Basic and Clinical Pharmacology. CI. Structures and small molecule modulators of mammalian adenylyl Cyclases, Pharmacol. Rev. 69 (2017) 93–139.
[3] W.J. Tang, A.G. Gilman, Type-specific regulation of adenylyl cyclase by G protein beta gamma subunits, Science 254 (1991) 1500–1503.
[4] W.J. Tang, A.G. Gilman, Adenylyl cyclases, Cell 70 (1992) 869–872.
[5] R.K. Sunahara, R. Taussig, Isoforms of mammalian adenylyl cyclase: multiplicities of signaling, Mol. Interv. 2 (2002) 168–184.
[6] J. Krupinski, et al., Adenylyl cyclase amino acid sequence: possible channel- or transporter-like structure, Science 244 (1989) 1558–1564.
[7] J.E. Schultz, The evolutionary conservation of eukaryotic membrane-bound adenylyl cyclase isoforms, Front. Pharmacol. 13 (2022) 1009797.
[8] J.E. Schultz, S. Klumpp, R. Benz, W.J. Schurhoff-Goeters, A. Schmid, Regulation of adenylyl cyclase from Paramecium by an intrinsic potassium conductance, Science 255 (1992) 600–603.
[9] J.E. Schultz, J. Natarajan, Regulated unfolding: a basic principle of intraprotein signaling in modular proteins, Trends Biochem. Sci. 38 (2013) 538–545.
[10] Y.L. Guo, T. Seebacher, U. Kurz, J.U. Linder, J.E. Schultz, Adenylyl cyclase Rv1625c of mycobacterium tuberculosis: a progenitor of mammalian adenylyl cyclases, EMBO J. 20 (2001) 3667–3675.
[11] K. Kanchan, et al., Transmembrane signaling in chimeras of the Escherichia coli aspartate and serine chemotaxis receptors and bacterial class III adenylyl cyclases, J. Biol. Chem. 285 (2010) 2090–2099.
[12] S. Beltz, J. Bassler, J.E. Schultz, Regulation by the quorum sensor from Vibrio indicates a receptor function for the membrane anchors of adenylate cyclases, Elife 5 (2016).
[13] T. Seebacher, J.U. Linder, J.E. Schultz, An isoform-specific interaction of the membrane anchors affects mammalian adenylyl cyclase type V activity, Eur. J. Biochem. 268 (2001) 105–110.

[14] M. Ziegler, et al., A novel signal transducer element intrinsic to class IIIa and IIIb adenylate cyclases, FEBS J. 284 (2017) 1204–1217.
[15] J. Bassler, J.E. Schultz, A.N. Lupas, Adenylate cyclases: receivers, transducers, and generators of signals, Cell. Signal. 46 (2018) 135–144.
[16] C. Qi, S. Sorrentino, O. Medalia, V.M. Korkhov, The structure of a membrane adenylyl cyclase bound to an activated stimulatory G protein, Science 364 (2019) 389–394.
[17] A. Seth, M. Finkbeiner, J. Grischin, J.E. Schultz, Gsalpha stimulation of mammalian adenylate cyclases regulated by their hexahelical membrane anchors, Cell. Signal. 68 (2020), 109538.
[18] S. Diel, K. Klass, B. Wittig, C. Kleuss, Gbetagamma activation site in adenylyl cyclase type II. Adenylyl cyclase type III is inhibited by Gbetagamma, J. Biol. Chem. 281 (2006) 288–294.
[19] M.P. Graziano, M. Freissmuth, A.G. Gilman, Expression of Gs alpha in Escherichia coli. Purification and properties of two forms of the protein, J. Biol. Chem. 264 (1989) 409–418.
[20] M.P. Graziano, M. Freissmuth, A.G. Gilman, Purification of recombinant Gs alpha, Methods Enzymol. 195 (1991) 192–202.
[21] T.A. Baldwin, Y. Li, C.S. Brand, V.J. Watts, C.W. Dessauer, Insights into the regulatory properties of human adenylyl cyclase type 9, Mol. Pharmacol. 95 (2019) 349–360.
[22] M.G. Cumbay, V.J. Watts, Novel regulatory properties of human type 9 adenylate cyclase, J. Pharmacol. Exp. Ther. 310 (2004) 108–115.
[23] M. Soto-Velasquez, M.P. Hayes, A. Alpsoy, E.C. Dykhuizen, V.J. Watts, A novel CRISPR/Cas9-based cellular model to explore adenylyl cyclase and cAMP signaling, Mol. Pharmacol. 94 (2018) 963–972.
[24] J.E. Schultz, B.H. Schmidt, Treatment of rats with thyrotropin (TSH) reduces the adrenoceptor sensitivity of adenylate cyclase from cerebral cortex, Neurochem. Int. 10 (1987) 173–178.
[25] E.G. Bligh, W.J. Dyer, A rapid method of total lipid extraction and purification, Can. J. Biochem. Physiol. 37 (1959) 911–917.
[26] M. Gledhill, The detection of iron protoporphyrin (heme b) in phytoplankton and marine particulate material by electrospray ionisation mass spectrometry - comparison with diode array detection, Anal. Chim. Acta 841 (2014) 33–43.
[27] Y. Isaji, N.O. Ogawa, Y. Takano, N. Ohkouchi, Quantification and carbon and nitrogen isotopic measurements of Heme B in environmental samples, Anal. Chem. 92 (2020) 11213–11222.
[28] M.S. Detzel, et al., Revisiting the interaction of heme with hemopexin, Biol. Chem. 402 (2021) 675–691.
[29] E. Tolosano, F. Altruda, Hemopexin: structure, function, and regulation, DNA Cell Biol. 21 (2002) 297–306.
[30] E. Tolosano, S. Fagoonee, N. Morello, F. Vinchi, V. Fiorito, Heme scavenging and the other facets of hemopexin, Antioxid. Redox Signal. 12 (2010) 305–320.
[31] N. Izadi, et al., Purification and characterization of an extracellular heme-binding protein, HasA, involved in heme iron acquisition, Biochemistry 36 (1997) 7050–7057.
[32] R. Glueck, D. Green, I. Cohen, C.H. Ts'ao, Hematin: unique effects of hemostasis, Blood 61 (1983) 243–249.
[33] B. Andria, et al., Biliverdin protects against liver ischemia reperfusion injury in swine, PLoS One 8 (2013), e69972.
[34] K. Winkler, A. Schultz, J.E. Schultz, The S-helix determines the signal in a Tsr receptor/adenylyl cyclase reporter, J. Biol. Chem. 287 (2012) 15479–15488.
[35] Tews, et al., The structure of a pH-sensing mycobacterial adenylyl cyclase holoenzyme, Science 308 (2005) 1020–1023.
[36] J.E. Owen, G.M. Bishop, S.R. Robinson, Uptake and toxicity of hemin and Iron in cultured mouse astrocytes, Neurochem. Res. 41 (2016) 298–306.
[37] V.C. Tsolaki, et al., Hemin accumulation and identification of a heme-binding protein clan in K562 cells by proteomic and computational analysis, J. Cell. Physiol. 237 (2022) 1315–1340.
[38] V. Jeney, et al., Pro-oxidant and cytotoxic effects of circulating heme, Blood 100 (2002) 879–887.
[39] C. Sanabra, G. Mengod, Neuroanatomical distribution and neurochemical characterization of cells expressing adenylyl cyclase isoforms in mouse and rat brain, J. Chem. Neuroanat. 41 (2011) 43–54.
[40] W. Durante, et al., cAMP induces heme oxygenase-1 gene expression and carbon monoxide production in vascular smooth muscle, Am. J. Phys. 273 (1997) H317–H323.
[41] S. Immenschuh, et al., Transcriptional activation of the haem oxygenase-1 gene by cGMP via a cAMP response element/activator protein-1 element in primary cultures of rat hepatocytes, Biochem. J. 334 (Pt 1) (1998) 141–146.
[42] S. Immenschuh, et al., The rat heme oxygenase-1 gene is transcriptionally induced via the protein kinase a signaling pathway in rat hepatocyte cultures, Mol. Pharmacol. 53 (1998) 483–491.
[43] T. Szkudelski, K. Frackowiak, K. Szkudelska, Hemin attenuates response of primary rat adipocytes to adrenergic stimulation, PeerJ 9 (2021), e12092.
[44] H.M. Lander, D.M. Levine, A. Novogrodsky, Hemin stimulation of cAMP production in human lymphocytes, FEBS Lett. 303 (1992) 242–246.
[45] S.M. Mense, L. Zhang, Heme: a versatile signaling molecule controlling the activities of diverse regulators ranging from transcription factors to MAP kinases, Cell Res. 16 (2006) 681–692.
[46] S. Schneider, J. Marles-Wright, K.H. Sharp, M. Paoli, Diversity and conservation of interactions for binding heme in b-type heme proteins, Nat. Prod. Rep. 24 (2007) 621–630.
[47] Y. Kang, R. Liu, J.X. Wu, L. Chen, Structural insights into the mechanism of human soluble guanylate cyclase, Nature 574 (2019) 206–210.
[48] P.M. Schmidt, M. Schramm, H. Schroder, F. Wunder, J.P. Stasch, Identification of residues crucially involved in the binding of the heme moiety of soluble guanylate cyclase, J. Biol. Chem. 279 (2004) 3025–3032.
[49] S. Immenschuh, V. Vijayan, S. Janciauskiene, F. Gueler, Heme as a target for therapeutic interventions, Front. Pharmacol. 8 (2017) 146.
[50] M.T. Hopp, et al., Heme determination and quantification methods and their suitability for practical applications and everyday use, Anal. Chem. 92 (2020) 9429–9440.
[51] S. Kumar, U. Bandyopadhyay, Free heme toxicity and its detoxification systems in human, Toxicol. Lett. 157 (2005) 175–188.
[52] A.P. Pietropaoli, et al., Total plasma heme concentration increases after red blood cell transfusion and predicts mortality in critically ill medical patients, Transfusion 59 (2019) 2007–2015.
[53] U. Muller-Eberhard, J. Javid, H.H. Liem, A. Hanstein, M. Hanna, Plasma concentrations of hemopexin, haptoglobin and heme in patients with various hemolytic diseases, Blood 32 (1968) 811–815.

3.3 Publication III:

Landau, M., Elsabbagh, S., Gross, H., Fuchs, A., Schultz, A., Schultz, J.E. (2024). The membrane domains of mammalian adenylyl cyclases are lipid receptors.
Elife 2024 Vol. 13
https://doi.org/10.7554/eLife.101483.3

Position in list of authors: 1

Personal contributions:

Designed, carried out and analyzed experiments for the data represented in figures 4, 6, 7, 9 B-E and 10 and in part for figure 1D.

Maintained cell culture, transfected cell lines and harvested membranes for testing.

Extraction and fractionation of lung tissue.

Revised and edited the manuscript together with all authors.

Estimated contribution: 50%.

RESEARCH ARTICLE

The membrane domains of mammalian adenylyl cyclases are lipid receptors

Marius Landau[1], Sherif Elsabbagh[1], Harald Gross[1], Adrian CD Fuchs[2], Anita CF Schultz[1], Joachim E Schultz[1]*

[1]Pharmazeutisches Institut der Universität Tübingen, Tübingen, Germany; [2]Max-Planck-Institut für Biologie, Tübingen, Germany

eLife Assessment

This manuscript describes an **important** study of a new lipid-mediated regulation mechanism of adenylyl cyclases. The biochemical evidence provided is **convincing** and will trigger more research in this mechanism. This manuscript will be of interest to all scientists working on lipid regulation and adenylyl cyclases.

Abstract The biosynthesis of cyclic 3′,5′-adenosine monophosphate (cAMP) by mammalian membrane-bound adenylyl cyclases (mACs) is predominantly regulated by G-protein-coupled receptors (GPCRs). Up to now the two hexahelical transmembrane domains of mACs were considered to fix the enzyme to membranes. Here, we show that the transmembrane domains serve in addition as signal receptors and transmitters of lipid signals that control Gsα-stimulated mAC activities. We identify aliphatic fatty acids and anandamide as receptor ligands of mAC isoforms 1–7 and 9. The ligands enhance (mAC isoforms 2, 3, 7, and 9) or attenuate (isoforms 1, 4, 5, and 6) Gsα-stimulated mAC activities in vitro and in vivo. Substitution of the stimulatory membrane receptor of mAC3 by the inhibitory receptor of mAC5 results in a ligand inhibited mAC5–mAC3 chimera. Thus, we discovered a new class of membrane receptors in which two signaling modalities are at a crossing, direct tonic lipid and indirect phasic GPCR–Gsα signaling regulating the biosynthesis of cAMP.

***For correspondence:** joachim.schultz@uni-tuebingen.de

Competing interest: The authors declare that no competing interests exist.

Funding: See page 20

Sent for Review
06 August 2024
Preprint posted
07 August 2024
Reviewed preprint posted
01 October 2024
Reviewed preprint revised
23 October 2024
Version of Record published
29 November 2024

Reviewing Editor: Volker Dötsch, Goethe University Frankfurt, Germany

Introduction

The structure of the first second messenger, cyclic 3′,5′-adenosine monophosphate (cAMP), was reported in 1958 by Sutherland and Rall. It was generated by incubation of a liver extract with the first messengers adrenaline or glucagon (***Sutherland and Rall, 1958***). Since then, cAMP has been demonstrated to be an almost universal second messenger used to translate various extracellular stimuli into a uniform intracellular chemical signal (***Dessauer et al., 2017***; ***Ostrom et al., 2022***). The biosynthetic enzymes for cAMP from ATP, adenylyl cyclases (ACs), have been biochemically investigated in bacteria and eukaryotic cells (***Khandelwal and Hamilton, 1971***; ***Linder and Schultz, 2003***; ***Linder and Schultz, 2008***). Finally in 1989, the first mammalian AC was sequenced (***Krupinski et al., 1989***). The protein displayed two catalytic domains (C1 and C2) which are highly similar in all isoforms. The two hexahelical membrane anchors (TM1 and TM2) are dissimilar and isoform specifically conserved (***Bassler et al., 2018***). The latter were proposed to possess a channel or transporter-like function, properties, which were never confirmed (***Krupinski et al., 1989***). The domain architecture of mammalian ACs, TM1–C1–TM2–C2, clearly indicated a pseudoheterodimeric protein composed of two concatenated monomeric bacterial precursor proteins (***Guo et al., 2001***). To date, sequencing has identified nine mammalian membrane-delimited AC isoforms (mACs) with identical domain architectures (***Dessauer et al., 2017***). In all nine isoforms the catalytic domains are conserved and share extensive sequence

and structural similarities which indicate a similar biosynthetic mechanism (**Linder and Schultz, 2003**; **Linder and Schultz, 2008**; **Tesmer et al., 1997**; **Sinha and Sprang, 2006**). On the other hand, the associated two membrane domains differ substantially within each isoform and between all nine mAC isoforms (**Bassler et al., 2018**; **Schultz, 2022**; **Tang and Gilman, 1995**). Bioinformatic studies, however, revealed that the membrane domains, TM1 as well as TM2, are highly conserved in an isoform-specific manner for about 0.5 billion years of evolution (**Bassler et al., 2018**; **Schultz, 2022**).

Extensive studies on the regulation of the nine mAC isoforms revealed that the Gsα subunit of the trimeric G proteins activate cAMP formation. Gsα is released intracellularly upon stimulation of G-protein-coupled receptors (GPCRs), i.e., the receptor function for mAC regulation was assigned to the diversity of GPCRs, which presently are most prominent drug targets. In 1995 Tang and Gilman reported that Gsα regulation of mammalian mACs does not require the presence of the membrane anchors. A soluble C1–C2 dimer devoid of the membrane domains was fully activated by Gsα (**Tang and Gilman, 1995**). This reinforced the view that the mAC membrane anchors which comprise up to 40% of the protein were just that and otherwise functionally inert. The theoretical possibility of mACs to be regulated directly, bypassing the GPCRs, was dismissed (**Schuster et al., 2024**).

We were intrigued by the exceptional evolutionary conservation of the mAC membrane anchors for 0.5 billion years (**Bassler et al., 2018**; **Schultz, 2022**). In addition, we identified a cyclase-transducing element that connects the TM1 and TM2 domains to the attached C1 or C2 catalytic domains. These transducer elements are similarly conserved in a strictly isoform-specific manner (**Schultz, 2022**; **Ziegler, 2017**). Furthermore, cryo-EM structures of mAC holoenzymes clearly revealed that the two membrane domains, TM1 and TM2, collapse into a tight dodecahelical complex resembling membrane receptors (**Qi et al., 2019**; **Qi et al., 2022**; **Gu et al., 2001**). Lastly, we created a chimeric model involving the hexahelical quorum-sensing receptor from *Vibrio cholerae* which has a known aliphatic lipid ligand and the mAC 2 isoform. We observed that the ligand directly affected, i.e., attenuated the Gsα activation of mAC2 (**Seth et al., 2020**). As a proof-of-concept this demonstrated that the cytosolic catalytic AC dimer serves as a receiver for extracellular signals transmitted through the dyad-related membrane anchor. Accordingly, we proposed a general model of mAC regulation in which the extent of the indirect mAC activation via the GPCR/Gsα axis is under direct ligand control via the mAC membrane anchor (**Seth et al., 2020**).

Here, we report the results of a rigorous search for potential ligands of the mAC membrane domains. We identified aliphatic lipids as ligands for mAC isoforms 1–7 and 9. Isoform dependently, the ligands either attenuate or enhance Gsα activation in vitro and in vivo demonstrating a receptor function of the mAC proteins. The receptor properties are transferable as demonstrated by interchanging the membrane anchors between mAC3 and 5. Thus, the results define a new class of membrane receptors and establish a completely new level of regulation of cAMP biosynthesis in mammals in which tonic and phasic signaling processes intersect in a central signaling system, which is the target of frequently used drugs.

Results

Oleic acid enhances Gsα-stimulated mAC3, but not mAC5 activity

In earlier experiments, we demonstrated regulation of the mycobacterial AC Rv2212 by lipids (**Abdel Motaal et al., 2006**), the presence of oleic acid in the mycobacterial AC Rv1264 structure (**Findeisen et al., 2007**), and regulation of a chimera consisting of the quorum-sensing receptor from *Vibrio* and the mAC2 catalytic dimer by the aliphatic lipid 3-hydroxytridecan-4-one (**Beltz et al., 2016**). Therefore, we searched for lipids as ligands. Here, we used bovine lung as a starting material because lipids are important for lung development and function (**Änggård and Samuelsson, 1965**; **Dautel et al., 2017**). Lipids were extracted from a cleared lung homogenate, acidified to pH 1, with dichloromethane/methanol (2:1). The dried organic phase was chromatographed on silica gel (employing vacuum liquid chromatography; Si-VLC) and fractions A to Q were assayed (**Figure 1—figure supplement 1**). Fraction E enhanced mAC3 activity stimulated by 300 nM Gsα fourfold, whereas mAC5 activity was unaffected (**Figure 1A**). The non-maximal concentration of 300 nM Gsα was used because it enabled us to observe stimulatory as well as inhibitory effects.

Fraction E was further separated by reversed-phase high-performance liquid chromatography (RP-HPLC) into five subfractions (E1–E5; **Figure 1—figure supplement 2**). The mAC3 enhancing

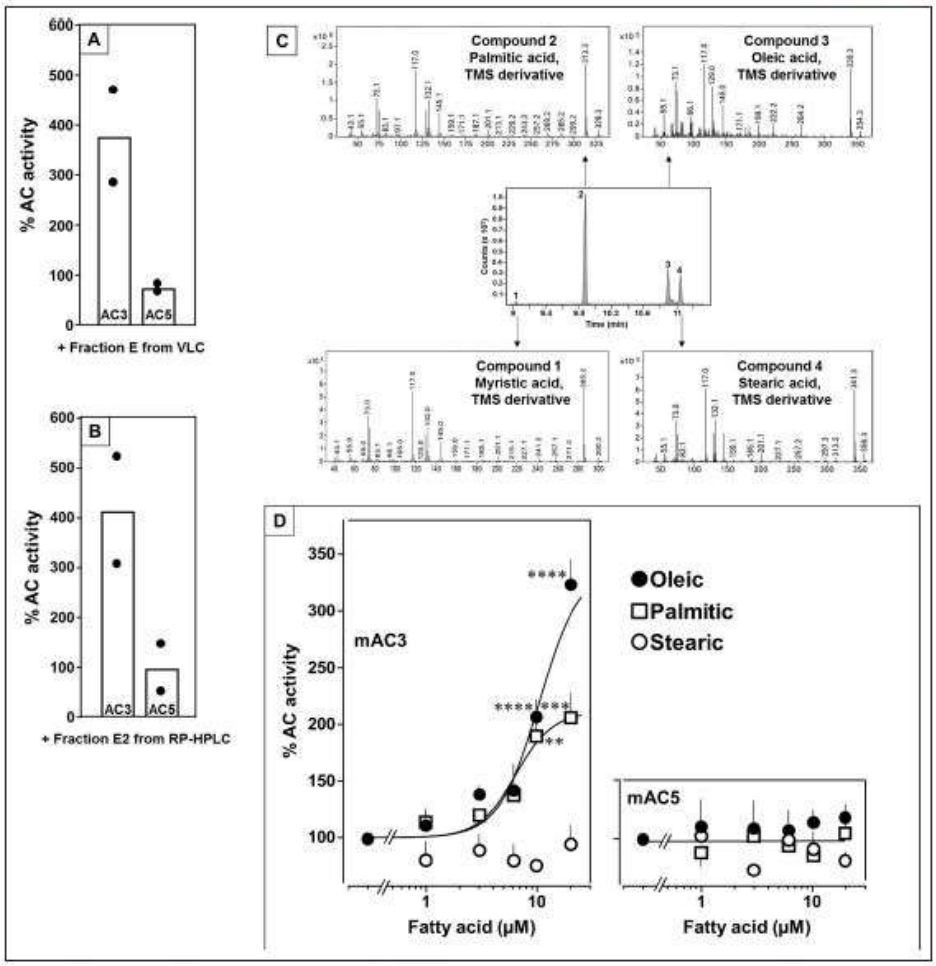

Figure 1. Identification of mAC3 activating fatty acids. Effect of 1 µg/assay of fractions E from vacuum liquid chromatography (**A**) and E2 from reversed-phase high-performance liquid chromatography (RP-HPLC) (**B**) on 300 nM Gsα-stimulated mAC isoforms 3 and 5. Activities are shown as % compared to 300 nM Gsα stimulation (100%). $n = 2$, each with two technical replicates. Basal and Gsα activities of mAC3 in (**A**) were 0.01 and 0.07 and of mAC5 0.06 and 1.32 nmol cAMP•mg^{-1}•min^{-1}, respectively. In (**B**), basal and Gsα activities of mAC3 were 0.02 and 0.12 and of mAC5 0.09 and 1.1 nmol cAMP•mg^{-1}•min^{-1}, respectively. (**C**) Gas chromatography–mass spectrometry (GC–MS) chromatogram of fraction E2. Mass spectra of the fatty acids are shown. Fatty acids' identity was confirmed by comparing with corresponding standards (TMS: Trimethylsilyl). (**D**) Effect of fatty acids identified by GC–MS on 300 nM Gsα-stimulated mAC3 (left) and mAC5 (right). Basal and Gsα activities of mAC3 were 0.023 ± 0.02 and 0.17 ± 0.03 and of mAC5 0.08 ± 0.02 and 0.44 ± 0.09 nmol cAMP•mg^{-1}•min^{-1}, respectively. $n = 3$–23. EC_{50} of palmitic and oleic acids for mAC3 were 6.4 and 10.4 µM, respectively. Data represent individual experiments (black dots in A and B) or mean ± SEM (D). One-sample *t* tests were performed. Significances: **p < 0.01; ***p < 0.001; ****p < 0.0001.

The online version of this article includes the following source data and figure supplement(s) for figure 1:

Figure supplement 1. Si-VLC: silica-vacuum liquid chromatography, RP-HPLC: reversed-phase high-performance liquid chromatography, EA: ethyl acetate, PE: petroleum ether, MeOH: methanol.

Figure supplement 2. Reversed-phase high-performance liquid chromatography (RP-HPLC) chromatogram of fraction E.

Figure 1 continued on next page

Figure 1 continued

Figure supplement 3. NMR spectra of fraction E2 in d_4-MeOH.

Figure supplement 4. Time-dependent stimulation of mAC3 by oleic acid.

Figure supplement 5. Hanes–Woolf plot of mAC3 ± 20 µM oleic acid.

Figure supplement 6. Oleic acid has no stimulatory effect on the soluble catalytic dimer.

Source data 1. Including data used for generating ***Figure 1A, B, D***.

Figure supplement 4—source data 1. Including data used for generating ***Figure 1—figure supplement 4***.

Figure supplement 5—source data 1. Including data used for generating ***Figure 1—figure supplement 5***.

Figure supplement 6—source data 1. Including data used for generating ***Figure 1—figure supplement 6***.

constituents appeared in fraction E2. It enhanced Gsα-stimulated mAC3 fourfold but had no effect on mAC5 (***Figure 1B***). ^{1}H- and ^{13}C-NMR spectra of fraction E2 indicated the presence of aliphatic lipids (***Figure 1—figure supplement 3***). Subsequent GC/MS analysis identified palmitic, stearic, oleic, and myristic acid in E2 (***Figure 1C***). Concentration–response curves were established for these fatty acids with mAC3 and mAC5 stimulated by 300 nM Gsα (***Figure 1D***). 20 µM oleic acid enhanced Gsα-stimulated mAC3 activity threefold (EC_{50} = 10.4 µM) and 20 µM palmitic acid twofold (EC_{50} = 6.4 µM), while stearic or myristic acid had no significant effect. None of these fatty acids affected mAC5 activity (***Figure 1D***).

The action of oleic acid on mAC3 was linear for >25 min (***Figure 1—figure supplement 4***). The Km of mAC3 for ATP (335 µM) was unaffected. Vmax was increased from 0.62 to 1.23 nmol cAMP/mg/min (***Figure 1—figure supplement 5***). Oleic acid did not affect the activity of a soluble, Gsα-stimulated construct formerly used for generating a C1 and C2 catalytic dimer from mAC1 and 2, ruling out spurious detergent effects (***Tang and Gilman, 1995***; ***Figure 1—figure supplement 6***). The effect of oleic acid was further evaluated by Gsα concentration–response curves of mAC3 and mAC5 in presence and absence of 20 µM oleic acid (***Figure 2***, left and center). For mAC3 the calculated EC_{50} of Gsα

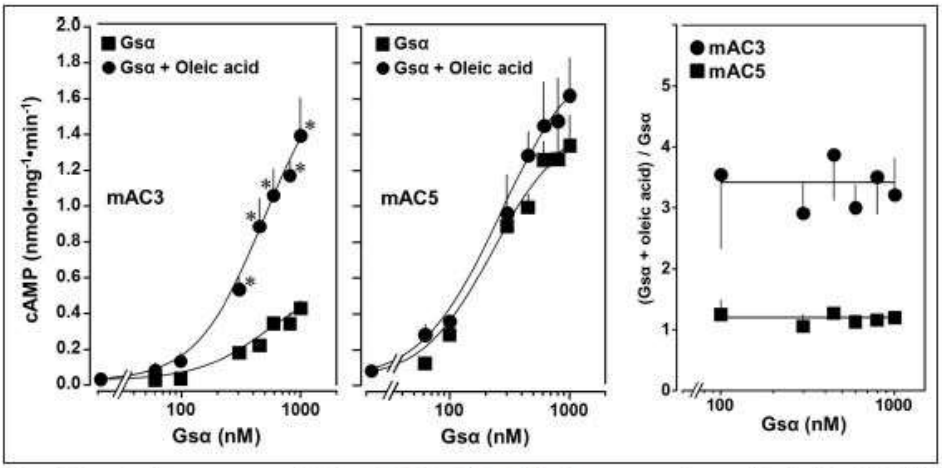

Figure 2. Concentration–response curves for Gsα and mAC3 and five activities in presence or absence of 20 µM oleic acid. 20 µM oleic acid enhances Gsα stimulation of mAC3 (left) but not of mAC5 (center). (Left) EC_{50} of Gsα in the absence of oleic acid was 549 nM and in the presence of 20 µM oleic acid, it was 471 nM (not significant). mAC3 basal activity was 30 ± 24 pmol cAMP•mg^{-1}•min^{-1}. *n* = 3, each with two technical replicates. (Center) The EC_{50} of Gsα in the absence of oleic acid was 245 nM and in the presence of oleic acid, it was 277 nM (not significant). mAC5 basal activity was 84 ± 60 cAMP•mg^{-1}•min^{-1}. *n* = 2, each with two technical replicates. (Right) (Gsα + oleic acid stimulation)/(Gsα stimulation) ratio of mAC3 and mAC5 from left and center (*n* = 2–3). Data are mean ± SEM, paired *t* test for left and center, and one-way ANOVA for right. Significances: *p < 0.05.

The online version of this article includes the following source data for figure 2:

Source data 1. Including data used for generating ***Figure 2***, left, center, and right.

Table 1. List of lipids tested against mAC isoforms.

Lauric (dodecanoic) acid
Myristic (tetradecanoic) acid
Myristoleic ((9Z)-tetradecenoic) acid
Palmitic (hexadecanoic) acid
Palmitoleic ((9Z)-hexadecenoic) acid
Octadecane
1,18-Octadecanedicarboxylic acid
Stearic (octadecanoic) acid
9-Hydroxystearic acid
Oleic ((9Z)-octadecenoic) acid
Oleamide ((9Z)-octadecenamide)
Methyl oleate
2-Oleoylglycerol
Triolein
Elaidic ((9E)-octadecenoic) acid
cis-Vaccenic ((11E)-octadecenoic) acid
Linoleic ((9Z,12Z)-octadecadienoic) acid
Linolenic ((9Z,12Z,15Z)-octadecatrienoic) acid
Arachidonic ((5Z,8Z,11Z,14Z)-eicosatetraenoic) acid
Eicosapentaenoic ((5Z,8Z,11Z,14Z,17Z)-eicosapentaenoic) acid

in presence and absence of oleic acid were 549 and 471 nM, respectively (not significant). Over the Gsα concentration range tested with mAC3 the enhancement of cAMP formation by 20 µM oleic was uniformly about 3.4-fold (***Figure 2***, right). In the case of mAC5, Gsα stimulation was not enhanced by oleic acid (***Figure 2***, center and right).

To explore the ligand space, we tested 18 aliphatic C_{12} to C_{20} lipids (***Table 1***; structures in ***Figure 3—figure supplement 1***). At 20 µM, elaidic, *cis*-vaccenic and linoleic acids were efficient enhancers of Gsα-stimulated mAC3 activity. Palmitic, palmitoleic, linolenic, eicosa-pentaenoic acids, and oleamide were less efficacious; other compounds were inactive (***Figure 3***). Notably, the saturated C_{18} stearic acid was inactive here and throughout, albeit otherwise variations in chain length, and the number, location, and conformation of double bonds were tolerated to some extent, e.g., *cis*-vaccenic, linoleic, and linolenic acids. The relaxed ligand specificity was anticipated as aliphatic fatty acids are highly bendable and bind to a flexible dodecahelical protein dimer embedded in a fluid lipid membrane. The ligand space of mAC3 somewhat resembled the fuzzy and overlapping ligand specificities of the free fatty acid receptors 1 and 4 (***Kimura et al., 2020***; ***Samovski et al., 2023***; ***Grundmann et al., 2021***).

Next, the effect of oleic acid was probed in vivo using HEK293 cells permanently transfected with mAC3 (HEK-mAC3) or mAC5 (HEK-mAC5). Intracellular cAMP formation via Gsα was triggered via stimulation of the endogenous β-receptor with 2.5 µM of the β-agonist isoproterenol (concentration of isoproterenol is based on a respective concentration–response curve with HEK-mAC3 cell; see ***Figure 4—figure supplement 1***). Addition of oleic acid enhanced cAMP formation in HEK-mAC3 1.5-fold (***Figure 4***). Stearic acid was inactive. Under identical conditions, cAMP formation in HEK-mAC5 cells was unaffected (***Figure 4***). The EC_{50} of oleic acid in HEK293-mAC3 cells was 0.5 µM, i.e., the potency appeared to be increased compared to respective membrane preparations whereas the efficiency was reduced, possibly reflecting the regulatory interplay within the cell. To exclude experimental artifacts, transfection efficiencies were tested by PCR. mAC3 and mAC5 transfections were similar (***Figure 4—figure supplement 2***). Taken together, the results suggest that the enhancement of Gsα-stimulated mAC3 by oleic acid might be due to binding of oleic acid to or into an mAC3 membrane receptor (***Schultz, 2022***; ***Beltz et al., 2016***).

Oleic acid enhances Gsα-stimulated mAC 2, 7, and 9 activities

Next, we examined other AC isoforms with oleic acid as a ligand. 20 µM oleic acid significantly enhanced Gsα-stimulated activities of isoforms 2, 7, and 9, mAC1 was slightly attenuated, and isoforms 4, 5, 6, and 8 were unaffected (***Figure 5A***).

Concentration–response curves were carried out for mACs 2, 7, and 9 (***Figure 5B***). The EC_{50} of oleic acid were 8.6, 6.7, and 7.8 µM, respectively, comparable to that determined for mAC3. Exploration of the ligand space for mACs 2, 7, and 9 with the panel of 18 aliphatic lipids uncovered more active lipids (***Figure 5C***). In the case of mAC2, 20 µM *cis*-vaccenic acid doubled cAMP formation (EC_{50} 10.6 µM) while other compounds were inactive (***Figure 5C*** and for additional concentration–response curves see ***Figure 5—figure supplement 1***). For mAC7 the EC_{50} of elaidic was 9.7 µM

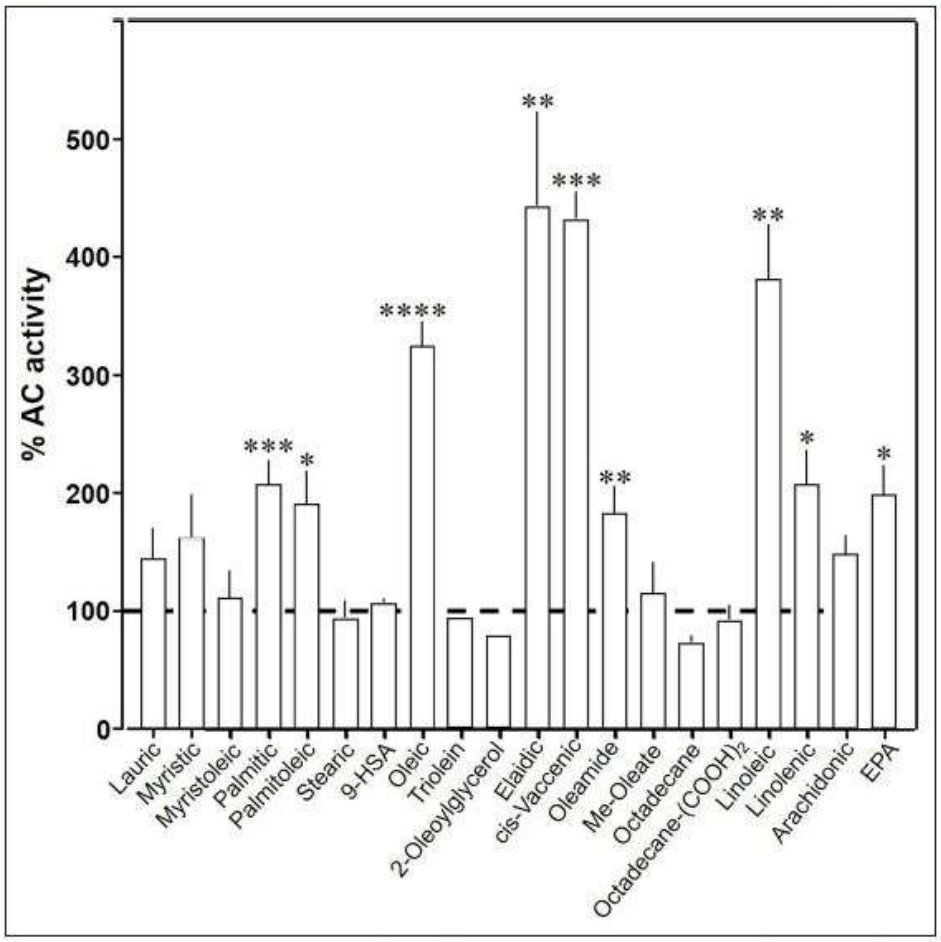

Figure 3. Effect of 20 µM lipids on 300 nM Gsα-stimulated mAC3. Basal and Gsα-stimulated activities were 0.02 ± 0.001 and 0.17 ± 0.01 nmol cAMP•mg^{-1}•min^{-1}, respectively. EPA: eicosapentaenoic acid; 9-HSA: 9-hydroxystearic acid. Data are mean ± SEM, n = 2–23. One-sample t tests, Significances: *p < 0.05; **p < 0.01; ***p < 0.001; ****p < 0.0001.

The online version of this article includes the following source data and figure supplement(s) for figure 3:

Source data 1. Including data used for generating ***Figure 3***.

Figure supplement 1. Structures of the tested aliphatic lipids listed in ***Table 1***.

(concentration–response curve see ***Figure 5—figure supplement 2***). The range of potential ligands for mAC9 was more comprehensive: three- to fourfold enhancement was observed with 20 µM palmitoleic, oleic, elaidic, *cis*-vaccenic, and linoleic acid. With 20 µM myristic, palmitic, palmitoleic, linolenic, and arachidonic acid 1.5- to 2-fold enhancements were observed (***Figure 5C*** and for concentration–response curves see ***Figure 5—figure supplements 3 and 4***).

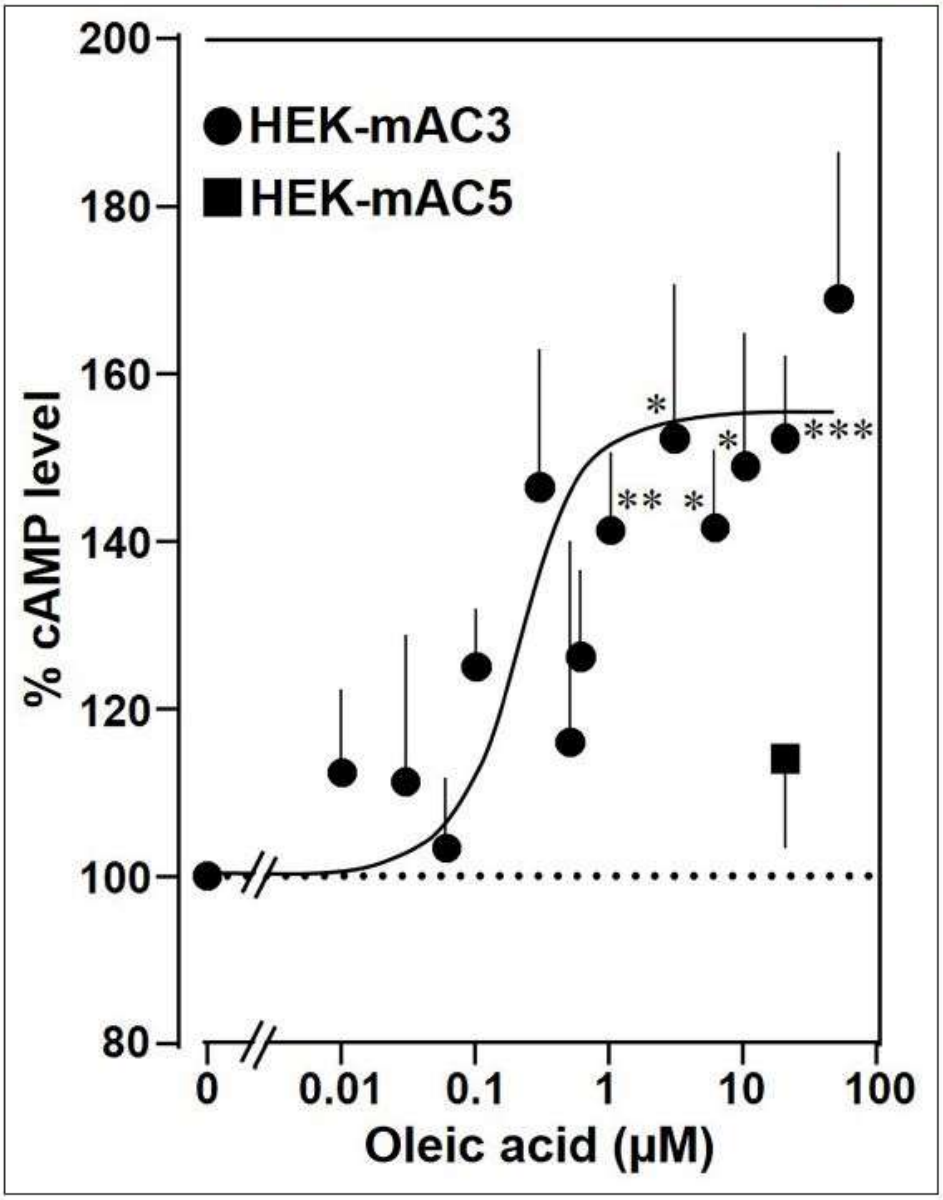

Figure 4. Oleic acid enhances cAMP formation in mAC3-transfected HEK293 cells. Effect of oleic acid on HEK293 cells permanently transfected with mACs 3 and 5 stimulated by 2.5 μM isoproterenol (set as 100%). Basal and isoproterenol-stimulated cAMP levels of HEK-mAC3 were 0.02 ± 0.006 and 1.35 ± 0.24 and of HEK-mAC5 2.13 ± 0.69 and 2.60 ± 0.88 pmol cAMP/10,000 cells, respectively. $n = 3$–9, carried out in technical triplicates. Data are mean ± SEM. One-sample t tests. Significances: *$p < 0.05$; **$p < 0.01$; ***$p < 0.001$.

The online version of this article includes the following source data and figure supplement(s) for figure 4:

Figure 4 continued on next page

Figure 4 continued

Figure supplement 1. Effect of isoproterenol on cAMP formation in HEK293 cells transfected with mAC3.

Figure supplement 2. Agarose gels of PCR products from HEK293 cells permanently transfected with mAC1–9.

Source data 1. Including data used for generating ***Figure 4***.

Figure supplement 1—source data 1. Including data used for generating ***Figure 4—figure supplement 1***.

Figure supplement 2—source data 1. PDF file containing original gels for ***Figure 4—figure supplement 2***, indicating the relevant bands.

Figure supplement 2—source data 2. Original files containing gels for ***Figure 4—figure supplement 2***.

Arachidonic acid and anandamide inhibit Gsα-stimulated activities of mAC1, 4, 5, and 6

Testing the panel of lipids at 20 µM with mAC isoforms 1, 4, 5, 6, and 8 we found that isoforms 1 and 4 were significantly attenuated by arachidonic acid, and somewhat less by palmitoleic acid. Other lipids had no effect (for bar plots and dose–response curves see ***Figure 6—figure supplements 1–3***). Of note, eicosa-pentaenoic acid which resembles arachidonic acid but for an additional *cis*-Δ^{-17} double bond had no effect on mAC activities (***Figure 6—figure supplements 1 and 2***). Concentration–response curves for arachidonic acid with 300 nM Gsα-stimulated mAC1 and 4 yielded IC_{50} of 23 and 36 µM, respectively, i.e., about twofold higher compared to the EC_{50} of enhancing ligands (***Figure 6A***).

Next, we examined whether arachidonic acid attenuates mAC1 and 4 in intact HEK 293 cells. Surprisingly, cAMP formation in HEK-mAC1 cells stimulated by 10 µM isoproterenol was attenuated by arachidonic acid with high potency (IC_{50} = 250 pM), i.e., with higher potency compared to data with membranes prepared from the same cell line. In contrast, mAC4 activity examined under identical conditions was not attenuated (***Figure 6B***). Currently, we are unable to rationalize these discrepancies. Possibly, mAC4 has another, more specific lipid ligand which is needed in in vivo. In general, the enhancing and attenuating effects bolster the hypothesis of specific receptor-ligand interactions and divergent intrinsic activities for different ligands. Of note, it was reported that arachidonic acid at concentrations up to 1 mM inhibits AC activity in brain membrane fractions and that essential fatty acid deficiency effects AC activity in rat heart (***Nakamura et al., 2001***; ***Alam et al., 1995***).

At this point we were lacking ligands for mACs 5, 6, and 8 (***Figure 7—figure supplements 1 and 2*** and Figure 8). Possibly, the negative charge of the fatty acid headgroups might impair receptor interactions. A neutral lipid neurotransmitter closely related to arachidonic acid is arachidonoylethanolamide (anandamide) (***Mock et al., 2023***). Indeed, anandamide attenuated 300 nM Gsα stimulation of mAC5 and 6 with IC_{50} of 42 and 23 µM, respectively, i.e., comparable to the effect of arachidonic acid on mACs 1 and 4, and distinctly less potently than the ligands for mAC 2, 3, 7, and 9 (***Figure 7A***). mACs 5 and 6 may thus represent new targets for anandamide which is part of a widespread neuromodulatory system (***Lu and Mackie, 2016***). The concentrations of arachidonic acid and anandamide required may be achieved in vivo by local biosynthesis and degradation. An interfacial membrane-embedded phosphodiesterase cleaves the phosphodiester bond of the membrane lipid *N*-arachidonoyl-ethanolamine-glycerophosphate releasing anandamide into the extracellular space (***Mock et al., 2023***; ***Simon and Cravatt, 2008***; ***Liu et al., 2006***). The lipophilicity and lack of charge should enable it to diffuse readily. Whether the mACs and this biosynthetic phosphodiesterase colocalize or associate with its target mACs is unknown. Degradation of anandamide is by a membrane-bound amidase, generating arachidonic acid and ethanolamine (***McKinney and Cravatt, 2005***). Therefore, we examined whether anandamide at higher concentrations might also affect mAC1 and 4. In fact, anandamide significantly attenuated Gsα-stimulated mAC1, but distinctly not mAC4 (***Figure 7B***). The IC_{50} of anandamide for mAC1 was 29 µM. We also tested whether anandamide attenuated cAMP formation in vivo using HEK-mAC5 cells primed by 2.5 µM isoproterenol (***Figure 7C***). 100 µM anandamide attenuated cAMP formation by only 23% in HEK293-mAC5 cells, the effect was significant ($p < 0.01$). At this point, we were unable to identify a ligand for mAC8, presumably another lipid (***Figure 8***).

Receptor properties are exchangeable between mAC isoforms 3 and 5

To unequivocally validate specific mAC–ligand–receptor interactions and regulation we generated a chimera in which the enhancing membrane domains of mAC3, i.e., mAC3-TM1 and TM2, were

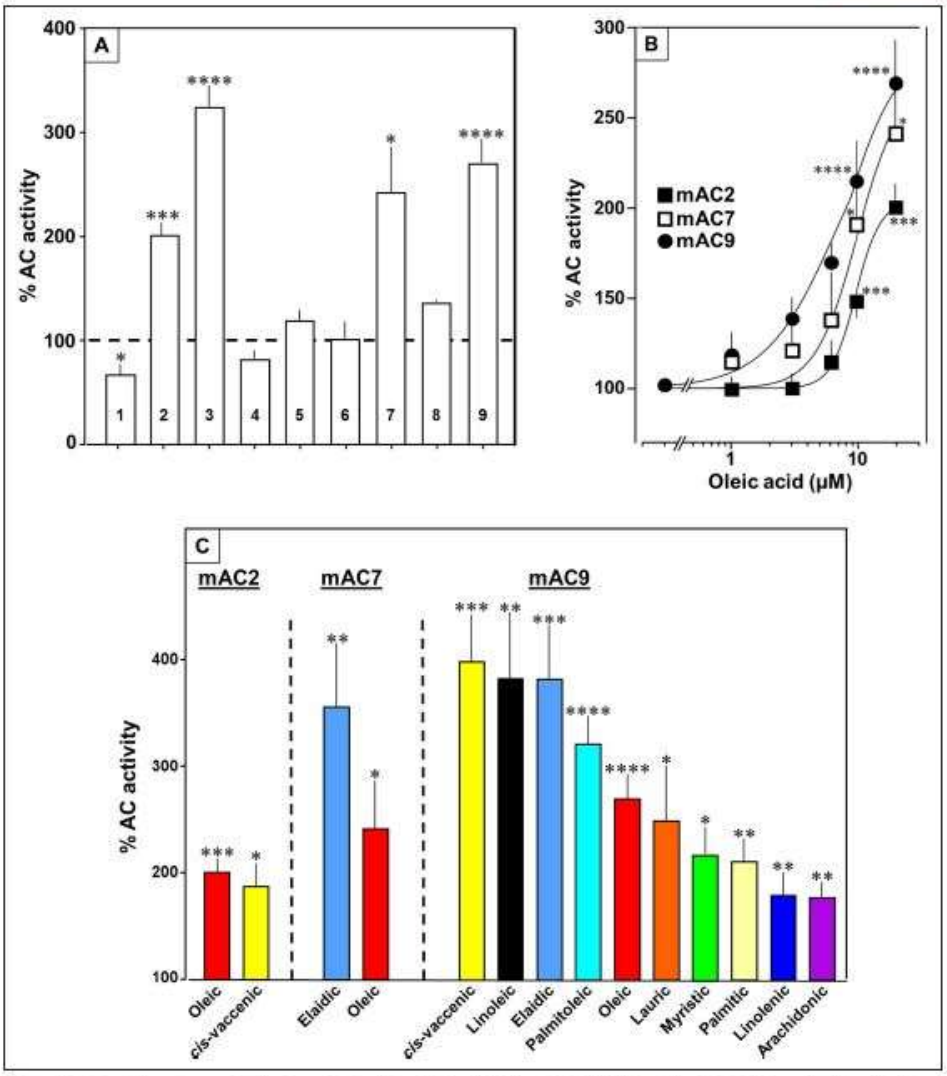

Figure 5. Fatty acids enhance mAC isoforms 2, 7, and 9 activities. (**A**) Effect of 20 μM oleic acid on 300 nM Gsα-stimulated mAC activities normalized to 100%. Basal and Gsα-stimulated activities for each isoform are in ***Figure 5—figure supplement 1***. $n = 2–23$. (**B**) Oleic acid activates mACs 2, 7, and 9 stimulated by 300 nM Gsα. $n = 7–23$. (**C**) Fatty acids activating mACs 2, 7, and 9 at 20 μM. For basal and Gsα-stimulated activities, see ***Figure 5—figure supplements 1–4***. $n = 5–15$. Identical colors indicate identical compounds. Data are mean ± SEM. One-sample *t* tests were performed. Significances: *p < 0.05; **p < 0.01; ***p < 0.001; ****p < 0.0001.

The online version of this article includes the following source data and figure supplement(s) for figure 5:

Source data 1. Including data used for generating ***Figure 5A–C***.

Figure supplement 1. Effect of lipids on 300 nM Gsα-stimulated mAC2.

Figure supplement 1—source data 1. Including basal and Gsα-stimulated activities of mAC1–mAC9.

Figure 5 continued on next page

Figure 5 continued

Figure supplement 1—source data 2. Including data used for generating ***Figure 5—figure supplement 1***, left and right.

Figure supplement 2. Effect of lipids on 300 nM Gsα-stimulated mAC7.

Figure supplement 2—source data 1. Including data used for generating ***Figure 5—figure supplement 2***, left and right.

Figure supplement 3. Effect of lipids on 300 nM Gsα-stimulated mAC9.

Figure supplement 3—source data 1. Including data used for generating ***Figure 5—figure supplement 3***, left and right.

Figure supplement 4. Concentration–response curves of fatty acids activating Gsα-stimulated mAC9.

Figure supplement 4—source data 1. Including data used for generating ***Figure 5—figure supplement 4***, left and right.

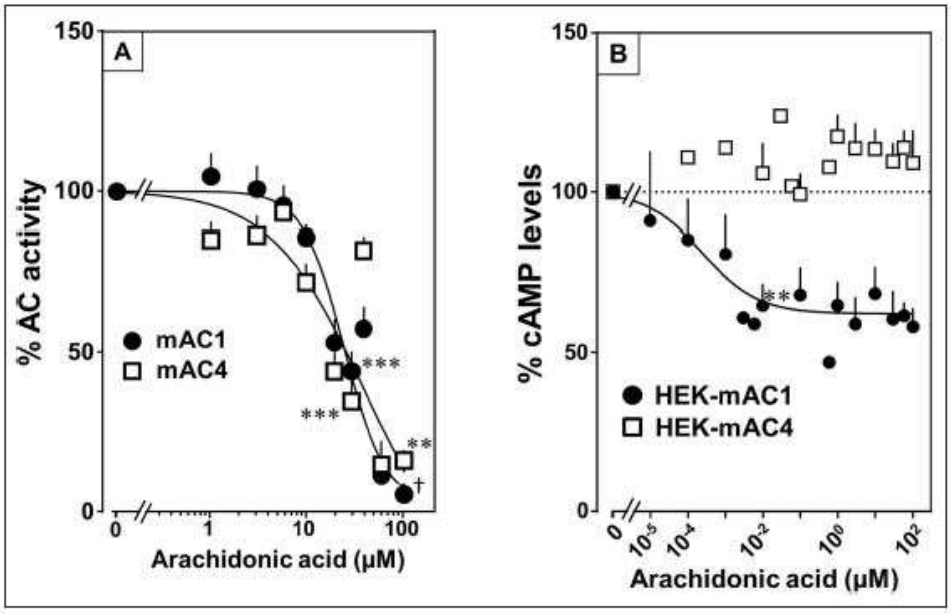

Figure 6. Arachidonic acid attenuates 300 nM Gsα-stimulated activities of mACs 1 and 4. (**A**) Arachidonic acid attenuates Gsα-stimulated mACs 1 and 4. Basal and Gsα-stimulated activities of mAC1 were 0.12 ± 0.01 and 0.42 ± 0.03 and of mAC4 0.02 ± 0.002 and 0.14 ± 0.02 nmol cAMP•mg^{-1}•min^{-1}, respectively. IC_{50} of arachidonic acid for mAC1 and mAC4 were 23 and 36 μM, respectively. n = 3–9. (**B**) Effect of arachidonic acid on HEK-mAC1 and HEK-mAC4 cells. Cells were stimulated by 10 μM isoproterenol (set as 100 %) in the presence of 0.5 mM IBMX (3-isobutyl-1-methylxanthine). Basal and isoproterenol-stimulated cAMP levels in HEK-mAC1 were 1.03 ± 0.15 and 1.66 ± 0.28 and in HEK-mAC4 0.20 ± 0.04 and 0.86 ± 0.24 pmol cAMP/10,000 cells, respectively. IC_{50} for HEK-mAC1 was 250 pM. n = 2–11, each with three replicates. Data are mean ± SEM. One-sample t tests were performed. Significances: **$p < 0.01$; ***$p < 0.001$; †$p < 0.0001$. For clarity, not all significances are indicated.

The online version of this article includes the following source data and figure supplement(s) for figure 6:

Source data 1. Including data used for generating ***Figure 6A, B***.

Figure supplement 1. Effect of 20 μM lipids on 300 nM Gsα-stimulated mAC1.

Figure supplement 1—source data 1. Including data used for generating ***Figure 6—figure supplement 1***.

Figure supplement 2. Effect of 20 μM lipids on 300 nM Gsα-stimulated mAC4.

Figure supplement 2—source data 1. Including data used for generating ***Figure 6—figure supplement 2***.

Figure supplement 3. Palmitoleic acid inhibits mACs 1 and 4 stimulated by 300 nM Gsα.

Figure supplement 3—source data 1. Including data used for generating ***Figure 6—figure supplement 3***.

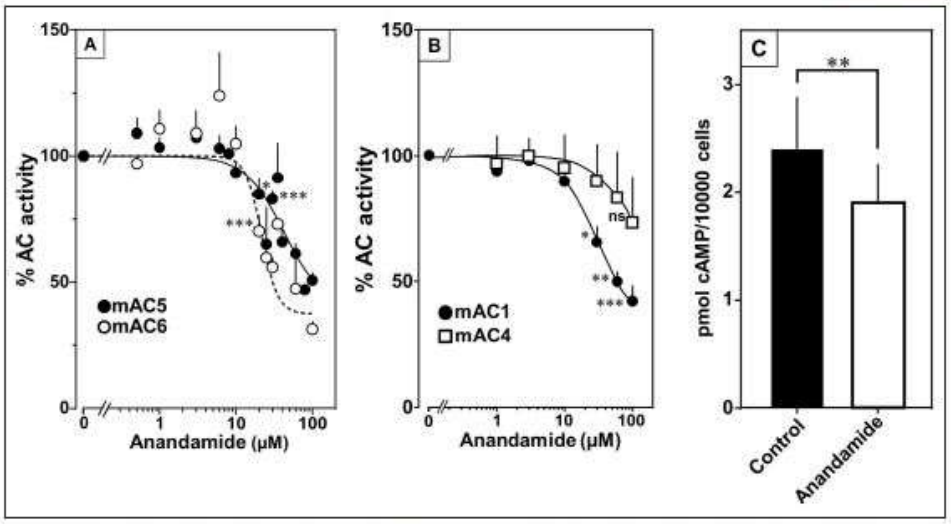

Figure 7. Anandamide attenuates 300 nM Gsα-stimulated activities of mACs 1, 4, 5, and 6. (**A**) Effect of anandamide on Gsα-stimulated mAC5 and 6. Basal and Gsα activities of mAC5 were 0.05 ± 0.01 and 0.98 ± 0.12 and of mAC6 0.05 ± 0.01 and 0.78 ± 0.12 nmol cAMP•mg^{-1}•min^{-1}, respectively. IC_{50} of anandamide were 42 and 22 μM, respectively. *n* = 3–32. (**B**) Anandamide attenuates mAC1 but not mAC4 stimulated by Gsα. Basal and Gsα-stimulated activities of mAC1 were 0.12 ± 0.01 and 0.40 ± 0.03 and of mAC4 0.02 ± 0.002 and 0.15 ± 0.02 nmol cAMP•mg^{-1}•min^{-1}, respectively. IC_{50} for mAC1 was 29 μM. *n* = 3–4, each with two technical replicates. (**C**) Effect of anandamide on 2.5 μM isoproterenol-stimulated HEK-mAC5. Basal and isoproterenol-stimulated cAMP levels of HEK-mAC5 were 1.8 ± 0.22 and 2.4 ± 0.48 pmol cAMP/10,000 cells, respectively. The control bar represents 2.5 μM isoproterenol stimulation alone. *n* = 5–6, each with three technical replicates. IC_{50} of anandamide was 133 μM. Data are mean ± SEM. One-sample *t* tests (A, B) and paired *t* test (C) were performed. Significances: ns: not significant p > 0.05; *p < 0.05; **p < 0.01; ***p < 0.001. For clarity, not all significances are indicated.

The online version of this article includes the following source data and figure supplement(s) for figure 7:

Source data 1. Including data used for generating ***Figure 7A–C***.

Figure supplement 1. Effect of 20 μM lipids on 300 nM Gsα-stimulated mAC5.

Figure supplement 1—source data 1. Including data used for generating ***Figure 7—figure supplement 1***.

Figure supplement 2. Effect of 20 μM lipids on 300 nM Gsα-stimulated mAC6.

Figure supplement 2—source data 1. Including data used for generating ***Figure 7—figure supplement 2***.

substituted by those of mAC5 (design in ***Figure 9A***, right). The intention was to obtain a chimera, $mAC5_{(membr)}$–$AC3_{(cat)}$, with a loss of receptor function, i.e., no enhancement by oleic acid, and a gain of another receptor function, i.e., attenuation of activity by anandamide. Successful expression and membrane insertion of the chimera in HEK293 cells was demonstrated by specific conjugation to Cy5.5 fluorophore, using the protein ligase Connectase (***Figure 9A***, left; ***Fuchs, 2023***). cAMP synthesis of isolated membranes from these cells was stimulated up to 10-fold by addition of 300 nM Gsα, comparable to membranes with recombinant mAC3 or mAC5 proteins (***Figure 9B***). mAC activity in the $mAC5_{(membr)}$–$AC3_{(cat)}$ chimera was not enhanced by oleic acid, i.e., loss of receptor function, but was attenuated by anandamide, i.e., gain of receptor function (***Figure 9C, D***). The attenuation was comparable to results obtained with mAC5 membranes, i.e., IC_{50} was 29 μM $mAC5_{(membr)}$–$AC3_{(cat)}$ (***Figure 9E***) compared to 42 μM for mAC5. This means that the attenuating receptor property of mAC5 was successfully grafted onto the mAC3-catalytic dimer. We take this to support the hypothesis that the mammalian mAC membrane domains operate as receptors using lipid ligands. The data virtually rule out unspecific lipid effects such as disturbance of membrane integrity by intercalation and surfactant or detergent effects. In addition, the data demonstrated that the signal most likely originates from the receptor entity and is transmitted through the subsequent linker regions to the catalytic dimer.

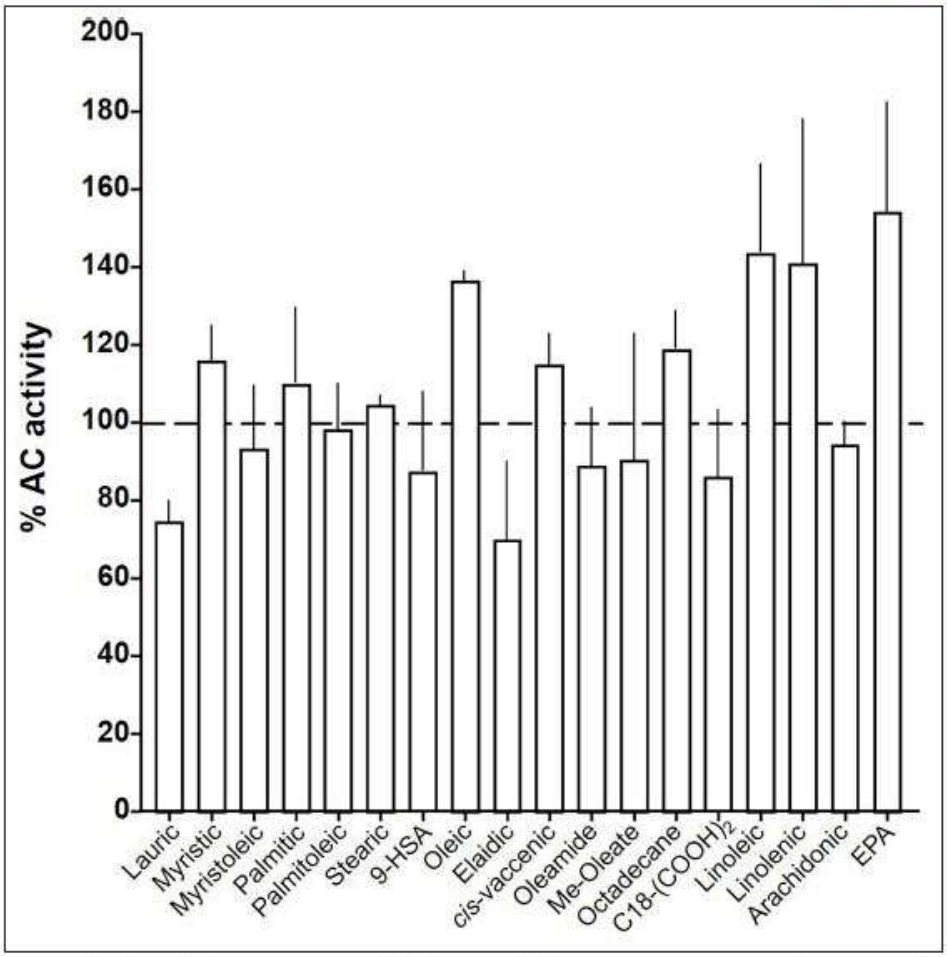

Figure 8. Effect of 20 μM lipids on 300 nM Gsα-stimulated mAC8. Basal and Gsα activities were 0.19 ± 0.01 and 1.04 ± 0.19 nmol cAMP•mg^{-1}•min^{-1}, respectively. Error bars denote SEM of n = 2–5.

The online version of this article includes the following source data for figure 8:

Source data 1. Including data used for generating ***Figure 8***.

The findings were further substantiated in vivo using HEK293-mAC5$_{(membr)}$–AC3$_{(cat)}$ cells. cAMP formation primed by 2.5 μM isoproterenol was attenuated by anandamide in HEK293-mAC5$_{(membr)}$–AC3$_{(cat)}$ cells by 66%, (***Figure 10***), i.e., a gain of function which remarkably exceeded the anandamide attenuation in HEK293-mAC5 cells of 23%. In HEK293-mAC5$_{(membr)}$–AC3$_{(cat)}$ cells oleic acid was ineffective, i.e., loss of function (data not shown). The results bolster the notion that mAC isoforms are receptors with lipids as ligands.

Lastly, we prepared membranes from mouse brain cortex in which predominantly mAC isoforms 2, 3, and 9 are expressed, isoforms with demonstrated enhancement of Gsα stimulation by oleic acid (***Sanabra and Mengod, 2011***). In cortical membranes 20 μM oleic acid enhanced Gsα-stimulated cAMP formation 1.5-fold with an EC$_{50}$ of 5 μM, almost identical to the one determined for mAC2, 3,

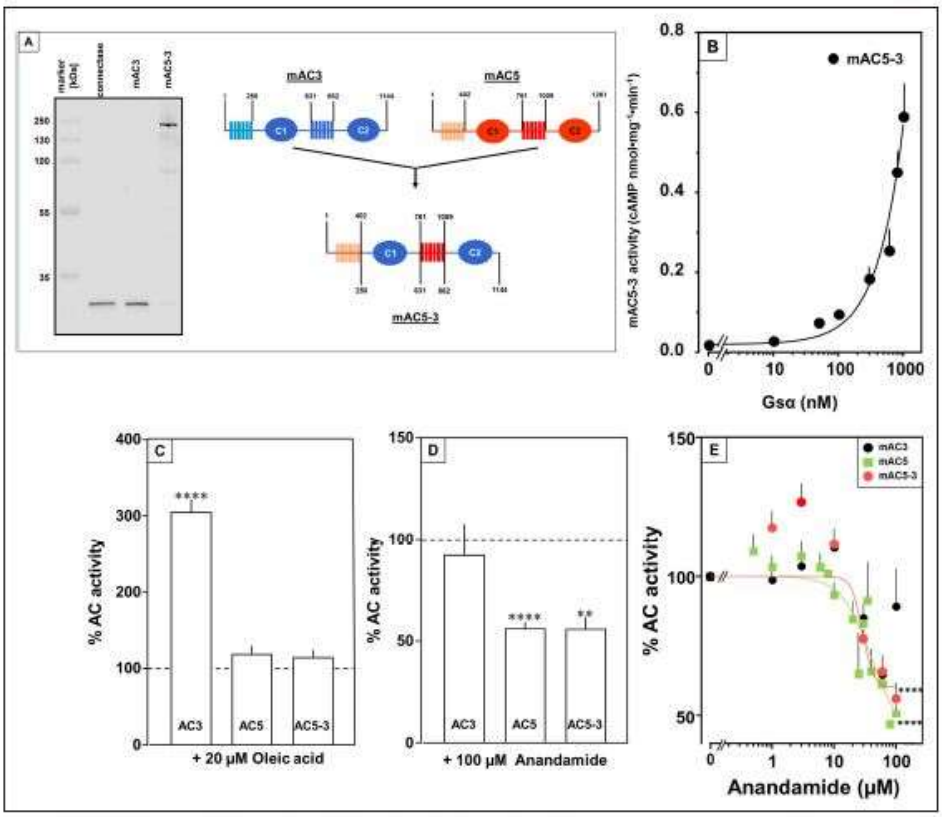

Figure 9. Receptor properties are exchangeable between mAC isoforms. (**A**, left) Detection of $AC5_{(membr)}$–$AC3_{(cat)}$ receptor chimeras. $AC5_{(membr)}$–$AC3_{(cat)}$ (AC5–3) (***Tews et al., 2005***) was expressed in HEK293 cells with an N-terminal tag for labeling with the protein ligase Connectase. The membrane preparation was incubated with fluorophore-conjugated Connectase and separated by sodium dodecyl sulfate–polyacrylamide gel electrophoresis (SDS–PAGE). A fluorescence scan of the gel detects $AC5_{(membr)}$–$AC3_{(cat)}$ (right), the reagent (fluorophore-conjugated Connectase) is detected when using HEK293 membrane (middle) or a buffer control (left); (A, right) Design of the chimeric AC5–3 construct. Numbers are amino acid positions in mAC3 and 5, respectively. (**B**) Gsα concentration–response curve of mAC5–3. Basal activity for mAC5–3 was 0.02 pmol cAMP•mg^{-1}•min^{-1}. Error bars denote SEM of $n = 3$, each with two technical replicates. (**C**) Effect of 20 µM oleic acid on 300 nM Gsα-stimulated mACs 3, 5, and 5–3. Basal and Gsα activities of mACs 3, 5, and 5–3 were 0.02 ± 0.003 and 0.11 ± 0.02, 0.05 ± 0.01 and 0.98 ± 0.12, and 0.01 ± 0.004 and 0.2 ± 0.02 nmol cAMP•mg^{-1}•min^{-1}, respectively. $n = 7$–33. (**D**) Effect of 100 µM Anandamide on 300 nM Gsα-stimulated mACs 3, 5, and 5–3. Basal and Gsα activities of mACs 3, 5, and 5–3 were 0.02 ± 0.002 and 0.19 ± 0.02, 0.05 ± 0.01 and 0.98 ± 0.12, and 0.02 ± 0.003 and 0.23 ± 0.04 nmol cAMP•mg^{-1}•min^{-1}, respectively. $n = 6$–9. IC_{50} for mAC5 and mAC5–3 were 42 and 29 µM, respectively. (**E**). Exchange of TM domains transfers anandamide effect on mAC3. Basal and Gsα-stimulated activities of mAC3 were 0.02 ± 0.002 and 0.12 ± 0.02 nmol cAMP•mg^{-1}•min^{-1}, respectively. Basal and Gsα-stimulated activities of mAC5 were 0.05 ± 0.005 and 0.98 ± 0.12 nmol cAMP•mg^{-1}•min^{-1}, respectively. Basal and Gsα-stimulated activities of mAC5–3 were 0.02 ± 0.002 and 0.22 ± 0.03 nmol cAMP•mg^{-1}•min^{-1}, respectively. Calculated IC_{50} concentrations of anandamide for mAC5 and mAC5–3 were 42 and 29 µM, respectively. Data are mean ± SEM. One-sample *t* tests. Significances: $^{**}p < 0.01$; $^{****}p < 0.0001$.

The online version of this article includes the following source data for figure 9:

Source data 1. PDF file containing original gel for ***Figure 9A***, indicating the relevant bands.

Source data 2. Original file containing gel for ***Figure 9A***.

Source data 3. Including data used for generating ***Figure 9B–E***.

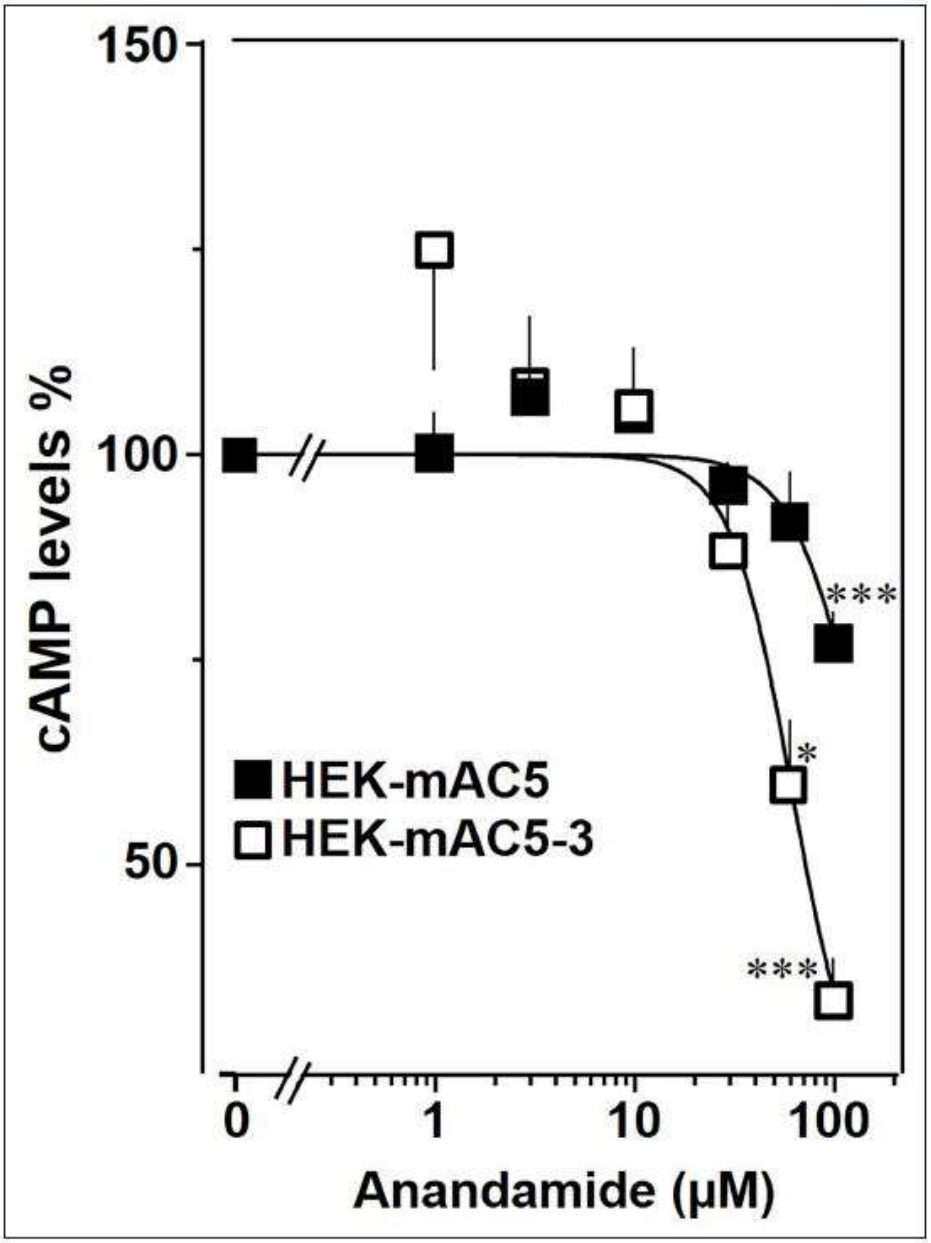

Figure 10. mAC5–mAC3 receptor transfer analyzed in HEK293 cells. Effect of anandamide on HEK-mAC5 and HEK-mAC5–3 cells stimulated by 2.5 μM isoproterenol (set as 100%). Basal and isoproterenol-stimulated cAMP levels in HEK-mAC5 were 1.80 ± 0.22 and 2.29 ± 0.39 and in HEK-mAC5–3 (+0.5 mM IBMX) 0.17 ± 0.02 and 3.11 ± 0.55 pmol cAMP/10,000 cells, respectively. $n = 4–11$. IC_{50} for HEK-mAC5 and HEK-mAC5–3 were 133 and 60 μM,

Figure 10 continued on next page

Figure 10 continued

respectively. Anandamide had no effect on basal activity of HEK-mAC5 and stimulated HEK-mAC3 cells in concentrations up to 100 µM (data not shown). Data are mean ± SEM. One-sample *t* tests were performed. Significances: *p < 0.05; ***p < 0.001.

The online version of this article includes the following source data for figure 10:

Source data 1. Including data used for generating ***Figure 10***.

7, and 9 (***Figure 11***). This suggests that mACs in brain cortical membranes are similarly affected by fatty acids.

Discussion

In the past, the biology of the two membrane anchors of mACs, highly conserved in an isoform-specific manner, remained unresolved. The theoretical possibility of a receptor function of these large hexahelical anchor domains, each comprising 150–170 amino acids, was considered unlikely (***Schuster et al., 2024***). Our data are a transformative step toward resolving this issue and introduce lipids as critical participants in regulating cAMP biosynthesis in mammals. The first salient discovery is the identification of the membrane domains of mACs as a new class of receptors for chemically defined ligands which set the level of stimulation by the GPCR/Gsα system. This conclusion is based on (1) the dodecahelical membrane domains of the nine mAC receptors have distinct, conserved isoform-specific sequences for the TM1 and TM2 domains ***Schultz, 2022***; (2) the receptors have distinct ligand specificities and affinities in the lower micromolar range; (3) isoform dependently ligands either enhance or attenuate Gsα-stimulated mAC activities; (4) receptor properties are transferable between isoforms by interchanging membrane domains; (5) isoproterenol-stimulated formation of cAMP in vivo is affected by addition of extracellular ligands; (6) Gsα-stimulated cAMP formation in mouse cortical membranes is enhanced by oleic acid. Therefore, the results establish a new class of receptors, the membrane domains of mACs, with lipids as ligands. The data question the utility of the currently used mAC subclassification, which groups mAC1, 3, 8, mAC2, 4, 7, mACs 5, 6, and mAC9 together (***Dessauer et al., 2017***). At this point, mAC 1, 4, 5, and 6, which are ligand-attenuated, may be grouped together and a second group may consist of isoforms 2, 3, 7, and 9 which are ligand-enhanced. Our data do not contradict earlier findings concerning regulation of mACs via GPCRs, cellular localization of mAC isoforms or regional cAMP signaling (***Dessauer et al., 2017***). Instead, the data reveal a completely new level of regulation of cAMP biosynthesis in which two independent modalities of signaling, i.e., direct, tonic lipid signaling and indirect phasic signaling via the GPCR/Gsα circuits intersect at the crucial biosynthetic step mediated by the nine mAC isoforms.

The second important finding is the observation that the extent of enhancement of mAC3 activity by 20 µM oleic acid is uniform up to 1000 nM Gsα (***Figure 2***, right). We suppose that in mAC3 the equilibrium of two differing ground states favors a Gsα unresponsive state and the effector oleic acid concentration dependently shifts this equilibrium to a Gsα responsive state (***Seth et al., 2020***). In contrast, the equilibrium of ground states of mAC5 probably is opposite, i.e., the one accessible to Gsα stimulation predominates and stimulation by Gsα is maximal. In addition, oleic acid has little effect because the mAC5 receptor domain does not bind oleic acid (***Figure 1D***, right, and ***Figure 2***, center). A ligand for mAC5, e.g., anandamide or arachidonic acid, likely shifts the equilibrium of ground states to a Gsα unresponsive state and inhibits stimulation. The biological balance of ground states appears to be an intrinsic property which is isoform specifically imprinted in mACs. Probably, it defines a major element of regulation and enables distinct inhibitory or stimulatory inputs by extracellular lipid ligands. The ground states probably are separated by a low transition energy and are stabilized by receptor occupancy. Hitherto available structures required Gsα and/or forskolin for stabilization and probably did not capture different ground states (***Schuster et al., 2024***; ***Qi et al., 2019***; ***Qi et al., 2022***; ***Sunahara et al., 1997b***; ***Tesmer and Sprang, 1998***; ***Vercellino et al., 2017***). Mechanistically, tonic levels of lipid ligands affect the ground states and thus set the bounds of cAMP formation elicited by phasic GPCR/Gsα stimulation. As such lipid signaling through the mAC membrane receptors appears to represent a higher level of a systemic regulatory input based on constant monitoring the physiological and nutritional status of an organism.

Lipid signaling is much less characterized than solute signaling (***Eyster, 2007***). Most of the highly functionalized ligands for GPCRs are storable in vesicles and the release, inactivation and removal

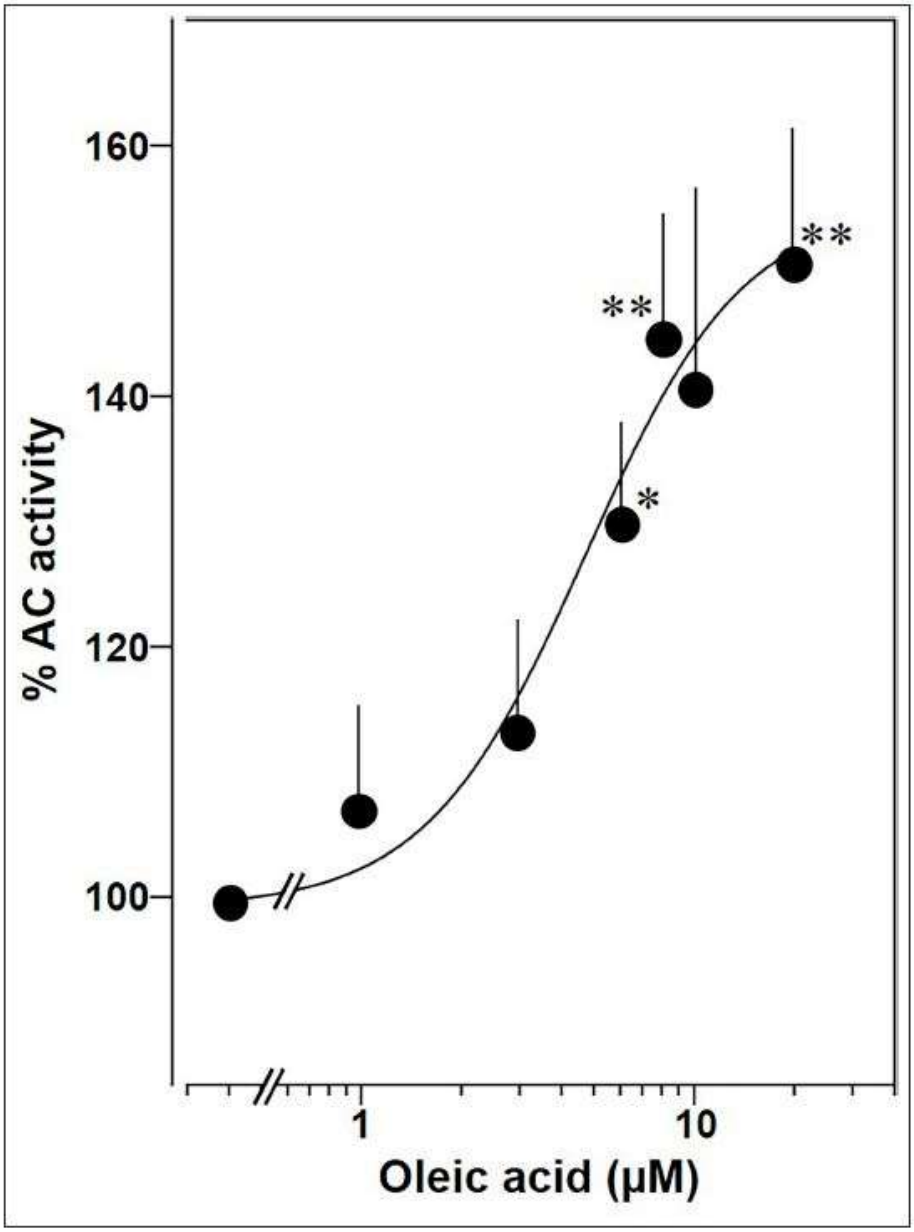

Figure 11. Oleic acid concentration dependently potentiates mAC activity in brain cortical membranes from mouse. Basal and 300 nM Gsα activities were 0.4 ± 0.1 and 2.7 ± 0.7 nmol cAMP•mg^{-1}•min^{-1}, respectively. n = 4–6. One-sample *t* test: *p < 0.05; **p < 0.01 compared to 100% (300 nM Gsα stimulation).

Figure 11 continued on next page

Figure 11 continued

The online version of this article includes the following source data for figure 11:

Source data 1. Including data used for generating ***Figure 11***.

are strictly controlled. On the other hand, the very nature of lipids, i.e., high flexibility of aliphatic chains, low water solubility, propensity for nonspecific protein binding, membrane permeability and potential effects on membrane fluidity complicate discrimination between extra- and intracellular lipid actions (***Samovski et al., 2023***). Yet, viewed from an evolutionary perspective, lipids possibly are ideal primordial signaling molecules because for the emergence of the first cell lipids were required to separate an intra- and extracellular space. Conceivably, lipids derived from membrane lipids were used for regulatory purposes early-on. In association with the evolution of bacterial mAC progenitors lipid ligands may have persisted in evolution and regulation by GPCR/Gsα in metazoans was acquired and expanded later.

The concentrations of free fatty acids in serum or interstitial fluid usually are rather low, mostly below the EC_{50} concentrations determined in this study (***Grundmann et al., 2021***; ***Ulven and Christiansen, 2015***; ***Huber and Kleinfeld, 2017***). This raises the question of the origin of lipid ligands under physiological conditions. It is well known that cell membranes are highly dynamic (***Alam et al., 1995***; ***McMahon and Gallop, 2005***). Within limits, cell morphology and lipid composition are in constant flux to accommodate diverse functional requirements. Remodeling of cell membranes is accomplished by targeted phospholipid biosynthesis and by regulated lipolysis of membrane lipids, e.g., by phospholipase A_2, mono- and diacylglycerol lipases or lipoprotein lipases (***Brown et al., 2003***). Therefore, a speculative possibility is that lipid ligands are acutely and locally generated directly from membrane lipids (***Liu et al., 2006***; ***Muccioli, 2010***). Such regulation probably happens at the level of individual cells, cellular networks, complex tissues, and whole organs. Additional potential lipid sources available for ligand generation may be, among others, lipids in nutrients (***Alam et al., 1995***), exosomes present in blood, serum lipids, chylomicrons, blood triglycerides, and lipids originating from the microbiome. On the one hand, the discovery of lipids as ligands for the mAC receptors broadens the basis of regulation of cAMP biosynthesis with potentially wide-ranging consequences in health and disease. On the other hand, the data pose the challenge to identify how the tonic signal is generated and regulated.

Materials and methods

Reagents and materials

ATP, creatine kinase, and creatine phosphate were from Merck. Except for lauric acid (Henkel) and 1,18-octadecanedicarboxylic acid (Thermo Fisher Scientific), lipids were from Merck. 10 mM stock solutions were prepared in analytical grade Dimethyl sulfoxide (DMSO) and kept under nitrogen. For assays the stock solution was appropriately diluted in 20 mM 3-(N-morpholino)propanesulfonic acid (MOPS) buffer, pH 7.5, suitable to be added to the assays resulting in the desired final concentrations. The final DMSO concentrations in in vitro and in vivo assays were maximally 1%, a concentration without any biochemical effect as checked in respective control incubations. The constitutively active GsαQ227L mutant protein was expressed and purified as described earlier (***Graziano et al., 1989***; ***Graziano et al., 1991***; ***Sunahara et al., 1997a***).

General experimental procedures

For HPLC analysis, a Waters HPLC system (1525 pump, 2996 photodiode array detector, 7725i injector, 200 series PerkinElmer vacuum degasser) was used. Solvents were HPLC or LC–MS grade from Merck-Sigma. One-dimensional ^{1}H- and ^{13}C-NMR spectra were recorded on a 400 MHz Bruker AVANCE III NMR spectrometer equipped with a 5-mm broadband SmartProbe and AVANCE III HD Nanobay console. Spectra were recorded in methanol-d_4 and calibrated to the residual solvent signal (δ_H 3.31 and δ_C 49.15 ppm).

Lung tissue extraction and fractionation

1.24 kg bovine lung was minced in a meat grinder, then mixed and homogenized with 1.2 l 50 mM MOPS, pH 7.5, in a Waring blender (4°C) resulting in 2.3 l homogenate. It was centrifuged (30 min,

4°C, 7200 × g) resulting in 1.2 l supernatant. The pH was adjusted to 1 using 7% HCl. Equal volumes of CH_2Cl_2/MeOH (2:1) were mixed with the supernatant in a separatory funnel and shaken vigorously. Centrifugation was at 5300 × g for 30 min. The lower organic CH_2Cl_2 layer was recovered and the solvent was evaporated yielding 2 g of dried material. It was dissolved in 100 ml petroleum ether and subjected to normal-phase silica gel vacuum liquid chromatography (60 H Supelco). The column was eluted stepwise with solvents of increasing polarity from 90:10 petroleum ether/EtOAc to 100% EtOAc, followed by 100% MeOH. 17 fractions (A–Q) of 300 ml were collected and dried. Fraction E (eluting at 40:60 petroleum ether/EtOAc) was analyzed by RP-HPLC using a linear MeOH/H_2O gradient from 80:20 to 100:0 (0.1% TFA Trifluoroacetic acid) for 15 min, followed by 100:0 for 30 min (Knauer Eurosphere II C18P 100-5, 250 × 8 mm, 1.2 ml/min flow rate, UV absorbance monitored at 210 nm) to yield five subfractions: E1–E5. Fraction E2 was analyzed by ^{1}H- and ^{13}C-NMR which indicated the presence of aliphatic lipids and fatty acids (***Figure 1—figure supplement 3***).

Gas chromatography–mass spectrometry analysis

Fraction E2 was analyzed by gas chromatography–mass spectrometry. Acids were acid trimethylsilylated using *N,O*-bis(trimethylsilyl)trifluoroacetamide + trimethylchlorosilane (99:1 vol/vol). The mixture was heated for 2 hr at 90°C. After cooling and clearing the sample was transferred into a GC vial in 200 µl hexane.

An Agilent Technologies GC system (8890 gas chromatograph and 5977B mass spectrometer equipped with a DB-HP5MS UI column, 30 m × 0.25 mm, film thickness of 0.25 µm) was used. Injection volume was 1 µl. The temperature was kept at 100°C for 5 min, and then increased at 53°C/min to 240°C. The rate was decreased to 3°C/min to reach 305°C. Carrier gas was He_2 (99.9%; 1.2 ml/min). Ionization was with 70 eV and MS spectra were recorded for a mass range *m/z* 35–800 for 35 min. Compounds were identified by comparing the spectra with those in the NIST library. Individual compound content is given as a relative % of the total peak area.

Plasmid construction and protein expression

hAC sequences were from NCBI were: ADCY1: NM_021116.3; ADCY2: NM_020546.2; ADCY3: NM_004036.4; ADCY4: NM_001198568.2; ADCY5: NM_183357.2; ADCY6: NM_015270.4; ADCY7: NM_001114.4; ADCY8: NM_001115.2; ADCY9: NM_001116.3. Human mAC genes were from GenScript and fitted with a C-terminal FLAG-tag. The chimera mAC5(TM)_mAC3(cat) had an N-terminal connectase-tag, MPGAFDADPLVVEIAAAGA, followed by AC5(1–402)_AC3(250–631)_AC5(761–1009)_AC3(862–1144). The gene was synthesized by GenScript. HEK293 cells were maintained in Dulbeccos Modified Eagle Medium (DMEM) with 10% fetal bovine serum at 37°C and 5% CO_2. Transfection with AC plasmids was with PolyJet (SignaGen, Frederick, MD, USA). Permanent cell lines were generated by selection for 7 days with 600 µg/ml G418 and maintained with 300 µg/ml For membrane preparation, cells were tyrpsinized, collected by centrifugation (3000 × g, 5 min) and lysed and homogenized in 20 mM HEPES, pH 7.5, 1 mM Ethylenediaminetetraacetic acid (EDTA), 2 mM $MgCl_2$, 1 mM Dithiothreitol (DTT), one tablet of cOmplete, EDTA-free (per 50 ml) and 250 mM sucrose by 20 strokes in a potter homogenizer on ice. Debris was removed (5 min at 1000 × g, 0°C), membranes were collected at 100,000 × g, 60 min at 0°C, suspended and stored at −80°C in 20 mM MOPS, pH 7.5, 0.5 mM EDTA, 2 mM $MgCl_2$. Membrane preparation from mouse brain cortex was according to ***Seth et al., 2020***; ***Schultz and Schmidt, 1987***. Three cerebral cortices were dissected and homogenized in 4.5 ml cold 48 mM Tris–HCl, pH 7.4, 12 mM $MgC1_2$, and 0.1 mM Ethylene glycol-bis(β-aminoethyl ether)-N,N,N',N'-tetraacetic acid (EGTA) with a Polytron hand disperser (Kinematica AG, Switzerland). The homogenate was centrifuged for 15 min at 12,000 × g at 4°C. The pellet was washed once with 5 ml 1 mM $KHCO_3$. The final suspension in 2 ml 1 mM $KHCO_3$ was stored in aliquots at −80°C.

DNA extraction

DNA from 1 × 10^6 cells of permanently transfected and non-transfected HEK293 cells was extracted using the High Pure PCR Template Preparation Kit (Roche) according to the manufacturer's instructions. DNA concentrations were determined at 260 nm using a sub-microliter cell (IMPLEN) in a P330 NanoPhotometer (IMPLEN). Elution buffer (Roche) was used for blanks.

Polymerase chain reaction

100 ng of template DNA was mixed with 0.5 µM Forward primer and 0.5 µM Reverse primer. 12.5 µl 2X KAPA2G Fast (HotStart) Genotyping Mix with dye and water was added, total reaction volume 25 µl according to the KAPA2G Fast HotStart Genotyping Mix kit (Roche) protocol. PCR followed the cycling protocol in a Biometra T3000 thermocycler:

Step	Temperature (°C)	Duration	Cycles
Initial denaturation	95	3 min	1
Denaturation	95	15 s	35
Annealing	60	15 s	
Extension	72	30–60 s	
Final extension	72	2–4 min	1

Extension and final extension times were adjusted to the expected amplicon length.

The PCR products were directly loaded on a 1.5% agarose gel. A 1 kb DNA ladder (New England Bio Labs #N3232S) was mixed with Gel Loading Dye Purple 6X (New England Biolabs #B7024S) and water. After running the gel for 15–20 min at 90 V in 1× Tris(hydroxymethyl)aminomethane-acetate-ethylenediaminetetraacetic acid (TAE) buffer, the gel was stained in an Ethidium bromide bath and left running for another 10–20 min. The gels were then evaluated under UV light in a UVP GelStudio PLUS (Analytik Jena) gel imager.

AC isoform	Forward primer (5'–3')	Reverse primer (5'–3')
1	GTCAACAGGTACATCAGCCGCC	AGCCTCCTTCCCAGCTGCTGC
2	AGGAGACTGCTACTACTGTGTATCTGGAC	GGATGCCACGTTGCTCTGGGA
3	TTCATCCTGGTGATGGCAAATGTCGT	GGAGTTGTCCACCACCTGGTG
4	CGGGGATGCCAAGTTCTTCCAGGTCATTG	GCCTAGGGTAGCTGAAGGAGG
5	CCTCATCCTGCGCTGCACCCAGAAGCG	ACTGAGC
6	TCCTGAGCCGTGCCATCGA	ACTGCTGGGGCCCCCATTGAG
7	TCCTCGGCGACTGCTACTACTG	GTTCAGCCCCAGCCCCTGAAA
8	ACTTGCGGAGTGGCGATAAATTGAGA	TGGCAAATCAGATTTGTCGGTGCC
9	CGCTGTGCTTCCTCCTGGTG	CACACTCTTTGAAACGTTGAGC

AC assay

In a volume of 10 µl, AC activities were measured using 1 mM ATP, 2 mM $MgCl_2$, 3 mM creatine phosphate, 60 µg/ml creatine kinase, and 50 mM MOPS pH 7.5. The cAMP assay kit from Cisbio (Codolet, France) was used for detection according to the supplier's instructions. For each assay, a cAMP standard curve was established. EC_{50} and IC_{50} values were calculated by GraphPad Prism version 8.4.3 for Windows, GraphPad Software, San Diego, CA, USA, https://www.graphpad.com .

cAMP accumulation assay

HEK293 cells stably expressing mAC isoforms 3, 5, and mAC5(membr)_mAC3(cat) were plated at 2500–10,000 cells/well into 384-well plates. Cells were treated with varying concentrations of lipids and incubated for 10 min at 37°C and 5% CO_2. 2.5–10 µM isoproterenol was added to stimulate cAMP formation and cells were incubated for 5 min. HEK293-AC5–3 was assayed in the presence of the phosphodiesterase inhibitor 0.5 mM isobutyl-methyl-xanthine. Addition of Cisbio HTRF detection reagents stopped the reaction and cAMP levels were determined.

Data handling and analysis

Experimental results were evaluated using GraphPad Prism version 8.4.3. Assays were conducted with a minimum of two technical replicates from at least two independent assays, as specified in the

figure legends. Average values from duplicate or triplicate experiments were designated as single points and data are expressed as means ± SEM. Graphs were generated by GraphPad and assembled in PowerPoint. Outliers were identified using the 'Identify Outliers' function of GraphPad (ROUT method).

Acknowledgements

We are indebted to Prof. Andrei Lupas, Max-Planck-Institute of Biology, Tübingen, for support, advice, and critique. We thank to N Grzegorzek, Organic Chemistry, for GC/MS measurements. Funding was from the Deutsche Forschungsgemeinschaft (Schu275/45-1) and from institutional funds from the Max-Planck-Gesellschaft.

Additional information

Funding

Funder	Grant reference number	Author
Deutsche Forschungsgemeinschaft	Schu275/45-1	Joachim E Schultz
Max-Planck-Gesellschaft	institutional funds	Adrian CD Fuchs

The funders had no role in study design, data collection, and interpretation, or the decision to submit the work for publication.

Author contributions

Marius Landau, Data curation, Investigation, Methodology, Validation, Visualization, Writing – review and editing; Sherif Elsabbagh, Data curation, Investigation, Validation, Visualization, Writing – review and editing; Harald Gross, Data curation, Investigation, Methodology, Writing – review and editing; Adrian CD Fuchs, Data curation, Visualization; Anita CF Schultz, Formal analysis, Data curation, Visualization; Joachim E Schultz, Conceptualization, Formal analysis, Supervision, Writing - original draft, Project administration, Writing – review and editing

Author ORCIDs

Marius Landau https://orcid.org/0000-0002-4638-1908
Adrian CD Fuchs https://orcid.org/0000-0001-6550-1795
Joachim E Schultz https://orcid.org/0000-0002-1985-4853

Peer review material

Reviewer #1 (Public review): https://doi.org/10.7554/eLife.101483.3.sa1
Reviewer #3 (Public review): https://doi.org/10.7554/eLife.101483.3.sa2
Author response https://doi.org/10.7554/eLife.101483.3.sa3

Additional files

Supplementary files

- MDAR checklist

Data availability

All data generated or analyzed during this study are included in the manuscript and supporting files.

References

Abdel Motaal A, Tews I, Schultz JE, Linder JU. 2006. Fatty acid regulation of adenylyl cyclase Rv2212 from *Mycobacterium tuberculosis* H37Rv. *The FEBS Journal* **273**:4219–4228. DOI: https://doi.org/10.1111/j.1742-4658.2006.05420.x, PMID: 16925585

Alam SQ, Mannino SJ, Alam BS, McDonough K. 1995. Effect of essential fatty acid deficiency on forskolin binding sites, adenylate cyclase and cyclic AMP-dependent protein kinase activity, the levels of G proteins and

ventricular function in rat heart. *Journal of Molecular and Cellular Cardiology* **27**:1593–1604. DOI: https://doi.org/10.1016/s0022-2828(95)90491-3, PMID: 8523422

Änggård E, Samuelsson B. 1965. Biosynthesis of prostaglandins from arachidonic acid in guinea pig lung. *Journal of Biological Chemistry* **240**:3518–3521. DOI: https://doi.org/10.1016/S0021-9258(18)97174-7

Bassler J, Schultz JE, Lupas AN. 2018. Adenylate cyclases: receivers, transducers, and generators of signals. *Cellular Signalling* **46**:135–144. DOI: https://doi.org/10.1016/j.cellsig.2018.03.002

Beltz S, Bassler J, Schultz JE. 2016. Regulation by the quorum sensor from Vibrio indicates a receptor function for the membrane anchors of adenylate cyclases. *eLife* **5**:e13098. DOI: https://doi.org/10.7554/eLife.13098, PMID: 26920221

Brown WJ, Chambers K, Doody A. 2003. Phospholipase A2 (PLA2) enzymes in membrane trafficking: mediators of membrane shape and function. *Traffic* **4**:214–221. DOI: https://doi.org/10.1034/j.1600-0854.2003.00078.x, PMID: 12694560

Dautel SE, Kyle JE, Clair G, Sontag RL, Weitz KK, Shukla AK, Nguyen SN, Kim Y-M, Zink EM, Luders T, Frevert CW, Gharib SA, Laskin J, Carson JP, Metz TO, Corley RA, Ansong C. 2017. Lipidomics reveals dramatic lipid compositional changes in the maturing postnatal lung. *Scientific Reports* **7**:40555. DOI: https://doi.org/10.1038/srep40555, PMID: 28145528

Dessauer CW, Watts VJ, Ostrom RS, Conti M, Dove S, Seifert R. 2017. International union of basic and clinical pharmacology. CI. structures and small molecule modulators of mammalian adenylyl cyclases. *Pharmacological Reviews* **69**:93–139. DOI: https://doi.org/10.1124/pr.116.013078, PMID: 28255005

Eyster KM. 2007. The membrane and lipids as integral participants in signal transduction: lipid signal transduction for the non-lipid biochemist. *Advances in Physiology Education* **31**:5–16. DOI: https://doi.org/10.1152/advan.00088.2006, PMID: 17327576

Findeisen F, Linder JU, Schultz A, Schultz JE, Brügger B, Wieland F, Sinning I, Tews I. 2007. The structure of the regulatory domain of the adenylyl cyclase Rv1264 from *Mycobacterium tuberculosis* with bound oleic acid. *Journal of Molecular Biology* **369**:1282–1295. DOI: https://doi.org/10.1016/j.jmb.2007.04.013, PMID: 17482646

Fuchs ACD. 2023. Specific, sensitive and quantitative protein detection by in-gel fluorescence. *Nature Communications* **14**:2505. DOI: https://doi.org/10.1038/s41467-023-38147-8, PMID: 37130834

Graziano MP, Freissmuth M, Gilman AG. 1989. Purification and properties of two forms of the protein. *The Journal of Biological Chemistry* **264**:409–418. DOI: https://doi.org/10.1016/S0021-9258(17)31273-5

Graziano MP, Freissmuth M, Gilman AG. 1991. Purification of recombinant Gs alpha. *Methods in Enzymology* **195**:192–202. DOI: https://doi.org/10.1016/0076-6879(91)95166-h, PMID: 1903486

Grundmann M, Bender E, Schamberger J, Eitner F. 2021. Pharmacology of free fatty acid receptors and their allosteric modulators. *International Journal of Molecular Sciences* **22**:1763. DOI: https://doi.org/10.3390/ijms22041763, PMID: 33578942

Gu C, Sorkin A, Cooper DMF. 2001. Persistent interactions between the two transmembrane clusters dictate the targeting and functional assembly of adenylyl cyclase. *Current Biology* **11**:185–190. DOI: https://doi.org/10.1016/s0960-9822(01)00044-6, PMID: 11231154

Guo YL, Seebacher T, Kurz U, Linder JU, Schultz JE. 2001. Adenylyl cyclase Rv1625c of *Mycobacterium tuberculosis*: a progenitor of mammalian adenylyl cyclases. *The EMBO Journal* **20**:3667–3675. DOI: https://doi.org/10.1093/emboj/20.14.3667, PMID: 11447108

Huber AH, Kleinfeld AM. 2017. Unbound free fatty acid profiles in human plasma and the unexpected absence of unbound palmitoleate. *Journal of Lipid Research* **58**:578–585. DOI: https://doi.org/10.1194/jlr.M074260, PMID: 28082409

Khandelwal RL, Hamilton IR. 1971. Purification and properties of adenyl cyclase from Streptococcus salivarius. *The Journal of Biological Chemistry* **246**:3297–3304 PMID: 4324896.

Kimura I, Ichimura A, Ohue-Kitano R, Igarashi M. 2020. Free fatty acid receptors in health and disease. *Physiological Reviews* **100**:171–210. DOI: https://doi.org/10.1152/physrev.00041.2018, PMID: 31487233

Krupinski J, Coussen F, Bakalyar HA, Tang WJ, Feinstein PG, Orth K, Slaughter C, Reed RR, Gilman AG. 1989. Adenylyl cyclase amino acid sequence: possible channel- or transporter-like structure. *Science* **244**:1558–1564. DOI: https://doi.org/10.1126/science.2472670, PMID: 2472670

Linder JU, Schultz JE. 2003. The class III adenylyl cyclases: multi-purpose signalling modules. *Cellular Signalling* **15**:1081–1089. DOI: https://doi.org/10.1016/s0898-6568(03)00130-x, PMID: 14575863

Linder JU, Schultz JE. 2008. Versatility of signal transduction encoded in dimeric adenylyl cyclases. *Current Opinion in Structural Biology* **18**:667–672. DOI: https://doi.org/10.1016/j.sbi.2008.11.008, PMID: 19054664

Liu J, Wang L, Harvey-White J, Osei-Hyiaman D, Razdan R, Gong Q, Chan AC, Zhou Z, Huang BX, Kim HY, Kunos G. 2006. A biosynthetic pathway for anandamide. *PNAS* **103**:13345–13350. DOI: https://doi.org/10.1073/pnas.0601832103, PMID: 16938887

Lu HC, Mackie K. 2016. An introduction to the endogenous cannabinoid system. *Biological Psychiatry* **79**:516–525. DOI: https://doi.org/10.1016/j.biopsych.2015.07.028, PMID: 26698193

McKinney MK, Cravatt BF. 2005. Structure and function of fatty acid amide hydrolase. *Annual Review of Biochemistry* **74**:411–432. DOI: https://doi.org/10.1146/annurev.biochem.74.082803.133450, PMID: 15952893

McMahon HT, Gallop JL. 2005. Membrane curvature and mechanisms of dynamic cell membrane remodelling. *Nature* **438**:590–596. DOI: https://doi.org/10.1038/nature04396, PMID: 16319878

Mock ED, Gagestein B, van der Stelt M. 2023. Anandamide and other N-acylethanolamines: A class of signaling lipids with therapeutic opportunities. *Progress in Lipid Research* **89**:101194. DOI: https://doi.org/10.1016/j.plipres.2022.101194, PMID: 36150527

Muccioli GG. 2010. Endocannabinoid biosynthesis and inactivation, from simple to complex. *Drug Discovery Today* **15**:474–483. DOI: https://doi.org/10.1016/j.drudis.2010.03.007, PMID: 20304091

Nakamura J, Okamura N, Usuki S, Bannai S. 2001. Inhibition of adenylyl cyclase activity in brain membrane fractions by arachidonic acid and related unsaturated fatty acids. *Archives of Biochemistry and Biophysics* **389**:68–76. DOI: https://doi.org/10.1006/abbi.2001.2315, PMID: 11370673

Ostrom KF, LaVigne JE, Brust TF, Seifert R, Dessauer CW, Watts VJ, Ostrom RS. 2022. Physiological roles of mammalian transmembrane adenylyl cyclase isoforms. *Physiological Reviews* **102**:815–857. DOI: https://doi.org/10.1152/physrev.00013.2021, PMID: 34698552

Qi C, Sorrentino S, Medalia O, Korkhov VM. 2019. The structure of a membrane adenylyl cyclase bound to an activated stimulatory G protein. *Science* **364**:389–394. DOI: https://doi.org/10.1126/science.aav0778, PMID: 31023924

Qi Chao, Lavriha P, Mehta V, Khanppnavar B, Mohammed I, Li Y, Lazaratos M, Schaefer JV, Dreier B, Plückthun A, Bondar A-N, Dessauer CW, Korkhov VM. 2022. Structural basis of adenylyl cyclase 9 activation. *Nature Communications* **13**:1045. DOI: https://doi.org/10.1038/s41467-022-28685-y, PMID: 35210418

Samovski D, Jacome-Sosa M, Abumrad NA. 2023. Fatty acid transport and signaling: mechanisms and physiological implications. *Annual Review of Physiology* **85**:317–337. DOI: https://doi.org/10.1146/annurev-physiol-032122-030352, PMID: 36347219

Sanabra C, Mengod G. 2011. Neuroanatomical distribution and neurochemical characterization of cells expressing adenylyl cyclase isoforms in mouse and rat brain. *Journal of Chemical Neuroanatomy* **41**:43–54. DOI: https://doi.org/10.1016/j.jchemneu.2010.11.001, PMID: 21094251

Schultz JE, Schmidt BH. 1987. Treatment of rats with thyrotropin (TSH) reduces the adrenoceptor sensitivity of adenylate cyclase from cerebral cortex. *Neurochemistry International* **10**:173–178. DOI: https://doi.org/10.1016/0197-0186(87)90124-0, PMID: 20501067

Schultz JE. 2022. The evolutionary conservation of eukaryotic membrane-bound adenylyl cyclase isoforms. *Frontiers in Pharmacology* **13**:1009797. DOI: https://doi.org/10.3389/fphar.2022.1009797, PMID: 36238545

Schuster D, Khanppnavar B, Kantarci I, Mehta V, Korkhov VM. 2024. Structural insights into membrane adenylyl cyclases, initiators of cAMP signaling. *Trends in Biochemical Sciences* **49**:156–168. DOI: https://doi.org/10.1016/j.tibs.2023.12.002, PMID: 38158273

Seth A, Finkbeiner M, Grischin J, Schultz JE. 2020. Gsα stimulation of mammalian adenylate cyclases regulated by their hexahelical membrane anchors. *Cellular Signalling* **68**:109538. DOI: https://doi.org/10.1016/j.cellsig.2020.109538, PMID: 31931092

Simon GM, Cravatt BF. 2008. Anandamide biosynthesis catalyzed by the phosphodiesterase GDE1 and detection of glycerophospho-N-acyl ethanolamine precursors in mouse brain. *The Journal of Biological Chemistry* **283**:9341–9349. DOI: https://doi.org/10.1074/jbc.M707807200, PMID: 18227059

Sinha SC, Sprang SR. 2006. Structures, mechanism, regulation and evolution of class III nucleotidyl cyclases. *Reviews of Physiology, Biochemistry and Pharmacology* **157**:105–140. DOI: https://doi.org/10.1007/112_0603, PMID: 17236651

Sunahara RK, Dessauer CW, Whisnant RE, Kleuss C, Gilman AG. 1997a. Interaction of Gsalpha with the cytosolic domains of mammalian adenylyl cyclase. *The Journal of Biological Chemistry* **272**:22265–22271. DOI: https://doi.org/10.1074/jbc.272.35.22265, PMID: 9268375

Sunahara RK, Tesmer JJ, Gilman AG, Sprang SR. 1997b. Crystal structure of the adenylyl cyclase activator Gsalpha. *Science* **278**:1943–1947. DOI: https://doi.org/10.1126/science.278.5345.1943, PMID: 9395396

Sutherland EW, Rall TW. 1958. Fractionation and characterization of a cyclic adenine ribonucleotide formed by tissue particles. *The Journal of Biological Chemistry* **232**:1077–1091 PMID: 13549488.

Tang WJ, Gilman AG. 1995. Construction of a soluble adenylyl cyclase activated by Gs alpha and forskolin. *Science* **268**:1769–1772. DOI: https://doi.org/10.1126/science.7792604, PMID: 7792604

Tesmer JJ, Sunahara RK, Gilman AG, Sprang SR. 1997. Crystal structure of the catalytic domains of adenylyl cyclase in a complex with Gsalpha.GTPgammaS. *Science* **278**:1907–1916. DOI: https://doi.org/10.1126/science.278.5345.1907, PMID: 9417641

Tesmer JJ, Sprang SR. 1998. The structure, catalytic mechanism and regulation of adenylyl cyclase. *Current Opinion in Structural Biology* **8**:713–719. DOI: https://doi.org/10.1016/s0959-440x(98)80090-0, PMID: 9914249

Tews I, Findeisen F, Sinning I, Schultz A, Schultz JE, Linder JU. 2005. The structure of a pH-sensing mycobacterial adenylyl cyclase holoenzyme. *Science* **308**:1020–1023. DOI: https://doi.org/10.1126/science.1107642

Ulven T, Christiansen E. 2015. Dietary fatty acids and their potential for controlling metabolic diseases through activation of FFA4/GPR120. *Annual Review of Nutrition* **35**:239–263. DOI: https://doi.org/10.1146/annurev-nutr-071714-034410, PMID: 26185978

Vercellino I, Rezabkova L, Olieric V, Polyhach Y, Weinert T, Kammerer RA, Jeschke G, Korkhov VM. 2017. Role of the nucleotidyl cyclase helical domain in catalytically active dimer formation. *PNAS* **114**:E9821–E9828. DOI: https://doi.org/10.1073/pnas.1712621114, PMID: 29087332

Ziegler M. 2017. A novel signal transducer element intrinsic to class IIIa and IIIb adenylate cyclases. *The FEBS Journal* **284**:1204–1217. DOI: https://doi.org/10.1111/febs.14047

Additional, unpublished data

In the fractionation scheme in appendix 1 of publication III one can see that fraction F is having an enhancing effect on Gsα-stimulated mAC3 while it is slightly inhibiting mAC5. The fact that it shows by eye visible opposite effects on different isoforms leads to the assumption, that this fraction might contain compounds that regulate ACs in an isoform-specific manner.

Indeed, fraction F (dissolved in DMSO) is strongly enhancing Gsα-stimulated mAC3 activity in a concentration-dependent manner up to 0.5 µg/10µl. With increasing concentrations, the stimulation decreases and at high concentrations (> 4 µg/10µL) the fraction is inhibiting (Figure 9).

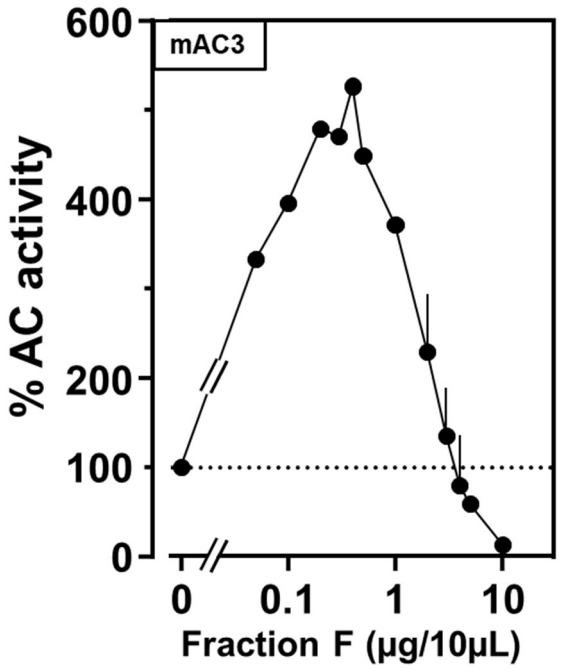

Figure 9. Concentration-response curve of fraction F on Gsα-stimulated mAC3. Basal and 600 nM Gsα (corresponds to 100%) activities of mAC3 were 0.02 and 0.36 nmol cAMP•mg^{-1}•min^{-1}, respectively. Error bars denote S.E.M. with n= 1-2. 10 µg/10µL equals a final DMSO concentration of 2%.

Obviously, fraction F itself was heterogenous. The next step was to further subfractionate. RP-HPLC resulted in 5 subfractions, F-1 to F-5 (Figure 10)

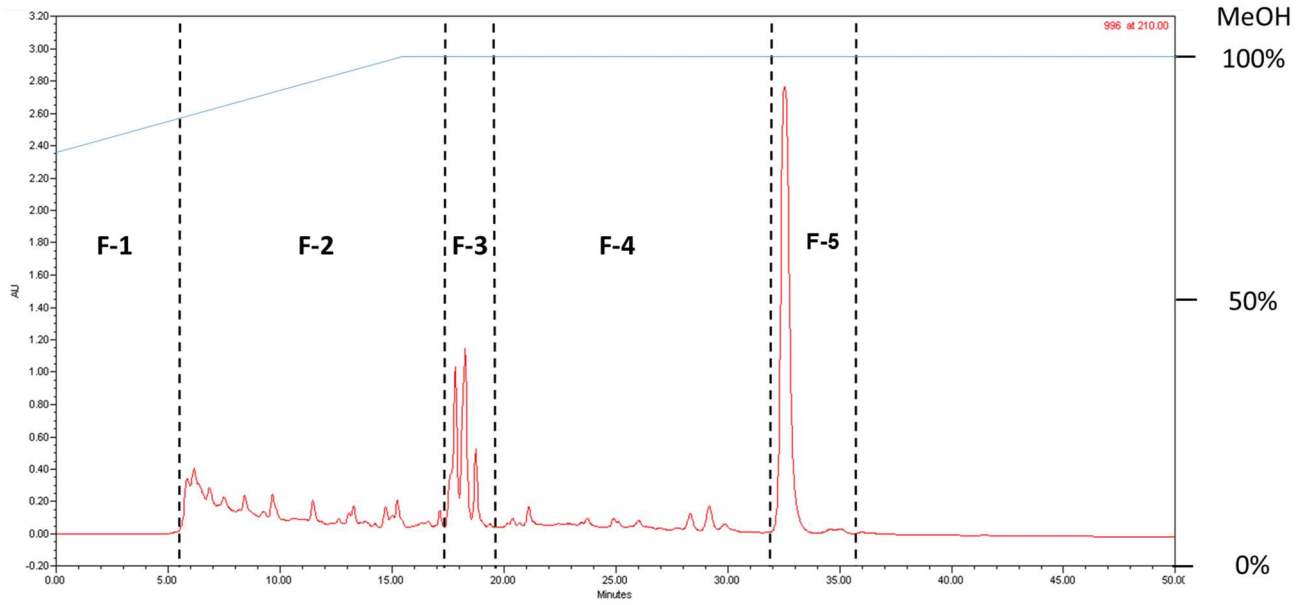

Figure 10. RP-HPLC chromatogram of fraction E.
UV-absorbance at 210 nm. MeOH/H_20 gradient indicated in blue. Flow rate: 1.5 mL/min. Column: Eurospher II 100-5 C18P, 250x8 mm (Knauer).

Next, I examined the effect of the subfractions on mAC3 and mAC5 activity, stimulated by Gsα. Subfraction F-1 was slightly enhancing mAC3 activity while it showed nearly no effect on mAC5. F-2, -3, and -4 were showing similar effects. Enhancement of mAC3 at certain concentrations, followed by a decrease of activity, like fraction F. The extent of enhancement differs between F-4 and the others. F-4 enhances mAC3 activity up to 700% compared to Gsα-stimulation alone, while F-2 and F-3 were enhancing up to 400%. The forementioned three subfractions were all inhibiting mAC5 activity similarly starting at concentrations higher than 1 µg/10µL assay volume. Subfraction F-5 enhances mAC3 activity up to 400% compared to Gsα-stimulated activity but lacks the decrease of activity at higher concentrations. The inhibitory effect on mAC5 is extenuated in comparison to F-2, -3, and -4 (Figure 11).

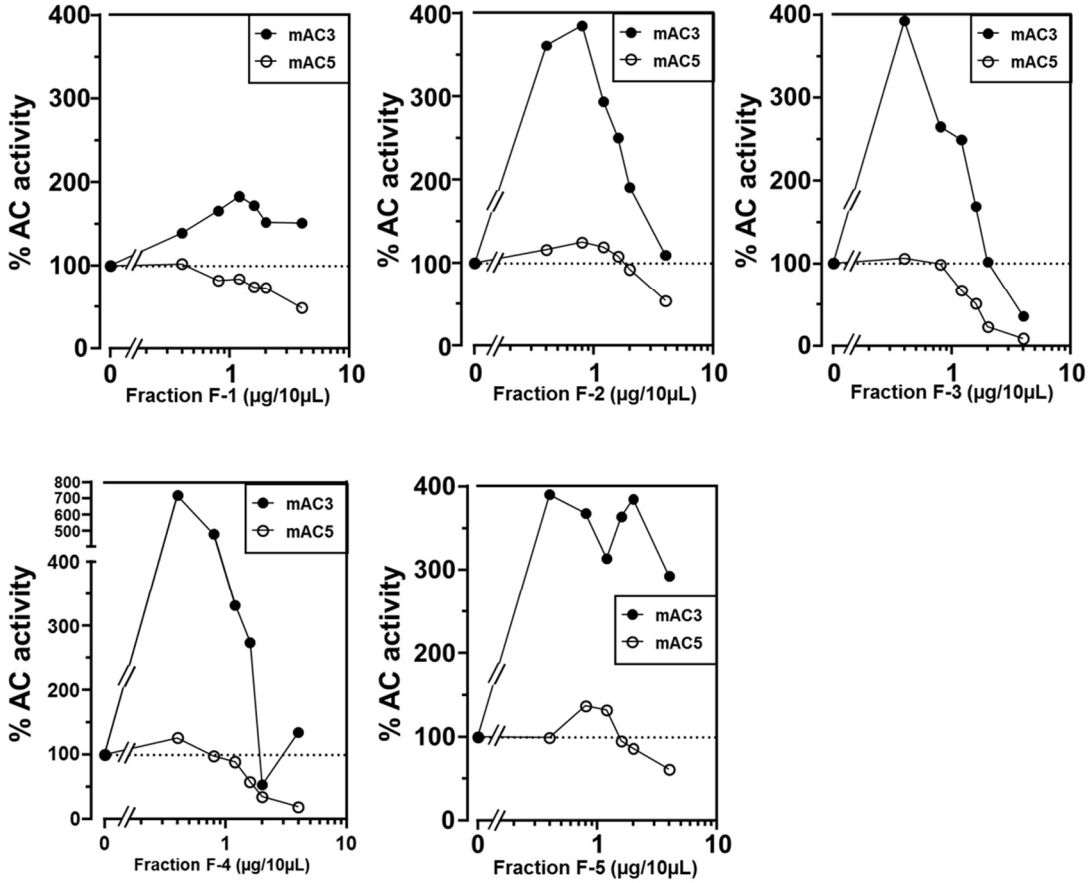

Figure 11. Effect of subfractions F-1 to F-5 on 600nm Gsα-stimulated mAC3 and mAC5.

The main reasons why I continued working on subfraction F-5 were the missing decrease of activity with higher concentrations and the isoform-specific enhancement of mAC3. Further, the RP-HPLC chromatogram (Figure 9) did show one major peak in this fraction, indicating the probability of dealing with a limited number of compounds in this fraction. NMR studies undertaken and analyzed by Prof. Dr. Harald Groß (Pharmaceutical Institute, University Tübingen) identified 7-ketocholesterol in subfraction F-5. 7-Ketocholesterol is an oxysterol associated with disease states, most prominently found in arterial plaques of coronary artery disease patients [29]. Surprisingly, 7-ketocholesterol did not affect Gsα-stimulated mAC3 in any way. The reduced form 7-hydroxycholesterol did also not affect Gsα -stimulated mAC3 activity, excluding loss of function through oxidation processes of the compound (Figure 12).

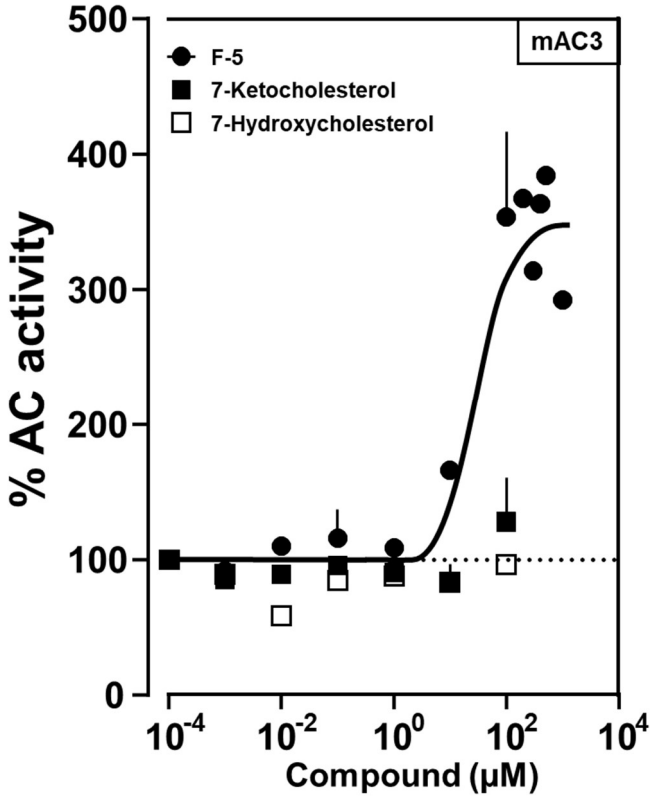

Figure 12. Effect of subfraction F-5, 7-keto- and 7-hydroxycholesterol on Gsα-stimulated mAC3.

The NMR data and some very minor peaks in the RP-HPLC chromatogram (Figure 9) were already indicating that the subfraction F-5 is not solely composed of 7-ketocholesterol but contains one or more unknown compounds. Together with Dr. Norbert Grzegorzek (Organic chemistry, University Tübingen) I performed GC/MS studies after trimethylsilylation according to publication III. The mass spectra were then compared to the NIST database for identification. It was no surprise that we identified 7-ketocholesterol in subfraction F-5. However, it was surprising to identify palmitic, stearic and oleic acid (Figure 13), the same fatty acids we identified in subfraction E-2. Therefore, I further cooperated with Dr. Sherif Elsabbagh investigating the effects of fatty acids.

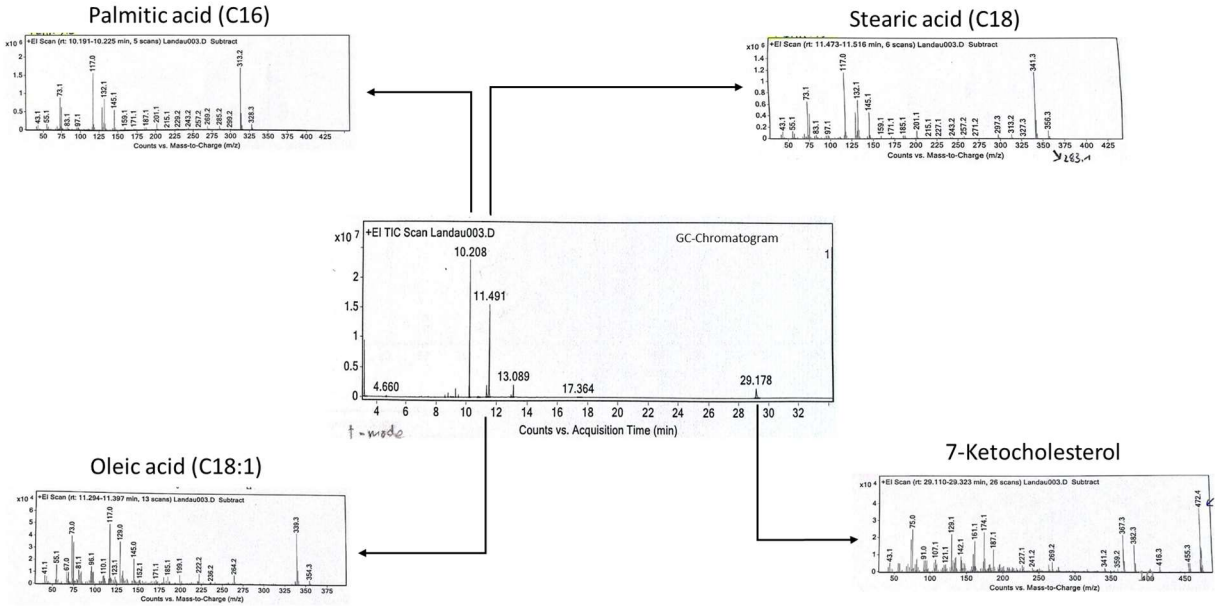

Figure 13. GC-chromatogram with respective mass spectra of subfraction F-5. Compounds were identified via comparisons with the NIST data base as their respective trimethylsilyl derivatives.

In addition to the chimeric protein mAC5-3, we also generated a chimera in which the transmembrane domain of mAC3 is fused to the cytosolic domain of mAC5 (mAC3-5). The expression was confirmed via in-gel fluorescence, performed by Dr. Adrian Fuchs (MPI Tübingen) (Figure 14). Gsα concentration-response curves revealed that this chimera was no longer regulated, exhibiting an activity at 300 nM Gsα that was 22 times higher than that of mAC5 at the same concentration (Figure 15). Due to this outcome, I decided not to pursue further research on this protein.

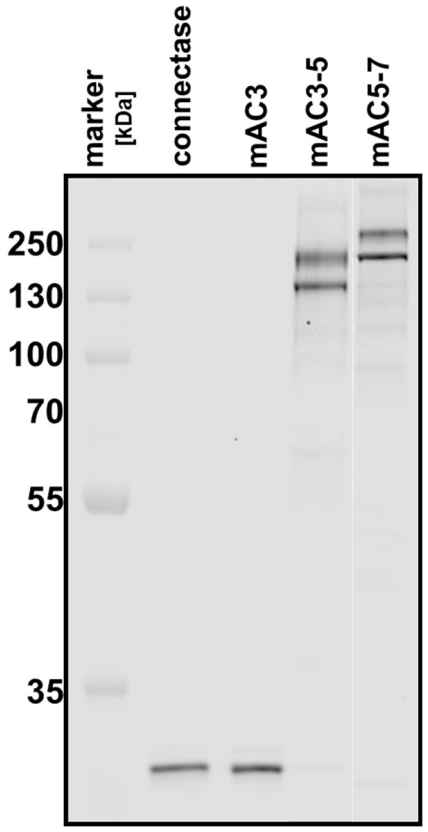

Figure 14. Detection of mAC3$_{(membr)}$-mAC5$_{(cat)}$ and mAC5$_{(membr)}$-mAC7$_{(cat)}$ chimeras.
Proteins were detected by in-gel fluorescence via the N-terminal Connectase-tag according to [30].

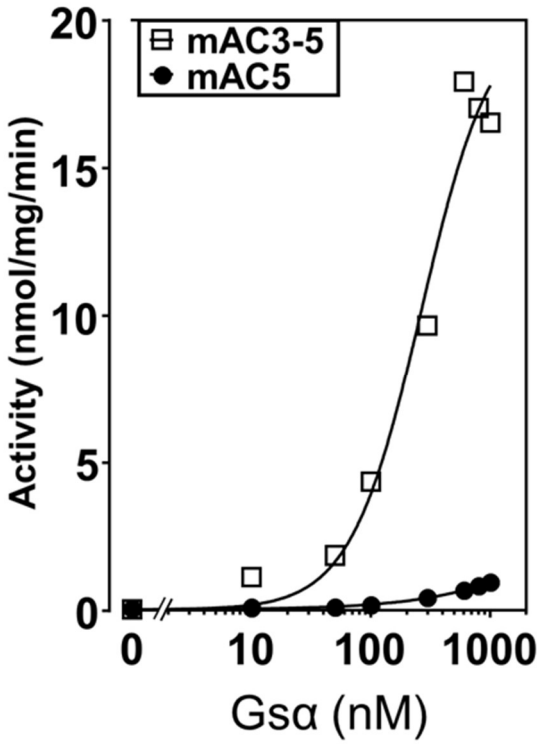

Figure 15. Gsα concentration response curves for mAC3-5 and mAC5.

Basal activities of mAC3-5 and mAC5 were 0.03 and 0.05 nmol•mg^{-1}•min^{-1}, respectively. EC_{50} were 264 and 245 nM, respectively. N=1, in technical duplicates.

Additionally, we designed and expressed a chimera combining the transmembrane domain of mAC5 with the cytosolic domain of mAC7 (mAC5-7). The expression was again confirmed through in-gel fluorescence (Figure 14). Anandamide concentration-response curves showed that the activity of this chimera, when stimulated by 300 nM Gsα, was attenuated comparable to mAC5. In contrast, mAC7 stimulated by Gsα remained unaffected by anandamide, even at concentrations up to 100 µM (Figure 16). These findings undermine the membrane receptor hypothesis by indicating that the anandamide receptor property of mAC5 is transferable not only to mAC3 but to another, anandamide-insensitive, isoform too.

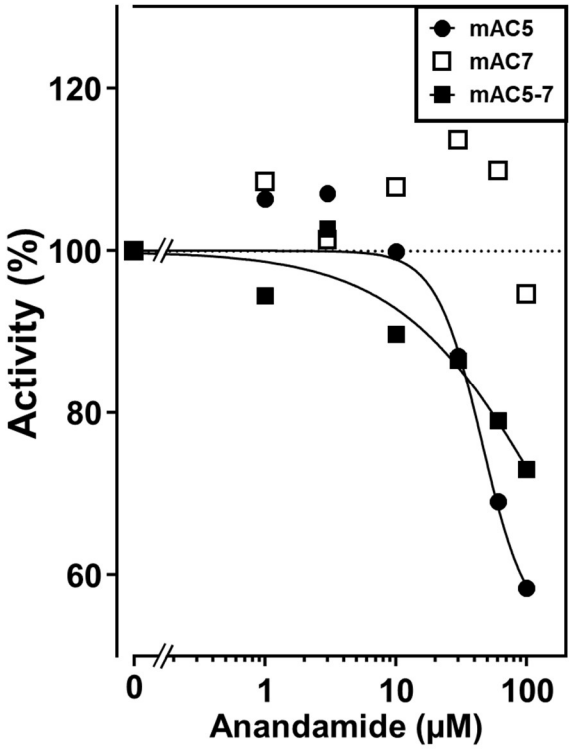

Figure 16. Anandamide attenuates mAC5-7 but not mAC7.
Basal and 300 nM Gsα-stimulated activities were 0.07 ± 0.01 and 1.78 ± 0.10 (AC5), 0.02 ± 0.01 and 0.09 ± 0.01 (AC7) and 0.02 ± 0.01 and 0.20 ± 0.02 nmol•mg^{-1}•min^{-1} (AC5-7), respectively. Calculated IC_{50} values were 45 and 140 µM for mAC5 and mAC5-7, respectively. Error bars are not shown for clarity, N=4-8.

Outlook and discussion

Not so many years ago, the TM domain of ACs was dismissed as a membrane anchor without further function. Bioinformatical, structural, and biochemical studies of the last couple of years indicated that the TM domains might be a novel class of receptors. On the search for potential ligands proofing this hypothesis, we came across some very interesting findings.

One major open question is dealing with the missing regulator specific for mAC8 activity. For all other isoforms we identified specific ligands. While we were focusing on the extraction of lipids from bovine lung at pH 1, preliminary data indicate that, yet unidentified, compounds extracted at pH 7 and pH 14 might have a stimulatory effect on mAC8. Further, the recently published cryo-EM structure of mAC8 indicates that there is a cavity in the TM domain at the interface of the TM1-7 helices formed by the TM4 helix and the loop between TMs 3-4, which is partially negatively charged and therefore a potential binding site for positively charged ligands [25]. This matches with the promising, but preliminary data of the pH 7 and pH 14 extraction data. mAC8 is best studied for its role in the brain, where it takes part in synaptic regulation and also in the heart, specifically in the sinoatrial node, where overexpression of AC8 increased heart rate [31, 32]. That given, using brain or heart tissue as starting material for ligand finding might be worthwhile.

Another aspect of the regulation via the TM domains that we did not directly address yet is, if the divalent cations nature is of importance for this kind of regulation. It is well known that Mn^{2+} is a more potent co-factor than Mg^{2+} but to this day it is not yet solved what exactly causes this difference in activity based on the cation's nature. Preliminary data suggest that the influence of the cation on AC regulation via its TM domain is at least given for the effect of oleic acid on mAC3. Membrane preparations incubated with Mn^{2+} instead of Mg^{2+} are not further enhanced by oleic acid, while the inhibiting effect of arachidonic acid and anandamide is not affected by exchanging the cations. This is something that needs to be investigated further.

The biochemical data that we generated over the last years are only the beginning of understanding how ACs are precisely regulated by their TM domains. Structural studies could be useful to identify the potential binding pocket of the ligands. Once the binding pocket is identified, bioinformatic studies could speed up the search for more potent ligands. The fatty acids that were described as potential ligands might not be the most potent ligands and presently, the existence of more specific ligands cannot be excluded. Predictions based on bioinformatic studies could then bear drugs with increased potency and/or efficacy.

Another question is where these lipophilic ligands come from. For GLPs it is known that the ones with ethanolamine-, choline-, and serine-headgroups are hydrolyzed by phospholipase D, resulting in phosphatidic acids [33].
Concentrations of heme b in blood are usually low but are reported to increase strongly upon hemolysis induced by pathologies like sickle cell disease, sepsis, malaria attacks but also after transfusion of packed red blood cells [34, 35].
While solute signaling is studied intensively, lipid signaling is less examined. The question of how the free fatty acids are getting to the TM domain of the ACs is something that, at this point, we cannot answer. It is described that free fatty acids actually bind to so called free fatty acid receptors, which are mostly, but not all GPCRs, but the authors also cannot explain how the fatty acids get there [36].

In publication III we put ACs at the crossing of direct, tonic lipid signaling and indirect phasic signaling via the GPCR/Gsα pathways. So, what is the tonic state that is constantly monitored by the mACs? The first thing that comes to mind is a general sensor system for the nutritional state, but this needs further investigation.

The second important finding described in publication III is the idea of two basal ground states, one Gsα-responsive state and one Gsα-unresponsive state (figure 17). The ligands then might shift the equilibrium from one state to the other. For example, mAC3, which seems to favor the Gsα-unresponsive state is shifted to the opposing state by oleic acid, seemingly an activating input. The opposite might be the case for mAC5. Arachidonic acid or anandamide, inhibitory inputs, shift the equilibrium to the Gsα-unresponsive state. So, we modified the model first described by Seth et al. a little bit, but the general idea is still the same: Ligands bind to the TM domain of ACs and then regulate the effect of Gsα without directly increasing or decreasing activity, somehow comparable to the pedals of a piano. Pressing the pedals of the piano is changing the way the piano will sound like, but one is unable to identify what changed until you start pressing the keys. In our case the TM domains are like the pedals, the keys represent the catalytic domains, the feet that are pushing the pedals are the ligands and the fingers playing the keys represent Gsα binding.

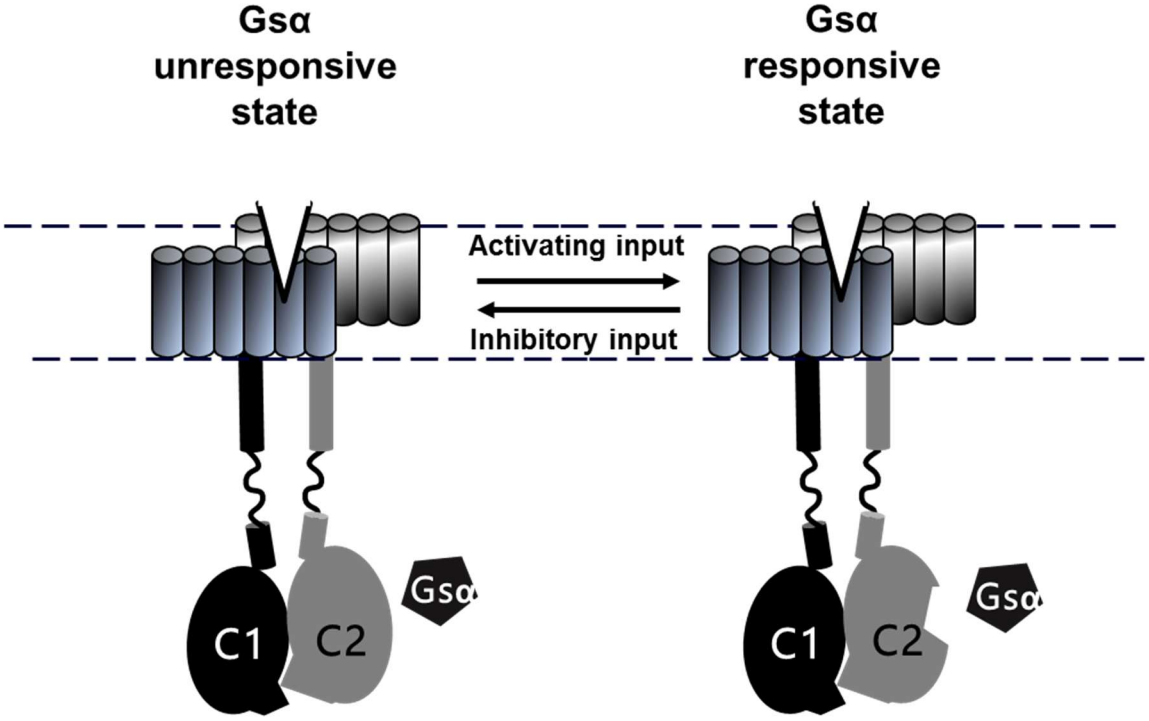

Figure 17. Two-state-model modified after [23].

An intriguing aspect of this research is the interconnectedness of glycerophospholipids, fatty acids, and endocannabinoids. Fatty acids and endocannabinoids are already recognized as ligands for receptors [37, 38]. Glycerophospholipids are described as “a reservoir for second messengers” [39] and therefore ligands. Two potential pathways of anandamide synthesis directly link these three substance classes. Anandamide can either be formed from arachidonic acid and ethanolamine or through the breakdown of *N*-arachidonoyl phosphatidylethanolamine, a membranous glycerophospholipid, by phosphodiesterase directly within the membrane [40]. The fact that all three substances can be formed into each other gives a hint, that mAC regulation might be controlled by a complex system of synthesis and degradation of lipophilic compounds.

Without any doubt, the results presented here are not describing the whole mechanism of AC regulation via its TM domains, but like my supervisor used to tell me at one of the first days in the lab: “Good science is not only answering questions, but also raises many more that are worth to investigate”. And this is the case here. There are so many open questions that are more than worth to go after.

1. Sutherland, E.W. and T.W. Rall, *Fractionation and characterization of a cyclic adenine ribonucleotide formed by tissue particles.* J Biol Chem, 1958. **232**(2): p. 1077-91.
2. Heldin, C.H., et al., *Signals and Receptors.* Cold Spring Harb Perspect Biol, 2016. **8**(4): p. a005900.
3. Casado, V. and V. Casado-Anguera, *What are the current trends in G protein-coupled receptor targeted drug discovery?* Expert Opin Drug Discov, 2023. **18**(8): p. 815-820.
4. Meinkoth, J.L., et al., *Signal transduction through the cAMP-dependent protein kinase.* Mol Cell Biochem, 1993. **127-128**: p. 179-86.
5. Kaupp, U.B. and R. Seifert, *Cyclic nucleotide-gated ion channels.* Physiol Rev, 2002. **82**(3): p. 769-824.
6. Bos, J.L., *Epac proteins: multi-purpose cAMP targets.* Trends Biochem Sci, 2006. **31**(12): p. 680-6.
7. Linder, J.U. and J.E. Schultz, *The class III adenylyl cyclases: multi-purpose signalling modules.* Cell Signal, 2003. **15**(12): p. 1081-9.
8. Bassler, J., J.E. Schultz, and A.N. Lupas, *Adenylate cyclases: Receivers, transducers, and generators of signals.* Cell Signal, 2018. **46**: p. 135-144.
9. Hahn, D.K., et al., *Catalytic Mechanism of Mammalian Adenylyl Cyclase: A Computational Investigation.* Biochemistry, 2015. **54**(40): p. 6252-62.
10. Tesmer, J.J. and S.R. Sprang, *The structure, catalytic mechanism and regulation of adenylyl cyclase.* Curr Opin Struct Biol, 1998. **8**(6): p. 713-9.
11. Yan, S.Z., et al., *The conserved asparagine and arginine are essential for catalysis of mammalian adenylyl cyclase.* J Biol Chem, 1997. **272**(19): p. 12342-9.
12. Dessauer, C.W., et al., *International Union of Basic and Clinical Pharmacology. CI. Structures and Small Molecule Modulators of Mammalian Adenylyl Cyclases.* Pharmacol Rev, 2017. **69**(2): p. 93-139.
13. Mitterauer, T., et al., *The C2 catalytic domain of adenylyl cyclase contains the second metal ion (Mn2+) binding site.* Biochemistry, 1998. **37**(46): p. 16183-91.
14. Ziegler, M., et al., *Characterization of a novel signal transducer element intrinsic to class IIIa/b adenylate cyclases and guanylate cyclases.* FEBS J, 2017. **284**(8): p. 1204-1217.
15. Qi, C., et al., *The structure of a membrane adenylyl cyclase bound to an activated stimulatory G protein.* Science, 2019. **364**(6438): p. 389-394.
16. Krupinski, J., et al., *Adenylyl cyclase amino acid sequence: possible channel- or transporter-like structure.* Science, 1989. **244**(4912): p. 1558-64.
17. Reddy, R., et al., *Voltage-sensitive adenylyl cyclase activity in cultured neurons. A calcium-independent phenomenon.* J Biol Chem, 1995. **270**(24): p. 14340-6.
18. Cooper, D.M. and A.J. Crossthwaite, *Higher-order organization and regulation of adenylyl cyclases.* Trends Pharmacol Sci, 2006. **27**(8): p. 426-31.
19. Tang, W.J. and A.G. Gilman, *Construction of a soluble adenylyl cyclase activated by Gs alpha and forskolin.* Science, 1995. **268**(5218): p. 1769-72.
20. Schultz, J.E., *The evolutionary conservation of eukaryotic membrane-bound adenylyl cyclase isoforms.* Front Pharmacol, 2022. **13**: p. 1009797.
21. Guo, Y.L., et al., *Adenylyl cyclase Rv1625c of Mycobacterium tuberculosis: a progenitor of mammalian adenylyl cyclases.* EMBO J, 2001. **20**(14): p. 3667-75.
22. Beltz, S., J. Bassler, and J.E. Schultz, *Regulation by the quorum sensor from Vibrio indicates a receptor function for the membrane anchors of adenylate cyclases.* Elife, 2016. **5**.

23. Seth, A., et al., *Gsalpha stimulation of mammalian adenylate cyclases regulated by their hexahelical membrane anchors.* Cell Signal, 2020. **68**: p. 109538.
24. Mehta, V., et al., *Structure of Mycobacterium tuberculosis Cya, an evolutionary ancestor of the mammalian membrane adenylyl cyclases.* Elife, 2022. **11**.
25. Khanppnavar, B., et al., *Regulatory sites of CaM-sensitive adenylyl cyclase AC8 revealed by cryo-EM and structural proteomics.* EMBO Rep, 2024. **25**(3): p. 1513-1540.
26. Yen, Y.C., et al., *Structure of adenylyl cyclase 5 in complex with Gbetagamma offers insights into ADCY5-related dyskinesia.* Nat Struct Mol Biol, 2024. **31**(8): p. 1189-1197.
27. Diau, G.Y., et al., *The influence of long chain polyunsaturate supplementation on docosahexaenoic acid and arachidonic acid in baboon neonate central nervous system.* BMC Med, 2005. **3**: p. 11.
28. Park, H.G., et al., *The fatty acid desaturase 2 (FADS2) gene product catalyzes Delta4 desaturation to yield n-3 docosahexaenoic acid and n-6 docosapentaenoic acid in human cells.* FASEB J, 2015. **29**(9): p. 3911-9.
29. Anderson, A., et al., *7-Ketocholesterol in disease and aging.* Redox Biol, 2020. **29**: p. 101380.
30. Fuchs, A.C.D., *Specific, sensitive and quantitative protein detection by in-gel fluorescence.* Nat Commun, 2023. **14**(1): p. 2505.
31. Ostrom, K.F., et al., *Physiological roles of mammalian transmembrane adenylyl cyclase isoforms.* Physiol Rev, 2022. **102**(2): p. 815-857.
32. Moen, J.M., et al., *Overexpression of a Neuronal Type Adenylyl Cyclase (Type 8) in Sinoatrial Node Markedly Impacts Heart Rate and Rhythm.* Front Neurosci, 2019. **13**: p. 615.
33. Jang, J.H., et al., *Understanding of the roles of phospholipase D and phosphatidic acid through their binding partners.* Prog Lipid Res, 2012. **51**(2): p. 71-81.
34. Immenschuh, S., et al., *Heme as a Target for Therapeutic Interventions.* Front Pharmacol, 2017. **8**: p. 146.
35. Pietropaoli, A.P., et al., *Total plasma heme concentration increases after red blood cell transfusion and predicts mortality in critically ill medical patients.* Transfusion, 2019. **59**(6): p. 2007-2015.
36. Kimura, I., et al., *Free Fatty Acid Receptors in Health and Disease.* Physiol Rev, 2020. **100**(1): p. 171-210.
37. Grundmann, M., et al., *Pharmacology of Free Fatty Acid Receptors and Their Allosteric Modulators.* Int J Mol Sci, 2021. **22**(4).
38. Estrada, J.A. and I. Contreras, *Endocannabinoid Receptors in the CNS: Potential Drug Targets for the Prevention and Treatment of Neurologic and Psychiatric Disorders.* Curr Neuropharmacol, 2020. **18**(8): p. 769-787.
39. Farooqui, A.A., L.A. Horrocks, and T. Farooqui, *Glycerophospholipids in brain: their metabolism, incorporation into membranes, functions, and involvement in neurological disorders.* Chem Phys Lipids, 2000. **106**(1): p. 1-29.
40. Sugiura, T., et al., *Biosynthesis and degradation of anandamide and 2-arachidonoylglycerol and their possible physiological significance.* Prostaglandins Leukot Essent Fatty Acids, 2002. **66**(2-3): p. 173-92.

Disclaimer AI-systems

I utilized OpenAI's ChatGPT language model to improve the quality of the language. I confirm that the AI was used exclusively for this purpose, and no information or data presented in this thesis was obtained through ChatGPT.